

**UNCONVENTIONAL FINITE ELEMENT MODELS FOR
NONLINEAR ANALYSIS OF BEAMS AND PLATES**

A Thesis

by

WOORAM KIM

Submitted to the Office of Graduate Studies of
Texas A&M University
in partial fulfillment of the requirements for the degree of

MASTER OF SCIENCE

August 2008

Major Subject: Mechanical Engineering

**UNCONVENTIONAL FINITE ELEMENT MODELS FOR
NONLINEAR ANALYSIS OF BEAMS AND PLATES**

A Thesis

by

WOORAM KIM

Submitted to the Office of Graduate Studies of
Texas A&M University
in partial fulfillment of the requirements for the degree of

MASTER OF SCIENCE

Approved by:

Chair of Committee,	J. N. Reddy
Committee Members,	Xinlin Gao
	Zoran Sunik
Head of Department,	Dennis O'Neal

August 2008

Major Subject: Mechanical Engineering

ABSTRACT

Unconventional Finite Element Models for
Nonlinear Analysis of Beams and Plates. (August 2008)

Wooram Kim, B.S., Korea Military Academy

Chair of Advisory Committee: Dr. J. N. Reddy

In this thesis, mixed finite element models of beams and plates bending are developed to include other variables (i.e., the membrane forces and shear forces) in addition to the bending moments and vertical deflection, and to see the effect of it on the nonlinear analysis. Models were developed based on the weighted residual method.

The effect of inclusion of additional variables is compared with other mixed models to show the advantage of the one type of model over other models.

For beam problems the Euler-Bernoulli beam theory and the Timoshenko beam theory are used. And for the plate problems the classical plate theory and the first-order shear deformation plate theory are used.

Each newly developed model is examined and compared with other models to verify its performance under various boundary conditions. In the linear convergence study, solutions are compared with analytical solutions available and solutions of existing models. For non-linear equation solving direct method and Newton-Raphson method are used to find non-linear solutions. Then, converged solutions are compared with available solutions of the displacement models.

Noticeable improvement in accuracy of force-like variables (i.e., shear resultant, membrane resultant and bending moments) at the boundary of elements can be achieved by using present mixed models in both linear and nonlinear analysis. Post processed data of newly developed mixed models show better accuracy than existing displacement based and mixed models in both of vertical displacement and force-like variables. Also present beam and plate finite element models allow use of relatively lower level of interpolation function without causing severe locking problems.

DEDICATION

To my God, my mother, grandfather, grandmother and all of my family members who have always been there for me.

ACKNOWLEDGMENTS

I am greatly indebted to my advisor Dr. J.N.Reddy for his valuable comments and advice. Without his help, this thesis would not have been completed. Sincere thanks to Dr. Xin-Lin Gao and Dr. Zoran Sunik for their valuable recommendations and consideration as committee members.

TABLE OF CONTENTS

	Page
ABSTRACT.....	iii
DEDICATION.....	iv
ACKNOWLEDGMENTS.....	v
TABLE OF CONTENTS.....	vi
LIST OF FIGURES.....	viii
LIST OF TABLES.....	x
CHAPTER I INTRODUCTION.....	1
1.1 Review of Euler-Bernoulli Beam Theory.....	3
1.1.1 Kinematics of EBT.....	4
1.1.2 Equilibriums of EBT.....	4
1.1.3 Constitutive Relations and Resultants of EBT.....	6
1.2 Review of Timoshenko Beam Theory (TBT).....	7
1.2.1 Kinematics of TBT.....	7
1.2.2 Equilibriums of TBT.....	8
1.2.3 Constitutive Relations and Resultants of TBT.....	10
1.3. Review of Classical Plate Theory (CPT).....	11
1.3.1 Kinematics of CPT.....	12
1.3.2 Equilibriums of CPT.....	13
1.3.3 Constitutive Relations and Resultants of CPT.....	16
1.4. Review of First Order Shear Deformation Theory (FSDT).....	18
1.4.1 Kinematics of FSDT.....	18
1.4.2 Equilibriums of FSDT.....	19
1.4.3 Constitutive Relations and Resultants of FSDT.....	19
CHAPTER II DEVELOPMENT OF BEAM BENDING MODELS.....	21
2.1 Model I of Beam Bending.....	22
2.1.1 Weighted Residual Statements of Model I.....	22
2.1.2 Finite Element Equations of Model I.....	23
2.2 Model II of Beam Bending.....	26
2.2.1 Weighted Residual Statements of Model II.....	26
2.2.2 Finite Element Equations of Model II.....	27
2.3 Model III of Beam Bending.....	29
2.3.1 Weighted Residual Statements of Model III.....	30
2.3.2 Finite Element Equations of Model III.....	31
2.4 Model IV of Beam Bending.....	34
2.4.1 Weighted Residual Statements of the Model IV.....	34
2.4.2 Finite Element Equations of Model IV.....	35
2.5 Lagrange Type Beam Finite Elements.....	37

	Page
CHAPTER III DEVELOPMENT OF PLATE BENDING MODELS.....	40
3.1 Model I of Plate Bending.....	42
3.1.1 Weighted Residual Statements of Model I.....	42
3.1.2 Finite Element Equations of Model I.....	43
3.2 Model II of Plate Bending.....	48
3.2.1 Weighted Residual Statements of Model II.....	48
3.2.2 Finite Element Equations of Model II.....	49
3.3 Model III of Plate Bending.....	53
3.3.1 Weighted Residual Statements of Model III.....	53
3.3.2 Finite Element Equations of Model III.....	55
3.4 Model IV of Plate Bending.....	60
3.4.1 Weighted Residual Statements of Model IV.....	60
3.4.2 Finite Element Equations of Model IV.....	62
3.5 The Lagrange Type Plate Finite Elements.....	67
CHAPTER IV NONLINEAR EQUATION SOLVING PROCEDURES.....	69
4.1 Direct Iterative Method.....	69
4.1.1 Algorithm of Direct Iterative Method.....	70
4.2 Newton-Raphson Iterative Method.....	72
4.2.1 Algorithm of Newton-Raphson Iterative Method.....	73
4.2.2 Calculation of Tangent Stiffness Matrices.....	75
4.2.3 Tangent Stiffness Matrices.....	76
4.3 Load Increment Vector.....	81
CHAPTER V NUMERICAL RESULTS.....	82
5.1. Numerical Analysis of Nonlinear Beam Bending.....	82
5.1.1 Description of Problem[1].....	82
5.1.2 Numerical Results.....	84
5.2. Numerical Analysis of Nonlinear Plate Bending.....	93
5.2.1 Description of Problem.....	93
5.2.2 Non-dimensional Analysis of Linear Solutions.....	94
5.2.3 Non-linear Analysis.....	100
CHAPTER VI CONCLUSION.....	111
REFERENCES.....	113
VITA.....	115

LIST OF FIGURES

		Page
Fig. 1.1	Undeformed and deformed EBT and TBT beams, source from[2]...	3
Fig. 1.2	A typical beam element with forces and bending moments.....	5
Fig. 1.3	Undeformed and deformed CPT and FSDT plates, source from[2]...	9
Fig. 1.4	A typical 2-D plate element[3] with forces and moments.....	11
Fig. 2.1	Node number and local coordinate of the line elements of the Lagrange family.....	38
Fig. 3.1	Node number and local coordinate of the rectangular elements of the Lagrange family.....	68
Fig. 4.1	A flow chart[1] of the direct iteration method.....	70
Fig. 4.2	A flow chart[1] of the Newton iteration method.....	72
Fig. 5.1	Description of the beam geometry.....	82
Fig. 5.2	Symmetry boundary conditions of beams.....	83
Fig. 5.3	A comparison of the non-linear solutions of beams.....	85
Fig. 5.4	A comparison of the membrane locking in various models.....	89
Fig. 5.5	A comparison of effect of the length-to-thickness ratio on the beam.....	91
Fig. 5.6	A description of the plate bending problem.....	93
Fig. 5.7	Symmetry boundary conditions[1, 25] of a quadrant of the square plate.....	94
Fig. 5.8	Plots of the membrane and normal stress of Model I, II and CPT displacement model under SS3 boundary condition.....	103
Fig. 5.9	Plots of the center deflection, normal and membrane stress of Model III with that of the FSDT displacement model under SS1 and SS3 boundary conditions.....	106
Fig. 5.10	Post processed quadrant images of the variables in various models, SS3, with converged solution at load parameter $\bar{P} = 250$	107

	Page
Fig. 5.11 Plots of the non-linear membrane stresses of Model III and FSDT displacement model along the $x = 2.5$	108
Fig. 5.12 Plots of the non-linear bending moments of Model III and FSDT displacement model along the $x = 2.5$	109

LIST OF TABLES

		Page
Table 5.1	Comparison of mixed models and displacement based models..	84
Table 5.2	Membrane locking in mixed models and the displacement models.....	87
Table 5.3	Effect of the membrane locking in the mode I and II.....	88
Table 5.4	Effect of the length-to-thickness ratio on the deflections in TBT beam.....	90
Table 5.5	Comparison of the effect of the length-to-thickness ratio in the EBT and the TBT beams.....	90
Table 5.6	Comparison of Model III with other mixed models	92
Table 5.7	Comparison of the linear solution of various CPT Models, isotropic ($\nu = 0.3$) square plate, simple supported (SS1).....	95
Table 5.8	Comparison of the linear solution of various CPT Models, isotropic ($\nu = 0.3$) square plate, clamped (CC).....	96
Table 5.9	Comparison of the CPT linear solution with that of the displacement model, isotropic ($\nu = 0.25$) square plate, simple supported (SS1).....	98
Table 5.10	Comparison of the CPT linear solution with that of the displacement Model, isotropic ($\nu = 0.25$) square plate, clamped(CC).....	98
Table 5.11	Comparison of the current mixed FSDT linear solution with that of the other mixed model (Reddy [7]), with isotropic($\nu = 0.25$, $K_s = 5/6$) square plate, simple supported(SS1).....	99
Table 5.12	Comparison of the linear solution of the FSDT with isotropic ($\nu = 0.25$, $K_s = 5/6$) square plate, simple supported (SS1).....	100
Table 5.13	Effect of reduced integration in Model I and II.....	101
Table 5.14	Comparison of the center deflection and normal stress of Model I and II with the CPT displacement model.....	102
Table 5.15	Comparison of the convergence of Model I, II, III and IV under the SS1 and SS3 boundary conditions.....	104
Table 5.16	Comparison of the center deflection and normal stress of Model III with the FSDT displacement model under SS1 and SS3 boundary conditions.....	105

CHAPTER I

INTRODUCTION

The objective of this study is to investigate the performance of finite element models based on mixed weighted-residual formulations of beams and plates. In particular, the study investigates merits and demerits of the newly developed mixed finite element models of beam and plate bending based on weighted-residual and mixed formulations. The von Karman nonlinear equations[1, 2] of beams and plates[1, 3] are used to develop alternative finite element models to the conventional, displacement-based, finite element models[4]. Once the basic models are developed and critically evaluated in comparison to the conventional, displacement-based, finite element models, they can be extended to other beam and plate structures with proper modifications. For example, the plate bending models can be extended to the laminated composite structures with proper laminate equations[3, 5].

The mixed finite element models of beams and plates were developed more than two decades ago by Putcha and Reddy[6, 7] to overcome the drawbacks of the displacement based models. The basic idea of mixed finite element model is to include more than two different types of fields in the finite element model as independent variables. For example, the bending moment of the beam element can be included as independent variable, in addition to the axial and transverse displacements.

The mixed finite element models[7] developed in past only included bending moments as independent variables to reduce the differentiability of the transverse displacement component[7]. This mixed models can provide the same level of accuracy for the bending moment as that for the displacement fields, whereas in the displacement based model the bending moment is calculated at points other than nodes in the post processing step[1, 4]. Thus, the displacement finite element models cannot provide the same level of accuracy for force-like variables as in the mixed finite element models.

In the present study, mixed finite element models are developed to include other variables (i.e., the membrane forces and shear forces) in addition to the bending moments, and to see the effect of them on the nonlinear analysis. The effect of including other variables will be compared with different mixed models to show the advantage of the one type of model over other models.

For the nonlinear beam bending problems[1, 8], three different mixed models based on the Euler-Bernoulli beam theory[4, 9] and one mixed model based on the Timoshenko beam theory[4, 9] are developed. For the nonlinear plate bending problems, two different mixed models based on the classical plate theory[1, 3] and two mixed models based on the first-order shear deformation plate theory [1, 3] are developed.

To verify the performance of the newly developed finite element models, numerical results of them are compared with those of the existing displacement based finite element models[1, 7]. For each beam bending model, three types of boundary conditions (i.e., clamped-clamped (CC), hinged-hinged (HH), and pined-pined (PP) boundary conditions.) are examined and the results are compared. For plate bending model, three types of boundary conditions (i.e., the simple support I (SS1), the simple support III (SS3), and the clamped (CC) boundary conditions.) are examined and the results are compared with those of the conventional finite element models[1, 7].

For each of the beam models, three different Lagrange type interpolation functions[4, 10] (i.e. linear, quadratic and cubic) are used for the approximation of the variables to see the relations between the degree of interpolation functions and the accuracy of the solutions. For each of the plate bending models, two different Lagrange type interpolation functions[4, 10] (i.e. 4-nodes and 9 nodes) are considered. Then, the post-processed data on the stresses and the moments of the equilibrium state in the various models are compared.

The finite element Models are implemented using Maple 9.5 [11] for the beam bending models and the Fortran [12] for the plates bending problems. All graphs and data are obtained by using the MS Excel and the Matlab 7.1[13].

1.1 Review of Euler-Bernoulli Beam Theory

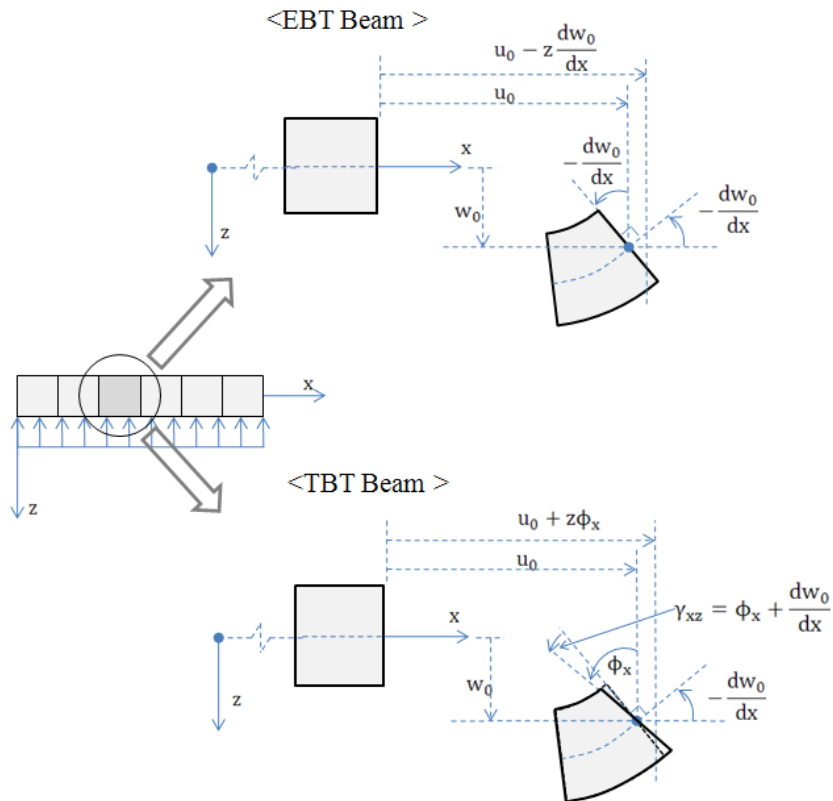


Fig. 1.1 Undeformed and deformed EBT and TBT beams, source from [2].

To develop new nonlinear mixed finite element models of beam bending, the Euler-Bernoulli beam theory and the Timoshenko beam theory are considered. Due to the assumption of moderate rotation[1] of a beam cross section perpendicular to the x -axis, a geometric nonlinearity[1] can be considered for the present study. As a consequence, the nonlinearity only appears as square of the slope (i.e., $(dw_0/dx)^2$) in the formulations. Detailed geometry and characteristics of both beam bending theories can be found in the Fig. 1.1.

1.1.1 Kinematics of EBT

By taking the horizontal axis (i.e., longitudinal direction of the beam) of the beam to be located along the x-axis, and the vertical axis (i.e., direction along the height) to be located along the z-axis, the displacement field[3, 8, 14] of the EBT can be given as follow (see Reddy[1]):

$$\begin{aligned} u_1 &= u_0(x) - z \left(\frac{dw_0(x)}{dx} \right) , \\ u_2 &= 0 , \\ u_3 &= w_0(x) . \end{aligned} \quad (1.1)$$

The von Karman strain[1, 2] associated with the displacement field of the EBT is given as follow:

$$\varepsilon_{xx} = \varepsilon_{xx}^0 + z\varepsilon_{xx}^1 . \quad (1.2)$$

where ε_{xx}^0 and ε_{xx}^1 are defined as

$$\begin{aligned} \varepsilon_{xx}^0 &= \frac{du_0}{dx} + \frac{1}{2} \left(\frac{dw_0}{dx} \right)^2 , \\ \varepsilon_{xx}^1 &= - \frac{d^2w_0}{dx^2} . \end{aligned} \quad (1.3)$$

1.1.2 Equilibriums of EBT

Here, the equilibrium equations[11] of the EBT are derived by using the force and the moment equilibrium of the infinitesimal free body diagram[1] given in the Fig. 1.2. The vertical shear force resultant can be defined only in terms of the bending moment, and certain portion of the membrane force with the nonlinear assumption.

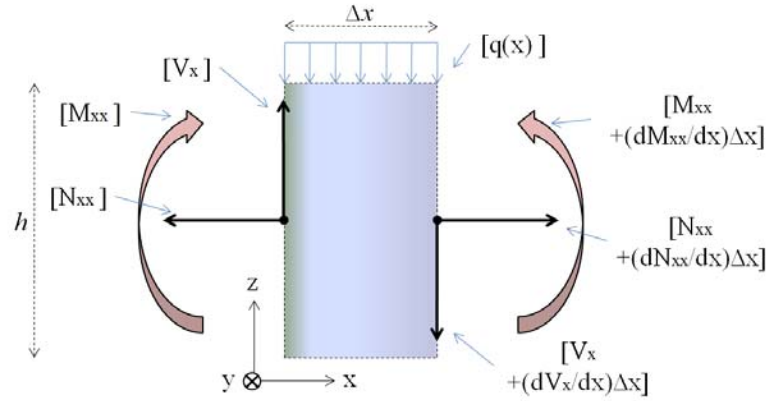


Fig. 1.2 A typical infinitesimal beam element with forces and bending moments.

By Taylor's expansion[15, 16], each of the resultants on the right hand side of the free body diagram (see Fig. 1.2) can be expanded to the left hand side by following equation [15, 17]

$$\begin{aligned}
 R_i(x + \Delta x) &= R_i(x) + \frac{\partial R_i(x)}{\partial x} (\Delta x) + \frac{1}{2!} \frac{\partial^2 R_i(x)}{\partial x^2} (\Delta x)^2 + \dots \\
 &+ \frac{1}{(n-1)!} \frac{\partial^{(n-1)} R_i(x)}{\partial x^{(n-1)}} (\Delta x)^{(n-1)} + \frac{1}{(n)!} \frac{\partial^{(n)} R_i(x)}{\partial x^n} (\Delta x)^{(n)} + \dots , \\
 R_i(x + \Delta x) &= R_i(x) + \frac{\partial R_i(x)}{\partial x} (\Delta x) , \tag{1.4}
 \end{aligned}$$

where $R_i(x)$ is an arbitrary resultant on the left side of the element, and $R_i(x + \Delta x)$ is the associated value on the right side of the element. Then, every term multiplied by $(\Delta x)^2$ from the expansion can be omitted by taking the limit of $\Delta x \rightarrow 0$. Then the x-direction and the z-direction force equilibrium can be obtained as follow:

$$\begin{aligned}
\rightarrow \sum F_x &= -N_{xx} + \left(N_{xx} + \frac{dN_{xx}}{dx} \Delta x \right) + f(x) \Delta x \\
&= \frac{dN_{xx}}{dx} \Delta x + f(x) \Delta x = 0 , \\
\uparrow \sum F_z &= V_x - \left(V_x + \frac{dV_x}{dx} \Delta x \right) - q(x) \Delta x \\
&= \frac{dV_x}{dx} \Delta x + q(x) \Delta x = 0 .
\end{aligned} \tag{1.5}$$

By taking the positive y-direction to be the direction of going through the board, the y-direction moment equilibrium can be written as follow:

$$\begin{aligned}
\curvearrowright \sum M_y &= M_{xx} - \left(M_{xx} + \frac{dM_{xx}}{dx} \Delta x \right) + \left(V_x + \frac{dV_x}{dx} \Delta x \right) \Delta x \\
&\quad - \left(N_{xx} + \frac{dN_{xx}}{dx} \Delta x \right) \left(\frac{dw_0}{dx} \right) \Delta x + q(x) \Delta x \left(\frac{\Delta x}{2} \right) \\
&= \left[-\frac{dM_{xx}}{dx} + V_x + N_{xx} \frac{dw_0}{dx} \right] \Delta x + \left[\frac{dV_x}{dx} + \frac{dN_{xx}}{dx} \frac{dw_0}{dx} + \frac{q(x)}{2} \right] (\Delta x)^2 = 0 .
\end{aligned} \tag{1.6}$$

We can obtain a point equilibrium of the forces and the moment, by dividing above equations by Δx , and taking the limit of $\Delta x \rightarrow 0$. Finally, following equilibrium equations of EBT[1] can be obtained.

$$\begin{aligned}
\frac{dN_{xx}}{dx} + f(x) &= 0 , \\
\frac{dV_x}{dx} + q(x) &= 0 , \\
V_x - \frac{dM_{xx}}{dx} - N_{xx} \frac{dw_0}{dx} &= 0 .
\end{aligned} \tag{1.7}$$

1.1.3 Constitutive Relations and Resultants of EBT

In the present study, the beam is assumed to obey the linear elastic relation, thus the stress of the EBT can be related to the strain by the relation known as Hooke's law, as follow:

$$\sigma_{xx} = E \varepsilon_{xx} . \quad (1.8)$$

The stress and moment resultants[1] can be defined as,

$$\begin{aligned} N_{xx} &= \int_A (\sigma_{xx}) dy dz = EA \left[\frac{du_0}{dx} + \frac{1}{2} \left(\frac{dw_0}{dx} \right)^2 \right] , \\ M_{xx} &= \int_A z(\sigma_{xx}) dy dz = EI \frac{d^2 w_0}{dx^2} , \end{aligned} \quad (1.9)$$

where the A is the cross section area of the beam, the I [1] is the second moment inertia of the cross section (about the y-axis) and the E is the Young's modulus[18, 19] or elastic modulus.

1.2 Review of Timoshenko Beam Theory (TBT)

1.2.1 Kinematics of TBT

By taking the horizontal axis (i.e., longitudinal direction) of the beam to be located along the x-axis and the vertical axis (i.e., direction along the height) along the z-axis, the displacement field [1, 9, 14] of the TBT can be given as follow:

$$\begin{aligned} u_1 &= u_0(x) + z\phi_x(x) , \\ u_2 &= 0 , \\ u_3 &= w_0(x) . \end{aligned} \quad (1.10)$$

Note that instead of the slope of the deformed beam axis (i.e., $-dw_0/dx$), the shear rotation[14] ϕ_x was included to account for the shear rotation of the cross section.

The von Karman strain[1] associated with the displacement field of TBT can be given as follow:

$$\begin{aligned}\varepsilon_{xz} &= \varepsilon_{xz}^0, \\ \varepsilon_{xx} &= \varepsilon_{xx}^0 + z\varepsilon_{xx}^1,\end{aligned}\quad (1.11)$$

where, ε_{xz}^0 , ε_{xx}^0 and ε_{xx}^1 are defined as,

$$\begin{aligned}\varepsilon_{xz}^0 &= \frac{1}{2}\left(\frac{dw_0}{dx} + \phi_x\right), \\ \varepsilon_{xx}^0 &= \frac{du_0}{dx} + \frac{1}{2}\left(\frac{dw_0}{dx}\right)^2, \\ \varepsilon_{xx}^1 &= \frac{d\phi_x}{dx}.\end{aligned}\quad (1.12)$$

1.2.2 Equilibriums of TBT

By substituting the strains into the virtual work statement[8], the equilibrium equations of the TBT can be obtained. By the principle of the virtual work[1, 8], it can be stated, *'if a body is in equilibrium, the total virtual work done by actual internal as well as external forces in moving through their respective virtual displacement is zero'*[1]. It can be expressed by following equation[8],

$$\delta W^e = \delta W_I^e + \delta W_E^e = 0, \quad (1.13)$$

where,

$$\begin{aligned}\delta W_I^e &= \int_{x_a}^{x_b} \left\{ \int_{A^e} [\sigma_{xx}\delta\varepsilon_{xx} + \sigma_{xz}\delta(2\varepsilon_{xz})]dA \right\} dx, \\ \delta W_E^e &= - \left[\int_{x_a}^{x_b} (q\delta w_0 dx) dx + \int_{x_a}^{x_b} (f\delta u_0 dx) dx + \sum_{i=1}^6 Q_i^e \delta\Delta_i^e \right].\end{aligned}$$

Note that Q_i^e are the generalized nodal forces[1] and $\delta\Delta_i^e$ are the virtual generalized nodal displacements[1].

And the virtual strains and the definitions of the resultant forces can be defined as follow:

$$\begin{aligned}
\delta(2\varepsilon_{xz}) &= \left(\frac{d\delta w_0}{dx} + \delta\phi_x \right) , \\
\delta\varepsilon_{xx} &= \left(\frac{d\delta u_0}{dx} + \frac{dw_0}{dx} \frac{d\delta w_0}{dx} \right) + z \frac{d\delta\phi_x}{dx} , \\
N_{xx} &= \int_A (\sigma_{xx}) dydz , \\
Q_x &= \int_A (\sigma_{xz}) dydz , \\
M_{xx} &= \int_A (\sigma_{xx}z) dydz .
\end{aligned} \tag{1.14}$$

By substituting the force resultants, the moment resultants and the virtual strains given in the (1.14) into the (1.13), the following energy equation can be directly obtained.

$$\begin{aligned}
0 &= \delta W_I^e + \delta W_E^e \\
&= \int_{x_a}^{x_b} \left[N_{xx} \left(\frac{d\delta u_0}{dx} + \frac{dw_0}{dx} \frac{d\delta w_0}{dx} \right) + M_{xx} \frac{d\delta\phi_x}{dx} + Q_x \left(\frac{d\delta w_0}{dx} + \delta\phi_x \right) \right] dx \\
&\quad - \int_{x_a}^{x_b} (q\delta w_0) dx - \int_{x_a}^{x_b} (f\delta u_0) dx - \sum_{i=1}^6 Q_i^e \delta\Delta_i^e = 0 .
\end{aligned} \tag{1.15}$$

Then, by collecting the coefficients of the variations of the displacement terms in the (1.15), following equilibrium equations[1, 8] of the TBT can be obtained(for details see Reddy[1]).

$$\begin{aligned}
\delta u_0 &: -\frac{dN_{xx}}{dx} - f(x) = 0 , \\
\delta w_0 &: -\frac{d}{dx} \left(Q_x + N_{xx} \frac{dw_0}{dx} \right) - q(x) = 0 , \\
\delta \phi_x &: -\frac{dM_{xx}}{dx} + Q_x = 0 .
\end{aligned} \tag{1.16}$$

By comparing the equilibrium equations of the EBT given in the (1.7) and the TBT given in the (1.16), it can be shown that the shear resultant V_x of the EBT can be related to the shear resultant Q_x of the TBT by the following equation[1].

$$V_x = Q_x + N_{xx} \frac{dw_0}{dx} . \tag{1.17}$$

Essentially, the equilibrium equations of the EBT and the TBT are the same, but the specific variables involved may have different meanings. In this case, V_x is the shear resultant acting on the plane perpendicular to the x axis, while Q_x is the shear resultant acting on the deformed plane (see Reddy[1]).

1.2.3 Constitutive Relations and Resultants of TBT

Since there are two non-zero strain components in the TBT, we have two stress components from the constitutive relations. By assuming that the beam obeys linear elastic relation, the stresses can be related to strains as follow:

$$\begin{aligned}
\sigma_{xz} &= 2G\varepsilon_{xz} , \\
\sigma_{xx} &= E\varepsilon_{xx} .
\end{aligned} \tag{1.18}$$

The generalized resultant forces can be calculated by the definition given in the (1.14) as follow:

$$\begin{aligned}
 Q_x &= K_s GA \left(\phi_x + \frac{dw_0}{dx} \right) , \\
 N_{xx} &= EA \left[\frac{du_0}{dx} + \frac{1}{2} \left(\frac{dw_0}{dx} \right)^2 \right] , \\
 M_{xx} &= EI \frac{d\phi_x}{dx} ,
 \end{aligned} \tag{1.19}$$

where A is the cross section area of the beam, I is the second moment inertia of the cross section, $K_s (= 5/6)$ is the shear correction factor[14], G is the shear modulus[19] and E is the Young's modulus.

1.3. Review of Classical Plate Theory (CPT)

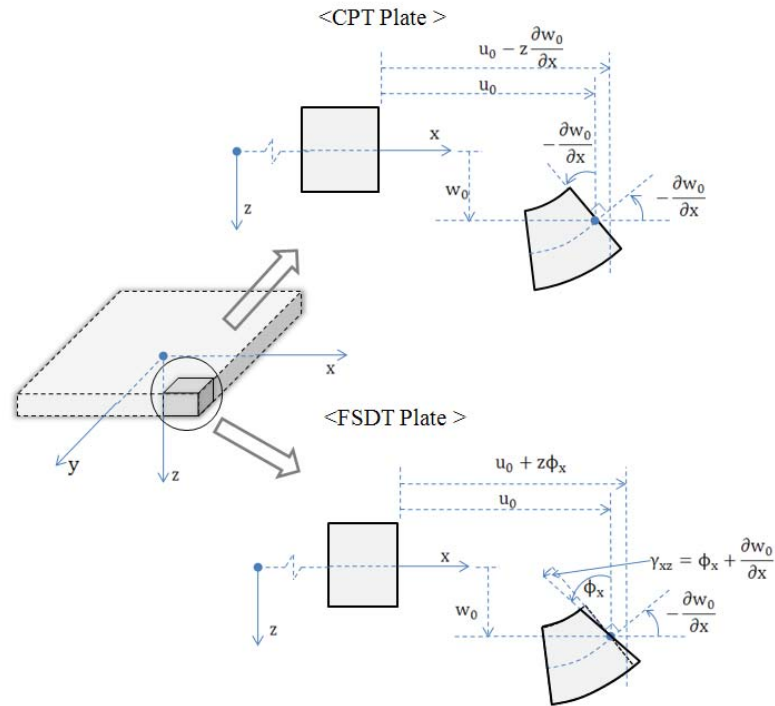


Fig. 1.3 Undeformed and deformed CPT and FSDT plates, source from [2].

The major difference between the CPT and FSDT comes from the displacement field given in the Fig. 1.3.

1.3.1 Kinematics of CPT

The CPT can be considered as an extended 2-D version of the EBT. Thus the displacement field of the CPT is very similar to that of the EBT. The displacement field of the CPT with Kirchhoff hypothesis[1, 3] can be given by,

$$\begin{aligned} u_1 &= u(x, y, z) = u_0(x, y) - z \left(\frac{\partial w_0(x, y)}{\partial x} \right), \\ u_2 &= v(x, y, z) = v_0(x, y) - z \left(\frac{\partial w_0(x, y)}{\partial y} \right), \\ u_3 &= w(x, y, z) = w_0(x, y). \end{aligned} \quad (1.20)$$

And with the assumption[1] of small strain but moderately large rotation, we can simplify the components of the nonlinear strain tensor[20]. Then the components of the strain tensor is given by,

$$\begin{aligned} \varepsilon_{xx} &= \frac{\partial u}{\partial x} + \frac{1}{2} \left(\frac{\partial \mathbf{w}}{\partial x} \right)^2, \\ \varepsilon_{xz} &= \frac{1}{2} \left(\frac{\partial u}{\partial z} + \frac{\partial \mathbf{w}}{\partial x} \right), \\ \varepsilon_{xy} &= \frac{1}{2} \left(\frac{\partial u}{\partial y} + \frac{\partial v}{\partial x} + \frac{\partial \mathbf{w}}{\partial x} \frac{\partial \mathbf{w}}{\partial y} \right), \\ \varepsilon_{yy} &= \frac{\partial v}{\partial y} + \frac{1}{2} \left(\frac{\partial \mathbf{w}}{\partial y} \right)^2, \\ \varepsilon_{yz} &= \frac{1}{2} \left(\frac{\partial v}{\partial z} + \frac{\partial \mathbf{w}}{\partial y} \right), \\ \varepsilon_{zz} &= \frac{\partial w}{\partial z}. \end{aligned} \quad (1.21)$$

By substituting the displacement field described in the (1.20) into the components of the strain tensor given in the (1.21), the following specific von Karman nonlinear strains[1] of the CPT can be obtained.

$$\begin{aligned}
\varepsilon_{xx} &= \frac{\partial u_0}{\partial x} + \frac{1}{2} \left(\frac{\partial w_0}{\partial x} \right)^2 - z \frac{\partial^2 w_0}{\partial x^2}, \\
\varepsilon_{yy} &= \frac{\partial v_0}{\partial y} + \frac{1}{2} \left(\frac{\partial w_0}{\partial y} \right)^2 - z \frac{\partial^2 w_0}{\partial y^2}, \\
\varepsilon_{xy} &= \frac{1}{2} \left(\frac{\partial u_0}{\partial y} + \frac{\partial v_0}{\partial x} + \frac{\partial w_0}{\partial x} \frac{\partial w_0}{\partial y} - 2z \frac{\partial^2 w_0}{\partial x \partial y} \right).
\end{aligned} \tag{1.22}$$

1.3.2 Equilibriums of CPT

The CPT can be derived by using vector approach[11] with the infinitesimal free diagram of the Fig. 1.4. Since it is assumed that the plane stress condition is still valid for the in-plane forces, the x, y and z-direction force equilibriums and x and y-direction moment equilibriums of the infinitesimal plate element[3] can be stated by using the generalized force resultants, as described in the (1.23a to e).

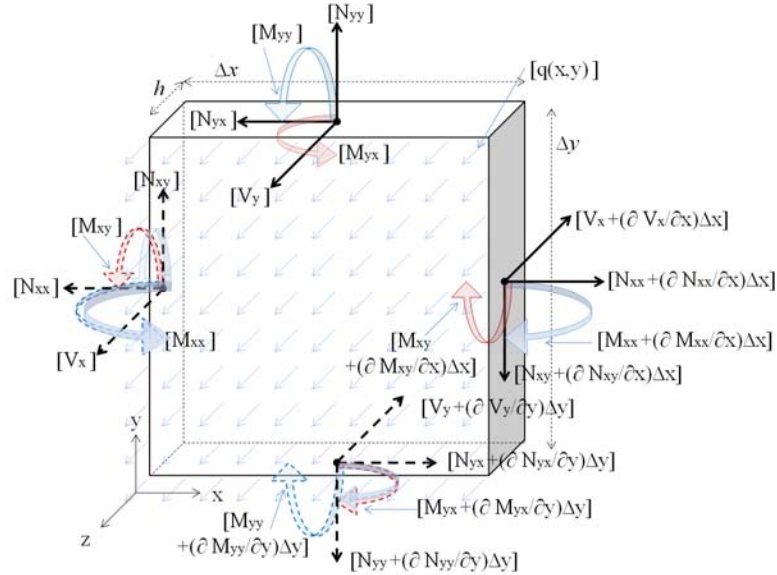


Fig. 1.4 A typical 2-D plate element[3] with forces and moments.

With the Taylor's expansion given in the (1.4), we can set the equilibriums of the forces and the moments in the given directions, as follow:

The x-direction force equilibrium:

$$\begin{aligned}
 \rightarrow \sum F_x &= \left[(N_{xx}) \times \Delta y - \left(N_{xx} + \frac{\partial N_{xx}}{\partial x} \Delta x \right) \times \Delta y \right] \\
 &\quad + \left[(N_{xy}) \times \Delta x - \left(N_{xy} + \frac{\partial N_{xy}}{\partial y} \Delta y \right) \times \Delta x \right] \\
 &= \left(\frac{\partial N_{xx}}{\partial x} + \frac{\partial N_{xy}}{\partial y} \right) \Delta x \Delta y = 0.
 \end{aligned} \tag{1.23a}$$

The y-direction force equilibrium:

$$\begin{aligned}
 \uparrow \sum F_y &= \left[(N_{yy}) \times \Delta x - \left(N_{yy} + \frac{\partial N_{yy}}{\partial y} \Delta y \right) \times \Delta x \right] \\
 &\quad + \left[(N_{xy}) \times \Delta y - \left(N_{xy} + \frac{\partial N_{xy}}{\partial x} \Delta x \right) \times \Delta y \right] \\
 &= \left(\frac{\partial N_{xy}}{\partial x} + \frac{\partial N_{yy}}{\partial y} \right) \Delta x \Delta y = 0.
 \end{aligned} \tag{1.23b}$$

The z-direction force equilibrium:

$$\begin{aligned}
 \sphericalangle \sum F_z &= \left[(V_x) \times \Delta y - \left(V_x + \frac{\partial V_x}{\partial x} \Delta x \right) \times \Delta y \right] \\
 &\quad + \left[(V_y) \times \Delta x - \left(V_y + \frac{\partial V_y}{\partial y} \Delta y \right) \times \Delta x \right] + [q(x, y) \times \Delta x \times \Delta y] \\
 &= \left(\frac{\partial V_x}{\partial x} + \frac{\partial V_y}{\partial y} + q(x) \right) \Delta x \Delta y = 0.
 \end{aligned} \tag{1.23c}$$

In the force equilibriums of the CPT, it is assumed that the plate is in the plane stress condition[18] for the in-plane forces. So by including some portion of in-plane

forces only for moment equilibriums, following equations of moment equilibrium can be obtained.

The y-direction moment equilibrium:

$$\begin{aligned}
\curvearrowright \sum M_x &= \left[(M_{xx}) - \left(M_{xx} + \frac{\partial M_{xx}}{\partial x} \Delta x \right) \right] \times \Delta y + \left[(M_{yx}) - \left(M_{yx} + \frac{\partial M_{yx}}{\partial y} \Delta y \right) \right] \\
&\quad \times \Delta x \\
&\quad - \left\{ - \left(V_x + \frac{\partial V_x}{\partial x} \Delta x \right) + \left[\left(N_{xx} + \frac{\partial N_{xx}}{\partial x} \Delta x \right) \times \frac{\partial w_0}{\partial x} \right] \right. \\
&\quad \left. + \left[\left(N_{xy} + \frac{\partial N_{xy}}{\partial x} \Delta x \right) \times \frac{\partial w_0}{\partial y} \right] \right\} \times \Delta y \times \Delta x \\
&\quad - \left[q(x, y) \times \Delta y \Delta x \left(\frac{\Delta x}{2} \right) \right] \\
&= \left(- \frac{\partial M_{xx}}{\partial x} - \frac{\partial M_{xy}}{\partial y} + V_x - N_{xx} \frac{\partial w_0}{\partial x} - N_{xy} \frac{\partial w_0}{\partial y} \right) \Delta x \Delta y \\
&\quad + \left(\frac{\partial V_x}{\partial x} \Delta x - \frac{\partial N_{xx}}{\partial x} \frac{\partial w_0}{\partial x} \Delta x - \frac{\partial N_{xy}}{\partial y} \frac{\partial w_0}{\partial y} \Delta y - q(x, y) \frac{\Delta x}{2} \right) \Delta x \Delta y = 0. \quad (1.23d)
\end{aligned}$$

The x-direction moment equilibrium:

$$\begin{aligned}
\curvearrowleft \sum M_y &= \left[(M_{yy}) - \left(M_{yy} + \frac{\partial M_{yy}}{\partial y} \Delta y \right) \right] \times \Delta x + \left[(M_{xy}) - \left(M_{xy} + \frac{\partial M_{xy}}{\partial x} \Delta x \right) \right] \\
&\quad \times \Delta y \\
&\quad - \left\{ - \left(V_y + \frac{\partial V_y}{\partial y} \Delta y \right) + \left[\left(N_{yy} + \frac{\partial N_{yy}}{\partial y} \Delta y \right) \times \left(\frac{\partial w_0}{\partial y} \right) \right] \right. \\
&\quad \left. + \left[\left(N_{yx} + \frac{\partial N_{yx}}{\partial y} \Delta y \right) \times \left(\frac{\partial w_0}{\partial x} \right) \right] \right\} \Delta x \Delta y \\
&\quad - \left[q(x, y) \times \Delta y \Delta x \left(\frac{\Delta y}{2} \right) \right] \\
&= \left(- \frac{\partial M_{yy}}{\partial y} - \frac{\partial M_{xy}}{\partial x} + V_y - N_{yy} \frac{\partial w_0}{\partial y} - N_{xy} \frac{\partial w_0}{\partial x} \right) \Delta x \Delta y \\
&\quad + \left(\frac{\partial V_y}{\partial y} \Delta y - \frac{\partial N_{yy}}{\partial y} \frac{\partial w_0}{\partial y} \Delta y - \frac{\partial N_{yx}}{\partial x} \frac{\partial w_0}{\partial x} \Delta x - q(x, y) \frac{\Delta y}{2} \right) \Delta x \Delta y = 0. \quad (1.23e)
\end{aligned}$$

1.3.3 Constitutive Relations and Resultants of CPT

In the present plate bending problem, it is assumed that every in-plane stress and strain remain plane stress[18] condition. For the orthotropic plane stress condition, the constitutive relations of stresses and strains can be given in the matrix form equation as follow:

$$\begin{Bmatrix} \sigma_{xx} \\ \sigma_{yy} \\ \sigma_{xy} \end{Bmatrix} = \begin{bmatrix} Q_{11} & Q_{12} & 0 \\ Q_{12} & Q_{22} & 0 \\ 0 & 0 & Q_{66} \end{bmatrix} \begin{Bmatrix} \varepsilon_{xx} \\ \varepsilon_{yy} \\ 2\varepsilon_{xy} \end{Bmatrix}, \quad (1.24)$$

where the components of the matrix $[Q]$ are given by,

$$\begin{aligned} Q_{11} &= \frac{E_1}{1 - \nu_{12}\nu_{21}}, & Q_{12} &= \frac{\nu_{12}E_2}{1 - \nu_{12}\nu_{21}} = \frac{\nu_{21}E_1}{1 - \nu_{12}\nu_{21}}, \\ Q_{22} &= \frac{E_2}{1 - \nu_{12}\nu_{21}}, & Q_{66} &= G_{12}. \end{aligned} \quad (1.25)$$

Note E_1 and E_2 are the elastic modulus [19] of the x and y-direction respectively, ν_{12} and ν_{21} are the Poisson's ratio and the G_{12} is the shear modulus.

By dividing the (1.23a to e) by $(\Delta x \Delta y)$, and taking the limit of $\Delta x, \Delta y \rightarrow 0$, the following equilibrium equations of the CPT can be obtained.

$$\begin{aligned} -\frac{\partial N_{xx}}{\partial x} - \frac{\partial N_{xy}}{\partial y} &= 0, \\ -\frac{\partial N_{xy}}{\partial x} - \frac{\partial N_{yy}}{\partial y} &= 0, \\ -\frac{\partial V_x}{\partial x} - \frac{\partial V_y}{\partial y} - q(x) &= 0, \\ V_x - \left(\frac{\partial M_{xx}}{\partial x} + \frac{\partial M_{xy}}{\partial y} + N_{xx} \frac{\partial w_0}{\partial x} + N_{xy} \frac{\partial w_0}{\partial y} \right) &= 0, \\ V_y - \left(\frac{\partial M_{xy}}{\partial x} + \frac{\partial M_{yy}}{\partial y} + N_{xy} \frac{\partial w_0}{\partial x} + N_{yy} \frac{\partial w_0}{\partial y} \right) &= 0. \end{aligned} \quad (1.26)$$

By locating the x axis along the mid-plane of the plate element, the resultants of the CPT can be defined by the following equations.

$$\begin{cases} N_{xx} \\ N_{yy} \\ N_{xy} \end{cases} = \int_{-\frac{h}{2}}^{\frac{h}{2}} \begin{cases} \sigma_{xx} \\ \sigma_{yy} \\ \sigma_{xy} \end{cases} dz ,$$

$$\begin{cases} M_{xx} \\ M_{yy} \\ M_{xy} \end{cases} = \int_{-\frac{h}{2}}^{\frac{h}{2}} \begin{cases} \sigma_{xx} \\ \sigma_{yy} \\ \sigma_{xy} \end{cases} z dz . \quad (1.27)$$

By using the constitutive relations given in the (1.25) and the definitions of the resultants given in the (1.26), the following equations of the resultants can be obtained.

$$\begin{aligned} N_{xx} &= A_{11} \left[\frac{\partial u_0}{\partial x} + \frac{1}{2} \left(\frac{\partial w_0}{\partial x} \right)^2 \right] + A_{12} \left[\frac{\partial v_0}{\partial y} + \frac{1}{2} \left(\frac{\partial w_0}{\partial y} \right)^2 \right], \\ N_{yy} &= A_{12} \left[\frac{\partial u_0}{\partial x} + \frac{1}{2} \left(\frac{\partial w_0}{\partial x} \right)^2 \right] + A_{22} \left[\frac{\partial v_0}{\partial y} + \frac{1}{2} \left(\frac{\partial w_0}{\partial y} \right)^2 \right], \\ N_{xy} &= A_{66} \left(\frac{\partial u_0}{\partial y} + \frac{\partial v_0}{\partial x} + \frac{\partial w_0}{\partial x} \frac{\partial w_0}{\partial y} \right), \\ M_{xx} &= -D_{11} \left(\frac{\partial^2 w_0}{\partial x^2} \right) - D_{12} \left(\frac{\partial^2 w_0}{\partial y^2} \right), \\ M_{yy} &= -D_{12} \left(\frac{\partial^2 w_0}{\partial x^2} \right) - D_{22} \left(\frac{\partial^2 w_0}{\partial y^2} \right), \\ M_{xy} &= -2D_{66} \left(\frac{\partial^2 w_0}{\partial x \partial y} \right) , \end{aligned} \quad (1.28)$$

The matrix $[A]$ and $[D]$ can be defined by,

$$(A_{ij}, D_{ij}) = \int_{-h/2}^{h/2} Q_{ij}(1, z) dz. \quad (1.29)$$

where $i, j = 1, 2, 6$.

1.4. Review of First Order Shear Deformation Theory (FSDT)

The FSDT can be considered as 2-D version of the TBT, as the CPT can be said to be the 2-D version of the EBT. In the FSDT the same nonlinearity used in the CPT is assumed. Thus the components of the strain tensor given in the (1.21) can be used to obtain the specific strains of the FSDT.

1.4.1 Kinematics of FSDT

The displacement field[3] of the FSDT with Kirchhoff hypothesis can be given by (see Reddy[1, 3] for details),

$$\begin{aligned} u_1 &= u(x, y, z) = u_0(x, y) + z\phi_x(x, y) , \\ u_2 &= v(x, y, z) = v_0(x, y) + z\phi_y(x, y) , \\ u_3 &= w_0(x, y) . \end{aligned} \tag{1.30}$$

By substituting the displacement field of the FSDT given in the (1.30) into components of the strain tensor given in the (1.21), strains[1] of the FSDT can be given by,

$$\begin{aligned} \varepsilon_{xx} &= \frac{\partial u_0}{\partial x} + \frac{1}{2} \left(\frac{\partial w_0}{\partial x} \right)^2 + z \frac{\partial \phi_x}{\partial x} , \\ \varepsilon_{yy} &= \frac{\partial v_0}{\partial y} + \frac{1}{2} \left(\frac{\partial w_0}{\partial y} \right)^2 + z \frac{\partial \phi_y}{\partial y} , \\ \varepsilon_{xy} &= \frac{1}{2} \left[\frac{\partial u_0}{\partial y} + \frac{\partial v_0}{\partial x} + \frac{\partial w_0}{\partial x} \frac{\partial w_0}{\partial y} + z \left(\frac{\partial \phi_x}{\partial y} + \frac{\partial \phi_y}{\partial x} \right) \right] , \\ \varepsilon_{xz} &= \frac{\partial w_0}{\partial x} + \phi_x , \\ \varepsilon_{yz} &= \frac{\partial w_0}{\partial y} + \phi_y . \end{aligned} \tag{1.31}$$

1.4.2 Equilibriums of FSDT

The equilibrium equations of the FSDT can be derived using the virtual work statement (see Reddy[1] for details), with strains given in the (1.31). The equilibrium equations[3] of the FSDT can be given by

$$\begin{aligned}
 -\frac{\partial N_{xx}}{\partial x} - \frac{\partial N_{xy}}{\partial y} &= 0 , \\
 -\frac{\partial N_{xy}}{\partial x} - \frac{\partial N_{yy}}{\partial y} &= 0 , \\
 \frac{\partial}{\partial x} \left(N_{xx} \frac{\partial w_0}{\partial x} + N_{xy} \frac{\partial w_0}{\partial y} + Q_x \right) + \frac{\partial}{\partial y} \left(N_{xy} \frac{\partial w_0}{\partial x} + N_{yy} \frac{\partial w_0}{\partial y} + Q_y \right) + q(x) &= 0 , \\
 Q_x - \left(\frac{\partial M_{xx}}{\partial x} + \frac{\partial M_{xy}}{\partial y} \right) &= 0 , \\
 Q_y - \left(\frac{\partial M_{xy}}{\partial x} + \frac{\partial M_{yy}}{\partial y} \right) &= 0 .
 \end{aligned} \tag{1.32}$$

In the part 1.1, the shear resultant V_x of the EBT was related to the shear resultant Q_x of the TBT by the relation given in the (1.17). In similar sense, the shear resultants of the CPT can be related to that of the FSDT by the following equations by comparing the equilibrium equations of the CPT and that of the FSDT.

$$\begin{aligned}
 V_x &= Q_x + \left(N_{xx} \frac{\partial w_0}{\partial x} + N_{xy} \frac{\partial w_0}{\partial y} \right) , \\
 V_y &= Q_y + \left(N_{xy} \frac{\partial w_0}{\partial x} + N_{yy} \frac{\partial w_0}{\partial y} \right) .
 \end{aligned} \tag{1.33}$$

1.4.3 Constitutive Relations and Resultants of FSDT

The FSDT has two more non-zero strains compared with the strains of the CPT. Additional strains of the FSDT can be related to the corresponding stress components by

$$\begin{Bmatrix} \sigma_{yz} \\ \sigma_{xz} \end{Bmatrix} = \begin{bmatrix} Q_{44} & 0 \\ 0 & Q_{55} \end{bmatrix} \begin{Bmatrix} 2\varepsilon_{yz} \\ 2\varepsilon_{xz} \end{Bmatrix} , \tag{1.34}$$

where Q_{44} and Q_{55} are the shear modulus G_{23} and G_{13} respectively.

In addition to the in-plane stresses and strains relations given in the (1.24), we have the following additional relations between the shear stresses and the shear resultants of the FSDT, which can be defined by

$$\begin{Bmatrix} Q_y \\ Q_x \end{Bmatrix} = \int_{-\frac{h}{2}}^{\frac{h}{2}} \begin{Bmatrix} \sigma_{yz} \\ \sigma_{xz} \end{Bmatrix} dz . \quad (1.35)$$

By substituting the constitutive relations given in the (1.24) and (1.34) into the definitions of the resultant forces given in the (1.27) and (1.35), the following equations of the resultants[3] of the FSDT can be obtained.

$$\begin{aligned} N_{xx} &= A_{11} \left[\frac{\partial u_0}{\partial x} + \frac{1}{2} \left(\frac{\partial w_0}{\partial x} \right)^2 \right] + A_{12} \left[\frac{\partial v_0}{\partial y} + \frac{1}{2} \left(\frac{\partial w_0}{\partial y} \right)^2 \right], \\ N_{yy} &= A_{12} \left[\frac{\partial u_0}{\partial x} + \frac{1}{2} \left(\frac{\partial w_0}{\partial x} \right)^2 \right] + A_{22} \left[\frac{\partial v_0}{\partial y} + \frac{1}{2} \left(\frac{\partial w_0}{\partial y} \right)^2 \right], \\ N_{xy} &= A_{66} \left(\frac{\partial u_0}{\partial y} + \frac{\partial v_0}{\partial x} + \frac{\partial w_0}{\partial x} \frac{\partial w_0}{\partial y} \right), \\ Q_x &= K_s A_{55} \left(\frac{\partial w_0}{\partial x} + \phi_x \right) \\ Q_y &= K_s A_{44} \left(\frac{\partial w_0}{\partial y} + \phi_y \right) \\ M_{xx} &= D_{11} \left(\frac{\partial \phi_x}{\partial x} \right) + D_{12} \left(\frac{\partial \phi_y}{\partial y} \right), \\ M_{yy} &= D_{12} \left(\frac{\partial \phi_x}{\partial x} \right) + D_{22} \left(\frac{\partial \phi_y}{\partial y} \right), \\ M_{xy} &= D_{66} \left(\frac{\partial \phi_x}{\partial y} + \frac{\partial \phi_y}{\partial x} \right), \end{aligned} \quad (1.36)$$

where, $K_s (= 5/6)$ is the shear correction factor[1] and $(A_{ij}, D_{ij}) = \int_{-\frac{h}{2}}^{\frac{h}{2}} (1, z) Q_{ij} dz$ (see the (1.25) and (1.34) for the specific values of the Q_{ij}).

CHAPTER II

DEVELOPMENT OF BEAM BENDING MODELS

In this chapter development of various types of the nonlinear mixed finite element models of the beam bending problem is discussed. In current models, force like physical variables are included as independent nodal variables with proper weighted residual statements[4]. Four different nonlinear mixed finite element models of beam bending are developed for the numerical analysis. The relation between the participation of a typical variable and the accuracy of the linear and the nonlinear solutions are investigated in the chapter V. To clarify the developing procedure the governing equations of the EBT and the TBT were brought from the chapter I.

- Governing equations of the EBT

$$\begin{aligned} \frac{dN_{xx}}{dx} + f(x) &= 0 \quad , \\ \frac{dV_x}{dx} + q(x) &= 0 \quad , \\ V_x - \frac{dM_{xx}}{dx} - N_{xx} \frac{dw_0}{dx} &= 0 \quad . \end{aligned} \tag{1.7}$$

$$\begin{aligned} N_{xx} &= EA \left[\frac{du_0}{dx} + \frac{1}{2} \left(\frac{dw_0}{dx} \right)^2 \right] , \\ M_{xx} &= -EI \frac{d^2w_0}{dx^2} . \end{aligned} \tag{1.9}$$

- Governing equations of the TBT

$$\begin{aligned} \delta u_0 : -\frac{dN_{xx}}{dx} - f(x) &= 0 \quad , \\ \delta w_0 : -\frac{d}{dx} \left(Q_x + N_{xx} \frac{dw_0}{dx} \right) - q(x) &= 0 \quad , \\ \delta \phi_x : -\frac{dM_{xx}}{dx} + Q_x &= 0 \quad . \end{aligned} \tag{1.16}$$

$$\begin{aligned}
N_{xx} &= EA \left[\frac{du_0}{dx} + \frac{1}{2} \left(\frac{dw_0}{dx} \right)^2 \right], \\
Q_x &= K_s GA \left(\phi_x + \frac{dw_0}{dx} \right), \\
M_{xx} &= EI \frac{d\phi_x}{dx}.
\end{aligned} \tag{1.19}$$

2.1 Model I of Beam Bending

2.1.1 Weighted Residual Statements of Model I

The governing equations of the EBT which were derived in the chapter I are used to develop the Model I of beam bending. The displacements (i.e., u_0 and w_0) and generalized forces (i.e., N_{xx} , V_x and M_{xx}) are included as independent variables in the beam bending Model I. By using the equilibrium equation and the resultant equations of the EBT, following weighted residual statements can be made.

$$\begin{aligned}
0 &= \int_{x_a}^{x_b} \left(\frac{d\bar{W}_1}{dx} N_{xx}^a - \bar{W}_1 f(x) \right) dx - \bar{W}_1(x_a) N_1 - \bar{W}_1(x_b) N_2 \\
0 &= \int_{x_a}^{x_b} \left(\frac{d\bar{W}_2}{dx} V_x^a - \bar{W}_2 q(x) \right) dx - \bar{W}_2(x_a) V_1 - \bar{W}_2(x_b) V_2 \\
0 &= \int_{x_a}^{x_b} \bar{W}_3 \left\{ -N_{xx}^a + EA \left[\frac{du_0^a}{dx} + \frac{1}{2} \left(\frac{dw_0^a}{dx} \right)^2 \right] \right\} dx \\
0 &= \int_{x_a}^{x_b} \bar{W}_4 \left(-V_x^a + \frac{dM_{xx}^a}{dx} + N_{xx}^a \frac{dw_0^a}{dx} \right) dx \\
0 &= \int_{x_a}^{x_b} \left(-\frac{\bar{W}_5 M_{xx}^a}{EI} + \frac{d\bar{W}_5}{dx} \frac{dw_0^a}{dx} \right) dx - \bar{W}_5(x_a) \theta_1 - \bar{W}_5(x_b) \theta_2
\end{aligned} \tag{2.1}$$

where,

$$N_1 = -N_{xx}(x_a), \quad N_2 = N_{xx}(x_b),$$

$$V_1 = -V_x(x_a), \quad V_2 = V_x(x_b),$$

$$\theta_1 = \frac{dw_0(x_a)}{dx} \quad \text{and} \quad \theta_2 = -\frac{dw_0(x_b)}{dx}.$$

Note that variables with superscripted 'a' (i.e., $u_0^a, w_0^a, N_{xx}^a, V_x^a$ and M_{xx}^a) denote approximated variables, $\bar{W}_i (i = 1, \dots, 5)$ denotes the i^{th} weight function of the i^{th} weighted residual statement. x_a and x_b are the global coordinates of element region. The boundary terms in the first, the second, and the third equations can be obtained by conducting the integration by parts[4] of the related terms.

2.1.2 Finite Element Equations of Model I

Next, with the weighted residual statements given in the (2.1), the variables can be approximated with the proper interpolation functions. Compared with the EBT displacement based model[1] whose variable (i.e., vertical displacement) should be approximated with the Hermite interpolation functions[1, 4], the model I allows the use of the Lagrange interpolation functions for the approximation of all variables of it, because weighted residual statements do not include any derivative of variable as primary variable.

$$\begin{aligned}
 u_0 &\cong u_0^a = \sum_{j=1}^m \psi_j^{u_0} \mathbb{U}_j, & \bar{W}_1 &= \psi_i^{u_0}, \\
 w_0 &\cong w_0^a = \sum_{j=1}^n \psi_j^{w_0} \mathbb{W}_j, & \bar{W}_2 &= \psi_i^{w_0}, \\
 N_{xx} &\cong N_{xx}^a = \sum_{j=1}^p \psi_j^{N_{xx}} \mathbb{N}_j, & \bar{W}_3 &= \psi_i^{N_{xx}}, \\
 V_x &\cong V_x^a = \sum_{j=1}^q \psi_j^{V_x} \mathbb{V}_j, & \bar{W}_4 &= \psi_i^{V_x}, \\
 M_{xx} &\cong M_{xx}^a = \sum_{j=1}^r \psi_j^{M_{xx}} \mathbb{M}_j, & \bar{W}_5 &= \psi_i^{M_{xx}}.
 \end{aligned} \tag{2.2}$$

By observing the boundary terms in the (2.1) which are produced by integration by parts with the chosen weight functions in the (2.2), the primary variables and the secondary variables can be specified as follow:

<The primary variable>	<The secondary variable>
$\bar{W}_1 \approx u_0$	N_{xx}
$\bar{W}_2 \approx w_0$	V_x
$\bar{W}_5 \approx M_{xx}$	$\frac{dw_0}{dx}$

By substituting the (2.2) into the (2.1), the following nonlinear mixed finite element equations can be obtained.

$$\begin{aligned}
& \sum_{j=1}^p \left[\int_{x_a}^{x_b} \left(\frac{d\psi_i^{u_0}}{dx} \psi_j^{N_{xx}} \right) dx \right] \mathbb{N}_j - \int_{x_a}^{x_b} \left(\psi_i^{u_0} f(x) \right) dx - \psi_i^{u_0}(x_a) N_1 - \psi_i^{u_0}(x_b) N_2 = 0 \quad , \\
& \sum_{j=1}^q \left[\int_{x_a}^{x_b} \left(\frac{d\psi_i^{w_0}}{dx} \psi_j^{V_x} \right) dx \right] \mathbb{V}_j - \int_{x_a}^{x_b} \left(\psi_i^{w_0} q(x) \right) dx - \psi_i^{w_0}(x_a) V_1 - \psi_i^{w_0}(x_b) V_2 = 0 \quad , \\
& \sum_{j=1}^p \left[\int_{x_a}^{x_b} \left(-\frac{\psi_i^{N_{xx}} \psi_j^{N_{xx}}}{EA} \right) dx \right] \mathbb{N}_j + \sum_{j=1}^m \left[\int_{x_a}^{x_b} \left(\psi_i^{N_{xx}} \frac{d\psi_j^{u_0}}{dx} \right) dx \right] \mathbb{W}_j \\
& \quad + \sum_{j=1}^n \left[\int_{x_a}^{x_b} \left(\frac{1}{2} \frac{d\mathbf{w}_0^a}{dx} \psi_i^{N_{xx}} \frac{d\psi_j^{w_0}}{dx} \right) dx \right] \mathbb{W}_j = 0 \quad , \\
& \sum_{j=1}^q \left[\int_{x_a}^{x_b} \left(-\psi_i^{V_x} \psi_j^{V_x} \right) dx \right] \mathbb{V}_j + \sum_{j=1}^r \left[\int_{x_a}^{x_b} \left(\psi_i^{V_x} \frac{d\psi_j^{M_{xx}}}{dx} \right) dx \right] \mathbb{M}_j \\
& \quad + \sum_{j=1}^p \left[\int_{x_a}^{x_b} \left(\frac{d\mathbf{w}_0^g}{dx} \psi_i^{V_x} \psi_j^{N_{xx}} \right) dx \right] \mathbb{N}_j = 0 \quad , \\
& \sum_{j=1}^r \left[\int_{x_a}^{x_b} \left(-\frac{\psi_i^{M_{xx}} \psi_j^{M_{xx}}}{EI} \right) dx \right] \mathbb{M}_j + \sum_{j=1}^n \left[\int_{x_a}^{x_b} \left(\frac{d\psi_i^{M_{xx}}}{dx} \frac{d\psi_j^{w_0}}{dx} \right) dx \right] \mathbb{W}_j \\
& \quad - \psi_i^{M_{xx}}(x_a) \theta_1 - \psi_i^{M_{xx}}(x_b) \theta_1 = 0 \quad .
\end{aligned} \tag{2.3}$$

Note that the boldface letters are used to indicate nonlinear terms. Above mixed finite element equations can be rewritten as algebraic matrix form by collecting coefficients of the unknowns in the form of the coefficient matrix $[K]$ and the rest of the terms as the force vector $\{F\}$ [4] as follow:

$$\begin{aligned}
& [K^e(\{U^e\})]\{U^e\} = \{F^e\} \\
& = \begin{bmatrix} [K^{11}] & [K^{12}] & [K^{13}] & [K^{14}] & [K^{15}] \\ [K^{21}] & [K^{22}] & [K^{23}] & [K^{24}] & [K^{25}] \\ [K^{31}] & [K^{32}] & [K^{33}] & [K^{34}] & [K^{35}] \\ [K^{41}] & [K^{42}] & [K^{43}] & [K^{44}] & [K^{45}] \\ [K^{51}] & [K^{52}] & [K^{53}] & [K^{54}] & [K^{55}] \end{bmatrix} \begin{Bmatrix} \{\mathbb{U}_j\} \\ \{\mathbb{W}_j\} \\ \{\mathbb{N}_j\} \\ \{\mathbb{V}_j\} \\ \{\mathbb{M}_j\} \end{Bmatrix} = \begin{Bmatrix} \{F^1\} \\ \{F^2\} \\ \{F^3\} \\ \{F^4\} \\ \{F^5\} \end{Bmatrix} . \quad (2.4)
\end{aligned}$$

where, the $[K^e(\{U^e\})]$ of the equation denotes that the coefficient matrix $[K]$ is the function of the unknowns $\{U^e\}$.

The sub-matrices and the specific terms of the force vectors are given as follow:

$$\begin{aligned}
[K^{13}] &= \int_{x_a}^{x_b} \left(\frac{d\psi_i^{u_0}}{dx} \psi_j^{N_{xx}} \right) dx , & [K^{24}] &= \int_{x_a}^{x_b} \left(\frac{d\psi_i^{w_0}}{dx} \psi_j^{V_x} \right) dx , \\
[K^{31}] &= \int_{x_a}^{x_b} \left(\psi_i^{N_{xx}} \frac{d\psi_j^{u_0}}{dx} \right) dx , & [K^{32}] &= \int_{x_a}^{x_b} \left(\frac{1}{2} \frac{d\mathbf{w}_0^a}{dx} \psi_i^{N_{xx}} \frac{d\psi_j^{w_0}}{dx} \right) dx , \\
[K^{33}] &= \int_{x_a}^{x_b} \left(-\frac{\psi_i^{N_{xx}} \psi_j^{N_{xx}}}{EA} \right) dx , & [K^{43}] &= \int_{x_a}^{x_b} \left(\frac{d\mathbf{w}_0^a}{dx} \psi_i^{V_x} \psi_j^{N_{xx}} \right) dx , \\
[K^{44}] &= \int_{x_a}^{x_b} \left(-\psi_i^{V_x} \psi_j^{V_x} \right) dx , & [K^{45}] &= \int_{x_a}^{x_b} \left(\psi_i^{V_x} \frac{d\psi_j^{M_{xx}}}{dx} \right) dx , \\
[K^{55}] &= \int_{x_a}^{x_b} \left(-\frac{\psi_i^{M_{xx}} \psi_j^{M_{xx}}}{EI} \right) dx , & [K^{52}] &= \int_{x_a}^{x_b} \left(\frac{d\psi_i^{M_{xx}}}{dx} \frac{d\psi_j^{w_0}}{dx} \right) dx , \\
\{F^1\} &= \int_{x_a}^{x_b} \left(\psi_i^{u_0} f(x) \right) dx + \psi_i^{u_0}(x_a) N_1 + \psi_i^{u_0}(x_b) N_2 , \\
\{F^2\} &= \int_{x_a}^{x_b} \left(\psi_i^{w_0} q(x) \right) dx + \psi_i^{w_0}(x_a) V_1 + \psi_i^{w_0}(x_b) V_2 , \\
\{F^5\} &= \psi_i^{M_{xx}}(x_a) \theta_1 + \psi_i^{M_{xx}}(x_b) \theta_1 . \quad (2.5)
\end{aligned}$$

All the sub-matrices and the force vectors which are not specified in the (2.5) are zero.

2.2 Model II of Beam Bending

The governing equations of the EBT which were derived in the chapter I can be also used for the development of the Model II. The Model II includes displacements (i.e., u_0 and w_0) and the generalized resultants (i.e., N_{xx} and M_{xx}), while the Model I included V_x in addition to those. Thus total number of the independent variables is 4 in the Model II. By eliminating the shear resultant V_x from the governing equations of the EBT, following equations can be obtained.

$$\begin{aligned}
\frac{dN_{xx}}{dx} + f(x) &= 0 \quad , \\
\frac{d}{dx} \left(\frac{dM_{xx}}{dx} + N_{xx} \frac{dw_0}{dx} \right) + q(x) &= 0 \quad , \\
N_{xx} &= EA \left[\frac{du_0}{dx} + \frac{1}{2} \left(\frac{dw_0}{dx} \right)^2 \right] , \\
M_{xx} &= -EI \frac{d^2w_0}{dx^2} .
\end{aligned} \tag{2.6}$$

2.2.1 Weighted Residual Statements of Model II

The equations given in the (2.6) are mathematically equivalent to the equations given in the (1.7) and (1.9), which were used for the Model I, but the effect of the elimination of the V_x can be observed both in the equation solving procedure and in the result of the numerical analysis, since it affects both the symmetry of the tangent matrix[1] and the accuracy of the solutions compared with other models. For the Model II, the following weighted residual statement can be made.

$$\begin{aligned}
0 &= \int_{x_a}^{x_b} \left(\frac{d\bar{W}_1}{dx} N_{xx}^a - \bar{W}_1 f(x) \right) dx - \bar{W}_1(x_a) N_1 - \bar{W}_1(x_b) N_2 , \\
0 &= \int_{x_a}^{x_b} \left[\frac{d\bar{W}_2}{dx} \left(\frac{dM_{xx}^a}{dx} + N_{xx}^a \frac{dw_0^a}{dx} \right) - \bar{W}_2 q(x) \right] dx - \bar{W}_2(x_a) V_1 - \bar{W}_2(x_b) V_2 , \\
0 &= \int_{x_a}^{x_b} \bar{W}_3 \left\{ -N_{xx}^a + EA \left[\frac{du_0^a}{dx} + \frac{1}{2} \left(\frac{dw_0^a}{dx} \right)^2 \right] \right\} dx , \\
0 &= \int_{x_a}^{x_b} \left(-\frac{\bar{W}_4 M_{xx}^a}{EI} + \frac{d\bar{W}_4}{dx} \frac{dw_0^a}{dx} \right) dx - \bar{W}_4(x_a) \theta_1 - \bar{W}_4(x_b) \theta_2 ,
\end{aligned} \tag{2.7}$$

where,

$$\begin{aligned}
 N_1 &= -N_{xx}(x_a), \quad N_2 = N_{xx}(x_b), \\
 V_1 &= -\left[\frac{dM_{xx}}{dx} + N_{xx} \frac{dw_0}{dx} \right]_{x=x_a} = -V_x(x_a), \\
 V_2 &= \left[\frac{dM_{xx}}{dx} + N_{xx} \frac{dw_0}{dx} \right]_{x=x_b} = V_x(x_b), \\
 \theta_1 &= \frac{dw_0(x_a)}{dx} \quad \text{and} \quad \theta_2 = -\frac{dw_0(x_b)}{dx} .
 \end{aligned}$$

Variables with superscripted ‘a’ (i.e. u_0^a , w_0^a , N_{xx}^a and M_{xx}^a) denote approximated variables, $\bar{W}_i (i = 1, \dots, 4)$ is the i^{th} weight function of the i^{th} weighted residual statement. x_a and x_b are the start and the end global coordinate of the element. The boundary terms V_1 and V_2 were obtained in the different forms compared with those of the Model I but the physical meaning are the same.

2.2.2 Finite Element Equations of Model II

All of the variables can be approximated by using the Lagrange type interpolations and the weigh functions can be chosen to be as

$$\begin{aligned}
 u_0 &\cong u_0^a = \sum_{j=1}^m \psi_j^{u_0} \mathbb{U}_j , & \bar{W}_1 &= \psi_i^{u_0} , \\
 w_0 &\cong w_0^a = \sum_{j=1}^n \psi_j^{w_0} \mathbb{W}_j , & \bar{W}_2 &= \psi_i^{w_0} , \\
 N_{xx} &\cong N_{xx}^a = \sum_{j=1}^p \psi_j^{N_{xx}} \mathbb{N}_j , & \bar{W}_3 &= \psi_i^{N_{xx}} , \\
 M_{xx} &\cong M_{xx}^a = \sum_{j=1}^r \psi_j^{M_{xx}} \mathbb{M}_j , & \bar{W}_4 &= \psi_i^{M_{xx}} .
 \end{aligned} \tag{2.8}$$

The primary and the secondary variables can be specified as follow:

<The primary variable>

<The secondary variable>

$$\bar{W}_1 \approx u_0$$

$$N_{xx}$$

$$\bar{W}_2 \approx w_0$$

$$V_x \left(= \frac{dM_{xx}}{dx} + N_{xx} \frac{dw_0}{dx} \right)$$

$$\bar{W}_4 \approx M_{xx}$$

$$\frac{dw_0}{dx}$$

By substituting the equation (2.8) into the equation (2.7), the following nonlinear mixed finite element equations of Model (II) can be obtained.

$$\begin{aligned}
& \sum_{j=1}^m \left[\int_{x_a}^{x_b} \left(\frac{d\psi_i^{u_0}}{dx} \psi_j^{N_{xx}} \right) dx \right] \mathbb{N}_j - \int_{x_a}^{x_b} \left(\psi_i^{u_0} f(x) \right) dx - \psi_i^{u_0}(x_a) N_1 - \psi_i^{u_0}(x_b) N_2 = 0 \quad , \\
& \sum_{j=1}^r \left[\int_{x_a}^{x_b} \frac{d\psi_i^{w_0}}{dx} \frac{d\psi_j^{M_{xx}}}{dx} dx \right] \mathbb{M}_j + \sum_{j=1}^m \left[\int_{x_a}^{x_b} \left(\frac{d\mathbf{w}_0^a}{d\mathbf{x}} \frac{d\psi_i^{w_0}}{dx} \psi_j^{N_{xx}} \right) dx \right] \mathbb{N}_j \\
& \quad - \int_{x_a}^{x_b} \left(\psi_i^{w_0} q(x) \right) dx - \psi_i^{w_0}(x_a) V_1 - \psi_i^{w_0}(x_b) V_2 = 0 \quad , \\
& \sum_{j=1}^p \left[\int_{x_a}^{x_b} \left(-\frac{\psi_i^{N_{xx}} \psi_j^{N_{xx}}}{EA} \right) dx \right] \mathbb{N}_j + \sum_{j=1}^m \left[\int_{x_a}^{x_b} \left(\psi_i^{N_{xx}} \frac{d\psi_j^{u_0}}{dx} \right) dx \right] \mathbb{W}_j \\
& \quad + \sum_{j=1}^n \left[\int_{x_a}^{x_b} \left(\frac{1}{2} \frac{d\mathbf{w}_0^a}{d\mathbf{x}} \psi_i^{N_{xx}} \frac{d\psi_j^{w_0}}{dx} \right) dx \right] \mathbb{W}_j = 0 \quad , \\
& \sum_{j=1}^r \left[\int_{x_a}^{x_b} \left(-\frac{\psi_i^{M_{xx}} \psi_j^{M_{xx}}}{EI} \right) dx \right] \mathbb{M}_j + \sum_{j=1}^n \left[\int_{x_a}^{x_b} \left(\frac{d\psi_i^{M_{xx}}}{dx} \frac{d\psi_j^{w_0}}{dx} \right) dx \right] \mathbb{W}_j \\
& \quad - \psi_i^{M_{xx}}(x_a) \theta_1 - \psi_i^{M_{xx}}(x_b) \theta_2 = 0 \quad .
\end{aligned} \tag{2.9}$$

The mixed finite element equations of Model II can be rewritten in algebraic matrix form by collecting the coefficients of the unknowns. Note that the Model II contains 4 variables as unknowns. Thus, the size of the $[K]$ of the Model II can be reduced, compared with that of the Model I.

$$\begin{aligned}
& [K^e(\{U^e\})]\{U^e\} = \{F^e\} \\
& = \begin{bmatrix} [K^{11}] & [K^{12}] & [K^{13}] & [K^{14}] \\ [K^{21}] & [K^{22}] & [K^{23}] & [K^{24}] \\ [K^{31}] & [K^{32}] & [K^{33}] & [K^{34}] \\ [K^{41}] & [K^{42}] & [K^{43}] & [K^{44}] \end{bmatrix} \begin{Bmatrix} \{\mathbb{U}_j\} \\ \{\mathbb{W}_j\} \\ \{\mathbb{N}_j\} \\ \{\mathbb{M}_j\} \end{Bmatrix} = \begin{Bmatrix} \{F^1\} \\ \{F^2\} \\ \{F^3\} \\ \{F^4\} \end{Bmatrix} . \tag{2.10}
\end{aligned}$$

The sub-matrices and the specific terms of the force vectors can be given by,

$$\begin{aligned}
[K^{13}] &= \int_{x_a}^{x_b} \left(\frac{d\psi_i^{u_0}}{dx} \psi_j^{N_{xx}} \right) dx , & [K^{24}] &= \int_{x_a}^{x_b} \frac{d\psi_i^{w_0}}{dx} \frac{d\psi_j^{M_{xx}}}{dx} dx \\
[K^{23}] &= \int_{x_a}^{x_b} \left(\frac{d\mathbf{w}_0^a}{dx} \frac{d\psi_i^{w_0}}{dx} \psi_j^{N_{xx}} \right) dx & [K^{33}] &= \int_{x_a}^{x_b} \left(-\frac{\psi_i^{N_{xx}} \psi_j^{N_{xx}}}{EA} \right) dx , \\
[K^{31}] &= \int_{x_a}^{x_b} \left(\psi_i^{N_{xx}} \frac{d\psi_j^{u_0}}{dx} \right) dx , & [K^{32}] &= \int_{x_a}^{x_b} \left(\frac{1}{2} \frac{d\mathbf{w}_0^a}{dx} \psi_i^{N_{xx}} \frac{d\psi_j^{w_0}}{dx} \right) dx , \\
[K^{44}] &= \int_{x_a}^{x_b} \left(-\frac{\psi_i^{M_{xx}} \psi_j^{M_{xx}}}{EI} \right) dx , & [K^{42}] &= \int_{x_a}^{x_b} \left(\frac{d\psi_i^{M_{xx}}}{dx} \frac{d\psi_j^{w_0}}{dx} \right) dx , \\
\{F^1\} &= \int_{x_a}^{x_b} \left(\psi_i^{u_0} f(x) \right) dx + \psi_i^{u_0}(x_a) N_1 + \psi_i^{u_0}(x_b) N_2 , \\
\{F^2\} &= \int_{x_a}^{x_b} \left(\psi_i^{w_0} q(x) \right) dx + \psi_i^{w_0}(x_a) V_1 + \psi_i^{w_0}(x_b) V_2 , \\
\{F^5\} &= \psi_i^{M_{xx}}(x_a) \theta_1 + \psi_i^{M_{xx}}(x_b) \theta_1 . \tag{2.11}
\end{aligned}$$

The sub-matrices and sub-vectors which are not specified above are zero.

2.3 Model III of Beam Bending

In displacement based model of the EBT, the slope ($\theta_x = -dw_0/dx$) was included as a primary variable with the use of the Hermite type interpolation for the vertical deflection w_0 . Because θ_x has a physical meaning, one can include it as an independent variable. This idea was proposed by Reddy by considering the following

equation as one of the governing equation of the EBT. It can be seen that the linear part of the coefficient matrix of the Model I given in the (2.4) and (2.5) cannot be symmetry, and the tangent matrix of the Model I, which will be discussed in the chapter III, cannot be symmetry either. In the computational point of view, the symmetry of the coefficient matrix of the algebraic equation system is very important because of the computational cost.

$$\theta_x = -\frac{dw_0}{dx} \quad (2.12)$$

By replacing every $-\frac{dw_0}{dx}$ in the EBT equations we can obtain the following differential equations, which can be modified for the Model III.

$$\begin{aligned} \frac{dN_{xx}}{dx} + f(x) &= 0 \quad , \\ \frac{dV_x}{dx} + q(x) &= 0 \quad , \\ V_x - \frac{dM_{xx}}{dx} - N_{xx}\theta_x &= 0 \quad , \\ N_{xx} &= EA \left[\frac{du_0}{dx} + \frac{1}{2}(\theta_x)^2 \right] \quad , \\ \theta_x + \frac{dw_0}{dx} &= 0 \quad , \\ M_{xx} &= EI \frac{d\theta_x}{dx} \quad . \end{aligned} \quad (2.13)$$

2.3.1 Weighted Residual Statements of Model III

With the equations of the (2.13), the weighted residual statements of the Model III of beam bending can be written as follow.

$$\begin{aligned}
0 &= \int_{x_a}^{x_b} \left(\frac{d\bar{W}_1}{dx} N_{xx}^a - \bar{W}_1 f(x) \right) dx - \bar{W}_1(x_a) N_1 - \bar{W}_1(x_b) N_2 , \\
0 &= \int_{x_a}^{x_b} \left(\frac{d\bar{W}_2}{dx} V_x^a - \bar{W}_2 q(x) \right) dx - \bar{W}_2(x_a) V_1 - \bar{W}_2(x_b) V_2 , \\
0 &= \int_{x_a}^{x_b} \bar{W}_3 \left(V_x^a - \frac{dM_{xx}^a}{dx} + \theta_x^a N_{xx}^a \right) dx , \\
0 &= \int_{x_a}^{x_b} \bar{W}_4 \left\{ -N_{xx}^a + EA \left[\frac{du_0^a}{dx} + \frac{1}{2} (\theta_x)^2 \right] \right\} dx , \\
0 &= \int_{x_a}^{x_b} \bar{W}_5 \left(\theta_x^a + \frac{dw_0^a}{dx} \right) dx , \\
0 &= \int_{x_a}^{x_b} \left(-\frac{\bar{W}_6 M_{xx}^a}{EI} - \frac{d\bar{W}_6}{dx} \theta_x^a \right) dx + \bar{W}_6(x_a) \theta_1 + \bar{W}_6(x_b) \theta_2 , \tag{2.14}
\end{aligned}$$

where,

$$\begin{aligned}
N_1 &= -N_{xx}(x_a) , \quad N_2 = N_{xx}(x_b) , \\
V_1 &= -V_x(x_a) , \quad V_2 = V_x(x_b) , \\
\theta_1 &= -\theta_x(x_a) \quad \text{and} \quad \theta_2 = \theta_x(x_b) .
\end{aligned}$$

2.3.2 Finite Element Equations of Model III

In a sense, the weighted residual statement of the (2.14) can be fully qualified for the Galerkin method[4], because each of the integral equation represents the work done in virtual work sense, with the following choice of the weight functions. The approximations of the variables and the chosen weight functions are as follow:

$$\begin{aligned}
u_0 &\cong u_0^a = \sum_{j=1}^l \psi_j^{u_0} \mathfrak{U}_j , & \bar{W}_1 &= \delta u_0 = \psi_i^{u_0} , \\
w_0 &\cong w_0^a = \sum_{j=1}^m \psi_j^{w_0} \mathfrak{W}_j , & \bar{W}_2 &= \delta w_0 = \psi_i^{w_0} , \\
\theta_x &\cong \theta_x^a = \sum_{j=1}^n \psi_j^{\theta_x} \mathfrak{S}_j , & \bar{W}_3 &= \delta \theta_x = \psi_i^{\theta_x} , \\
N_{xx} &\cong N_{xx}^a = \sum_{j=1}^p \psi_j^{N_{xx}} \mathfrak{N}_j , & \bar{W}_4 &= \delta N_{xx} = \psi_i^{N_{xx}} , \\
V_x &\cong V_x^a = \sum_{j=1}^q \psi_j^{V_x} \mathfrak{V}_j , & \bar{W}_5 &= \delta V_x = \psi_i^{V_x} , \\
M_{xx} &\cong M_{xx}^a = \sum_{j=1}^r \psi_j^{M_{xx}} \mathfrak{M}_j , & \bar{W}_6 &= \delta M_{xx} = \psi_i^{M_{xx}} . \tag{2.15}
\end{aligned}$$

The primary and the secondary variables can be specified as follow:

<The primary variable>	<The secondary variable>
$\bar{W}_1 \approx u_0$	N_{xx}
$\bar{W}_2 \approx w_0$	V_x
$\bar{W}_6 \approx M_{xx}$	θ_x

By substituting the equation (2.15) into the (2.14), the following nonlinear mixed finite element equations can be given by,

$$\begin{aligned}
& \sum_{j=1}^p \left[\int_{x_a}^{x_b} \left(\frac{d\psi_i^{u_0}}{dx} \psi_j^{N_{xx}} \right) dx \right] \mathbb{N}_j - \int_{x_a}^{x_b} \left(\psi_i^{u_0} f(x) \right) dx - \psi_i^{u_0}(x_a) N_1 - \psi_i^{u_0}(x_b) N_2 = 0 \quad , \\
& \sum_{j=1}^q \left[\int_{x_a}^{x_b} \left(\frac{d\psi_i^{w_0}}{dx} \psi_j^{V_x} \right) dx \right] \mathbb{V}_j - \int_{x_a}^{x_b} \left(\psi_i^{w_0} q(x) \right) dx - \psi_i^{w_0}(x_a) V_1 - \psi_i^{w_0}(x_b) V_2 = 0 \quad , \\
& \sum_{j=1}^q \left[\int_{x_a}^{x_b} \left(\psi_i^{\theta_x} \psi_j^{V_x} \right) dx \right] \mathbb{V}_j + \sum_{j=1}^r \left[\int_{x_a}^{x_b} \left(-\psi_i^{\theta_x} \frac{d\psi_j^{M_{xx}}}{dx} \right) dx \right] \mathbb{M}_j \\
& \quad + \sum_{j=1}^p \left[\int_{x_a}^{x_b} \left(\theta_x^a \psi_i^{\theta_x} \psi_j^{N_{xx}} \right) dx \right] \mathbb{N}_j = 0 \quad , \\
& \sum_{j=1}^p \left[\int_{x_a}^{x_b} \left(-\frac{\psi_i^{N_{xx}} \psi_j^{N_{xx}}}{EA} \right) dx \right] \mathbb{N}_j + \sum_{j=1}^l \left[\int_{x_a}^{x_b} \left(\psi_i^{N_{xx}} \frac{d\psi_j^{u_0}}{dx} \right) dx \right] \mathbb{U}_j \\
& \quad + \sum_{j=1}^n \left[\int_{x_a}^{x_b} \left(\frac{1}{2} \theta_x^a \psi_i^{N_{xx}} \psi_j^{\theta_x} \right) dx \right] \mathbb{S}_j = 0 \quad , \\
& \sum_{j=1}^n \left[\int_{x_a}^{x_b} \left(\psi_i^{V_x} \psi_j^{\theta_x} \right) dx \right] \mathbb{S}_j + \sum_{j=1}^m \left[\int_{x_a}^{x_b} \left(\psi_i^{V_x} \frac{d\psi_j^{w_0}}{dx} \right) dx \right] \mathbb{W}_j = 0 \quad , \\
& \sum_{j=1}^r \left[\int_{x_a}^{x_b} \left(-\frac{\psi_i^{M_{xx}} \psi_j^{M_{xx}}}{EI} \right) dx \right] \mathbb{M}_j + \sum_{j=1}^n \left[\int_{x_a}^{x_b} \left(-\frac{d\psi_i^{M_{xx}}}{dx} \psi_j^{\theta_x} \right) dx \right] \mathbb{S}_j \\
& \quad + \psi_i^{M_{xx}}(x_a) \theta_1 + \psi_i^{M_{xx}}(x_b) \theta_2 = 0 \quad .
\end{aligned} \tag{2.16}$$

The mixed finite element equations of the Model III can be rewritten as the algebraic matrix form by collecting the coefficients of the unknowns. Note that the Model III contains 6 variables as unknowns. Thus, the size of the $[K]$ is the largest among three mixed EBT models.

$$[K^e(\{U^e\})]\{U^e\} = \{F^e\}$$

$$= \begin{bmatrix} [K^{11}] & [K^{12}] & [K^{13}] & [K^{14}] & [K^{15}] & [K^{16}] \\ [K^{21}] & [K^{22}] & [K^{23}] & [K^{24}] & [K^{25}] & [K^{26}] \\ [K^{31}] & [K^{32}] & [K^{33}] & [K^{34}] & [K^{35}] & [K^{36}] \\ [K^{41}] & [K^{42}] & [K^{43}] & [K^{44}] & [K^{45}] & [K^{46}] \\ [K^{51}] & [K^{52}] & [K^{53}] & [K^{54}] & [K^{55}] & [K^{56}] \\ [K^{61}] & [K^{62}] & [K^{63}] & [K^{64}] & [K^{65}] & [K^{66}] \end{bmatrix} \begin{Bmatrix} \{\mathbb{U}_j\} \\ \{\mathbb{W}_j\} \\ \{\mathbb{S}_j\} \\ \{\mathbb{N}_j\} \\ \{\mathbb{V}_j\} \\ \{\mathbb{M}_j\} \end{Bmatrix} = \begin{Bmatrix} \{F^1\} \\ \{F^2\} \\ \{F^3\} \\ \{F^4\} \\ \{F^5\} \\ \{F^6\} \end{Bmatrix} . \quad (2.17)$$

The sub-matrices and the specific terms of the force vectors are given as follow:

$$\begin{aligned} [K^{14}] &= \int_{x_a}^{x_b} \left(\frac{d\psi_i^{u_0}}{dx} \psi_j^{N_{xx}} \right) dx , & [K^{25}] &= \int_{x_a}^{x_b} \left(\frac{d\psi_i^{w_0}}{dx} \psi_j^{V_x} \right) dx , \\ [K^{35}] &= \int_{x_a}^{x_b} (\psi_i^{\theta_x} \psi_j^{V_x}) dx , & [K^{36}] &= \int_{x_a}^{x_b} \left(-\psi_i^{\theta_x} \frac{d\psi_j^{M_{xx}}}{dx} \right) dx , \\ [K^{34}] &= \int_{x_a}^{x_b} (\theta_x^a \psi_i^{\theta_x} \psi_j^{N_{xx}}) dx , & [K^{41}] &= \int_{x_a}^{x_b} \left(\psi_i^{N_{xx}} \frac{d\psi_j^{u_0}}{dx} \right) dx , \\ [K^{44}] &= \int_{x_a}^{x_b} \left(-\frac{\psi_i^{N_{xx}} \psi_j^{N_{xx}}}{EA} \right) dx , & [K^{43}] &= \int_{x_a}^{x_b} \left(\frac{1}{2} \theta_x^a \psi_i^{N_{xx}} \psi_j^{\theta_x} \right) dx , \\ [K^{53}] &= \int_{x_a}^{x_b} (\psi_i^{V_x} \psi_j^{\theta_x}) dx , & [K^{52}] &= \int_{x_a}^{x_b} \left(\psi_i^{V_x} \frac{d\psi_j^{w_0}}{dx} \right) dx , \\ [K^{66}] &= \int_{x_a}^{x_b} \left(-\frac{\psi_i^{M_{xx}} \psi_j^{M_{xx}}}{EI} \right) dx , & [K^{63}] &= \int_{x_a}^{x_b} \left(-\frac{d\psi_i^{M_{xx}}}{dx} \psi_j^{\theta_x} \right) dx , \\ \{F^1\} &= \int_{x_a}^{x_b} (\psi_i^{u_0} f(x)) dx + \psi_i^{u_0}(x_a) N_1 + \psi_i^{u_0}(x_b) N_2 , \\ \{F^2\} &= \int_{x_a}^{x_b} (\psi_i^{w_0} q(x)) dx + \psi_i^{w_0}(x_a) V_1 + \psi_i^{w_0}(x_b) V_2 , \\ \{F^6\} &= -\psi_i^{M_{xx}}(x_a) \theta_1 - \psi_i^{M_{xx}}(x_b) \theta_2 . \end{aligned} \quad (2.18)$$

2.4 Model IV of Beam Bending

2.4.1 Weighted Residual Statements of the Model IV

The governing equations of the TBT are used to develop the Model IV. It can be shown that the mixed Model IV is equivalent to the Model III regarding the numbers and the dimensions of nodal variables. By using the governing equations of the TBT, Model IV includes 6 variables as independent variables (i.e. u_0 , w_0 , ϕ_x , N_{xx} , Q_x and M_{xx}). With the equilibrium equation and the resultants equations of the TBT, following weighted residual statements can be obtained.

$$\begin{aligned}
0 &= \int_{x_a}^{x_b} \left(\frac{d\bar{W}_1}{dx} N_{xx}^a - \bar{W}_1 f(x) \right) dx - \bar{W}_1(x_a) N_1 - \bar{W}_1(x_b) N_2 , \\
0 &= \int_{x_a}^{x_b} \left(\frac{d\bar{W}_2}{dx} Q_x^a + N_{xx}^a \frac{d\bar{W}_2}{dx} \frac{dw_0^a}{dx} - \bar{W}_2 q(x) \right) dx - \bar{W}_2(x_a) V_1 - \bar{W}_2(x_b) V_2 , \\
0 &= \int_{x_a}^{x_b} \left(\frac{d\bar{W}_3}{dx} M_{xx}^a + \bar{W}_3 Q_x^a \right) dx - \bar{W}_3(x_a) M_1 - \bar{W}_3(x_b) M_2 , \\
0 &= \int_{x_a}^{x_b} \bar{W}_4 \left(EA \left[\frac{du_0^a}{dx} + \frac{1}{2} \left(\frac{dw_0^a}{dx} \right)^2 \right] - N_{xx}^a \right) dx , \\
0 &= \int_{x_a}^{x_b} \bar{W}_5 \left(K_s GA \left[\frac{dw_0^a}{dx} + \phi_x^a \right] - Q_x^a \right) dx , \\
0 &= \int_{x_a}^{x_b} \bar{W}_6 \left(EI \frac{d\phi_x^a}{dx} - M_{xx}^a \right) dx , \tag{2.19}
\end{aligned}$$

where,

$$N_1 = -N_{xx}(x_a), \quad N_2 = N_{xx}(x_b) ,$$

$$V_1 = - \left[Q_x + N_{xx} \frac{dw_0}{dx} \right]_{x=x_a} , \quad V_2 = \left[Q_x + N_{xx} \frac{dw_0}{dx} \right]_{x=x_b} ,$$

$$M_1 = -M_{xx}(x_a) \quad \text{and} \quad M_2 = M_{xx}(x_b) .$$

2.4.2 Finite Element Equations of Model IV

Since no derivative of any variable is involved as a nodal unknown, the Lagrange type interpolation function[4] should be used for the approximations of variables of the Model IV. The approximations of the variables and the chosen weight functions are given as follow:

$$\begin{aligned}
 u_0 &\cong u_0^a = \sum_{j=1}^l \psi_j^{u_0} \mathbb{U}_j , & \bar{W}_1 &= \psi_i^{u_0} , \\
 w_0 &\cong w_0^a = \sum_{j=1}^m \psi_j^{w_0} \mathbb{W}_j , & \bar{W}_2 &= \psi_i^{w_0} , \\
 \phi_x &\cong \phi_x^a = \sum_{j=1}^n \psi_j^{\phi_x} \mathbb{P}_j , & \bar{W}_3 &= \psi_i^{\phi_x} , \\
 N_{xx} &\cong N_{xx}^a = \sum_{j=1}^p \psi_j^{N_{xx}} \mathbb{N}_j , & \bar{W}_4 &= \psi_i^{N_{xx}} , \\
 Q_x &\cong Q_x^a = \sum_{j=1}^q \psi_j^{Q_x} \mathbb{Q}_j , & \bar{W}_5 &= \psi_i^{Q_x} , \\
 M_{xx} &\cong M_{xx}^a = \sum_{j=1}^r \psi_j^{M_{xx}} \mathbb{M}_j , & \bar{W}_6 &= \psi_i^{M_{xx}} .
 \end{aligned} \tag{2.20}$$

The primary and the secondary variables can be specified as follow:

<The primary variable>

$$\bar{W}_1 \approx u_0$$

$$\bar{W}_2 \approx w_0$$

$$\bar{W}_3 \approx \phi_x$$

<The secondary variable>

$$N_{xx}$$

$$V_x \left(= Q_x + N_{xx} \frac{dw_0}{dx} \right)$$

$$M_{xx}$$

The finite element equations of the Model IV can be obtained by substituting approximations and the chosen weight functions of the (2.20) into the (2.19).

$$\begin{aligned}
& \sum_{j=1}^p \left[\int_{x_a}^{x_b} \left(\frac{d\psi_i^{u_0}}{dx} \psi_j^{N_{xx}} \right) dx \right] \mathbb{N}_j - \int_{x_a}^{x_b} (\psi_i^{u_0} f(x)) dx \\
& - \psi_i^{u_0}(x_a) N_1 - \psi_i^{u_0}(x_b) N_2 = 0 \quad , \\
& \sum_{j=1}^q \left[\int_{x_a}^{x_b} \left(\frac{d\psi_i^{w_0}}{dx} \psi_j^{Q_x} \right) dx \right] \mathbb{Q}_j + \sum_{j=1}^p \left[\int_{x_a}^{x_b} \left(\frac{d\mathbf{w}_0^a}{d\mathbf{x}} \frac{d\psi_i^{w_0}}{dx} \psi_j^{N_{xx}} \right) dx \right] \mathbb{N}_j \\
& - \int_{x_a}^{x_b} (\psi_i^{w_0} q(x)) dx - \psi_i^{w_0}(x_a) V_1 - \psi_i^{w_0}(x_b) V_2 = 0 \quad , \\
& \sum_{j=1}^r \left[\int_{x_a}^{x_b} \left(\frac{d\psi_i^{\phi_x}}{dx} \psi_j^{M_{xx}} \right) dx \right] \mathbb{M}_j + \sum_{j=1}^q \left[\int_{x_a}^{x_b} (\psi_i^{\phi_x} \psi_j^{Q_x}) dx \right] \mathbb{Q}_j \\
& - \psi_i^{\phi_x}(x_a) M_1 - \psi_i^{\phi_x}(x_b) M_2 = 0 \quad , \\
& \sum_{j=1}^l \left[\int_{x_a}^{x_b} \left(\psi_i^{N_{xx}} \frac{d\psi_j^{u_0}}{dx} \right) dx \right] \mathbb{U}_j + \sum_{j=1}^m \left[\int_{x_a}^{x_b} \left(\frac{1}{2} \frac{d\mathbf{w}_0^a}{d\mathbf{x}} \psi_i^{N_{xx}} \frac{d\psi_j^{w_0}}{dx} \right) dx \right] \mathbb{W}_j \\
& \quad + \sum_{j=1}^p \left[\int_{x_a}^{x_b} \left(-\frac{\psi_i^{N_{xx}} \psi_j^{N_{xx}}}{EA} \right) dx \right] \mathbb{N}_j = 0 \quad , \\
& \sum_{j=1}^m \left[\int_{x_a}^{x_b} \left(\psi_i^{Q_x} \frac{d\psi_j^{w_0}}{dx} \right) dx \right] \mathbb{W}_j dx + \sum_{j=1}^n \left[\int_{x_a}^{x_b} (\psi_i^{Q_x} \psi_j^{\phi_x}) dx \right] \mathbb{P}_j \\
& \quad + \sum_{j=1}^q \left[\int_{x_a}^{x_b} \left(-\frac{\psi_i^{Q_x} \psi_j^{Q_x}}{K_s GA} \right) dx \right] \mathbb{Q}_j = 0 \quad , \\
& \sum_{j=1}^n \left[\int_{x_a}^{x_b} \left(\psi_i^{M_{xx}} \frac{d\psi_j^{\phi_x}}{dx} \right) dx \right] \mathbb{P}_j + \sum_{j=1}^r \left[\int_{x_a}^{x_b} \left(-\frac{\psi_i^{M_{xx}} \psi_j^{M_{xx}}}{EI} \right) dx \right] \mathbb{M}_j = 0 \quad . \quad (2.21)
\end{aligned}$$

From the (2.21), the following matrix form of the algebraic equations can be obtained.

$$\begin{aligned}
& [K^e(\{U^e\})]\{U^e\} = \{F^e\} \\
& = \begin{bmatrix} [K^{11}] & [K^{12}] & [K^{13}] & [K^{14}] & [K^{15}] & [K^{16}] \\ [K^{21}] & [K^{22}] & [K^{23}] & [K^{24}] & [K^{25}] & [K^{26}] \\ [K^{31}] & [K^{32}] & [K^{33}] & [K^{34}] & [K^{35}] & [K^{36}] \\ [K^{41}] & [K^{42}] & [K^{43}] & [K^{44}] & [K^{45}] & [K^{46}] \\ [K^{51}] & [K^{52}] & [K^{53}] & [K^{54}] & [K^{55}] & [K^{56}] \\ [K^{61}] & [K^{62}] & [K^{63}] & [K^{64}] & [K^{65}] & [K^{66}] \end{bmatrix} \begin{Bmatrix} \{\mathbb{U}_j\} \\ \{\mathbb{W}_j\} \\ \{\mathbb{P}_j\} \\ \{\mathbb{N}_j\} \\ \{\mathbb{Q}_j\} \\ \{\mathbb{M}_j\} \end{Bmatrix} = \begin{Bmatrix} \{F^1\} \\ \{F^2\} \\ \{F^3\} \\ \{F^4\} \\ \{F^5\} \\ \{F^6\} \end{Bmatrix} . \quad (2.22)
\end{aligned}$$

where,

$$\begin{aligned}
[K^{14}] &= \int_{x_a}^{x_b} \left(\frac{d\psi_i^{u_0}}{dx} \psi_j^{N_{xx}} \right) dx , & [K^{24}] &= \int_{x_a}^{x_b} \left(\frac{d\mathbf{w}_0^a}{dx} \frac{d\psi_i^{w_0}}{dx} \psi_j^{N_{xx}} \right) dx , \\
[K^{25}] &= \int_{x_a}^{x_b} \left(\frac{d\psi_i^{w_0}}{dx} \psi_j^{Q_x} \right) dx , & [K^{36}] &= \int_{x_a}^{x_b} \left(\frac{d\psi_i^{\phi_x}}{dx} \psi_j^{M_{xx}} \right) dx , \\
[K^{35}] &= \int_{x_a}^{x_b} (\psi_i^{\phi_x} \psi_j^{Q_x}) dx , & [K^{41}] &= \int_{x_a}^{x_b} \left(\psi_i^{N_{xx}} \frac{d\psi_j^{u_0}}{dx} \right) dx , \\
[K^{42}] &= \int_{x_a}^{x_b} \left(\frac{1}{2} \frac{d\mathbf{w}_0^a}{dx} \psi_i^{N_{xx}} \frac{d\psi_j^{w_0}}{dx} \right) dx , & [K^{44}] &= \int_{x_a}^{x_b} \left(-\frac{\psi_i^{N_{xx}} \psi_j^{N_{xx}}}{EA} \right) dx , \\
[K^{52}] &= \int_{x_a}^{x_b} \left(\psi_i^{Q_x} \frac{d\psi_j^{w_0}}{dx} \right) , & [K^{53}] &= \int_{x_a}^{x_b} (\psi_i^{Q_x} \psi_j^{\phi_x}) dx , \\
[K^{55}] &= \int_{x_a}^{x_b} \left(-\frac{\psi_i^{Q_x} \psi_j^{Q_x}}{K_s GA} \right) dx , & [K^{63}] &= \int_{x_a}^{x_b} \left(\psi_i^{M_{xx}} \frac{d\psi_j^{\phi_x}}{dx} \right) dx , \\
[K^{66}] &= \int_{x_a}^{x_b} \left(-\frac{\psi_i^{M_{xx}} \psi_j^{M_{xx}}}{EI} \right) dx , \\
\{F^1\} &= \int_{x_a}^{x_b} (\psi_i^{u_0} f(x)) dx + \psi_i^{u_0}(x_a) N_1 + \psi_i^{u_0}(x_b) N_2 , \\
\{F^2\} &= \int_{x_a}^{x_b} (\psi_i^{w_0} q(x)) dx + \psi_i^{w_0}(x_a) V_1 + \psi_i^{w_0}(x_b) V_2 , \\
\{F^3\} &= \psi_i^{\phi_x}(x_a) M_1 + \psi_i^{\phi_x}(x_b) M_2 .
\end{aligned} \tag{2.23}$$

All of the sub-matrices and sub-vectors which are not specified above are zero.

2.5 Lagrange Type Beam Finite Elements

For present study, the mixed formula allows the use of the Lagrange type interpolation functions[4] for the approximations of every variable. Here, beam elements that were used for the computer implementation and the numerical analysis are

mentioned. For the beam problems, the Lagrange types of linear, quadratic and cubic elements were used. The geometry of the elements and the locations of associated interpolations are given in the Fig. 2.1.

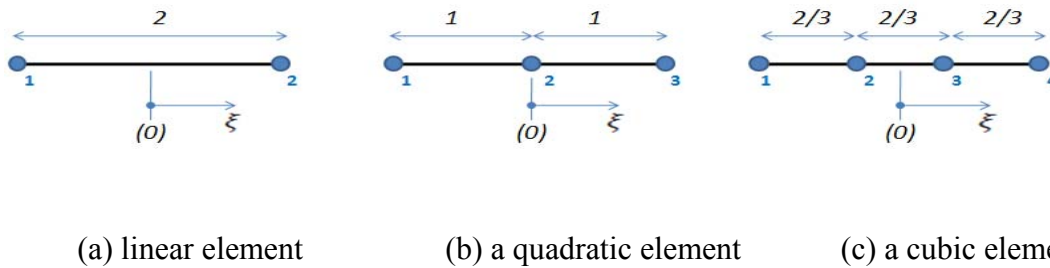


Fig. 2.1 Node number and local coordinate of the line elements of the Lagrange family.

Very well Known interpolation property [2] is known as partition of unity, which can be written as

$$\psi_i(x_j) = \begin{cases} 0 & \text{if } i \neq j \\ 1 & \text{if } i = j \end{cases}$$

$$\sum_{i=1}^n \psi_i(x) = 1.$$

So by considering the interpolation properties, we can derive interpolation functions which are associated with the nodal points with given set of polynomials. And, the specific interpolation functions associated with the nodal points are as follow:

- Linear interpolation functions

$$\psi_1 = \frac{1}{2}(1 - \xi) \quad , \quad \psi_2 = \frac{1}{2}(1 + \xi) \quad . \quad (2.24)$$

- Quadratic interpolation functions

$$\psi_1 = \frac{1}{2}\xi(\xi - 1), \quad \psi_2 = (1 + \xi)(1 - \xi), \quad \psi_3 = \frac{1}{2}\xi(1 + \xi). \quad (2.25)$$

- Cubic interpolation functions

$$\begin{aligned} \psi_1 &= -\frac{9}{16}\left(\xi + \frac{1}{3}\right)\left(\xi - \frac{1}{3}\right)(1 - \xi), \\ \psi_2 &= -\frac{27}{16}(1 + \xi)\left(\xi - \frac{1}{3}\right)(1 - \xi), \\ \psi_3 &= \frac{27}{16}(1 + \xi)\left(\xi + \frac{1}{3}\right)(1 - \xi), \\ \psi_4 &= \frac{9}{16}(1 + \xi)\left(\xi + \frac{1}{3}\right)\left(\xi - \frac{1}{3}\right). \end{aligned} \quad (2.26)$$

CHAPTER III

DEVELOPMENT OF PLATE BENDING MODELS

The 1-D beam bending problems which were discussed in the chapter II can be extended to the 2-D plate bending problems with simple modifications. Two CPT models and two FSDT models are developed. To clarify the developing procedure, the governing equations of the CPT and the FSDT are brought from the chapter I.

<The governing equations of the CPT>

$$\begin{aligned}
 -\frac{\partial N_{xx}}{\partial x} - \frac{\partial N_{xy}}{\partial y} &= 0 , \\
 -\frac{\partial N_{xy}}{\partial x} - \frac{\partial N_{yy}}{\partial y} &= 0 , \\
 -\frac{\partial V_x}{\partial x} - \frac{\partial V_y}{\partial y} - q(x) &= 0 , \\
 V_x - \left(\frac{\partial M_{xx}}{\partial x} + \frac{\partial M_{xy}}{\partial y} + N_{xx} \frac{\partial w_0}{\partial x} + N_{xy} \frac{\partial w_0}{\partial y} \right) &= 0 , \\
 V_y - \left(\frac{\partial M_{xy}}{\partial x} + \frac{\partial M_{yy}}{\partial y} + N_{xy} \frac{\partial w_0}{\partial x} + N_{yy} \frac{\partial w_0}{\partial y} \right) &= 0 ,
 \end{aligned} \tag{1.26}$$

and

$$\begin{aligned}
 A_{11}^* N_{xx} + A_{12}^* N_{yy} &= \left[\frac{\partial u_0}{\partial x} + \frac{1}{2} \left(\frac{\partial w_0}{\partial x} \right)^2 \right] , \\
 A_{12}^* N_{xx} + A_{22}^* N_{yy} &= \left[\frac{\partial v_0}{\partial y} + \frac{1}{2} \left(\frac{\partial w_0}{\partial y} \right)^2 \right] , \\
 A_{66}^* N_{xy} &= \left(\frac{\partial u_0}{\partial y} + \frac{\partial v_0}{\partial x} + \frac{\partial w_0}{\partial x} \frac{\partial w_0}{\partial y} \right) , \\
 D_{11}^* M_{xx} + D_{12}^* M_{yy} &= - \left(\frac{\partial^2 w_0}{\partial x^2} \right) , \\
 D_{12}^* M_{xx} + D_{22}^* M_{yy} &= - \left(\frac{\partial^2 w_0}{\partial y^2} \right) , \\
 D_{66}^* M_{xy} &= -2 \left(\frac{\partial^2 w_0}{\partial x \partial y} \right) .
 \end{aligned} \tag{1.28}$$

<The governing equations of the FSĐT>

$$\begin{aligned}
-\frac{\partial N_{xx}}{\partial x} - \frac{\partial N_{xy}}{\partial y} &= 0 , \\
-\frac{\partial N_{xy}}{\partial x} - \frac{\partial N_{yy}}{\partial y} &= 0 , \\
\frac{\partial}{\partial x} \left(N_{xx} \frac{\partial w_0}{\partial x} + N_{xy} \frac{\partial w_0}{\partial y} + Q_x \right) + \frac{\partial}{\partial y} \left(N_{xy} \frac{\partial w_0}{\partial x} + N_{yy} \frac{\partial w_0}{\partial y} + Q_y \right) + q(x) &= 0 , \\
Q_x - \left(\frac{\partial M_{xx}}{\partial x} + \frac{\partial M_{xy}}{\partial y} \right) &= 0 , \\
Q_y - \left(\frac{\partial M_{xy}}{\partial x} + \frac{\partial M_{yy}}{\partial y} \right) &= 0 ,
\end{aligned} \tag{1.33}$$

and

$$\begin{aligned}
A_{11}^* N_{xx} + A_{12}^* N_{yy} &= \left[\frac{\partial u_0}{\partial x} + \frac{1}{2} \left(\frac{\partial w_0}{\partial x} \right)^2 \right] , \\
A_{12}^* N_{xx} + A_{22}^* N_{yy} &= \left[\frac{\partial v_0}{\partial y} + \frac{1}{2} \left(\frac{\partial w_0}{\partial y} \right)^2 \right] , \\
A_{66}^* N_{xy} &= \left(\frac{\partial u_0}{\partial y} + \frac{\partial v_0}{\partial x} + \frac{\partial w_0}{\partial x} \frac{\partial w_0}{\partial y} \right) , \\
0 &= -\frac{Q_x}{K_s A_{55}} + \left(\frac{\partial w_0}{\partial x} + \phi_x \right) , \\
0 &= -\frac{Q_y}{K_s A_{44}} + \left(\frac{\partial w_0}{\partial y} + \phi_y \right) , \\
D_{11}^* M_{xx} + D_{12}^* M_{yy} &= \left(\frac{\partial \phi_x}{\partial x} \right) , \\
D_{12}^* M_{xx} + D_{22}^* M_{yy} &= \left(\frac{\partial \phi_y}{\partial y} \right) , \\
D_{66}^* M_{xy} &= \left(\frac{\partial \phi_x}{\partial y} + \frac{\partial \phi_y}{\partial x} \right) .
\end{aligned} \tag{1.36}$$

3.1 Model I of Plate Bending

3.1.1 Weighted Residual Statements of Model I

The governing equations of the CPT which were derived in the chapter I are modified to develop the plate bending Model I. Total eleven variables, i.e., u_0 , v_0 , w_0 , N_{xx} , N_{yy} , N_{xy} , V_x , V_y , M_{xx} , M_{yy} and M_{xy} , are treated as independent variable in the plate Model I. The Green-Gauss theorem[15] can be used to obtain the boundary terms when the integration by parts are conducted. The weighed residual statements of the Model I can be written as follow:

$$\begin{aligned} \int_{\Omega_e} \left(\frac{\partial \bar{W}_1}{\partial x} N_{xx}^a + \frac{\partial \bar{W}_1}{\partial y} N_{xy}^a \right) dx dy - \oint_{\Gamma_e} \bar{W}_1 \{n_x N_{xx} + n_y N_{xy}\} ds &= 0 , \\ \int_{\Omega_e} \left(\frac{\partial \bar{W}_2}{\partial x} N_{xy}^a + \frac{\partial \bar{W}_2}{\partial y} N_{yy}^a \right) dx dy - \oint_{\Gamma_e} \bar{W}_2 \{n_x N_{xy} + n_y N_{yy}\} ds &= 0 , \\ \int_{\Omega_e} \left(\frac{\partial \bar{W}_3}{\partial x} V_x^a + \frac{\partial \bar{W}_3}{\partial y} V_y^a - \bar{W}_3 q(x) \right) dx dy - \oint_{\Gamma_e} \bar{W}_3 \{n_x V_x + n_y V_y\} ds &= 0 , \\ \int_{\Omega_e} \bar{W}_4 \left\{ -A_{11}^* N_{xx}^a - A_{12}^* N_{yy}^a + \left[\frac{\partial u_0^a}{\partial x} + \frac{1}{2} \left(\frac{\partial w_0^a}{\partial x} \right)^2 \right] \right\} dx dy &= 0 , \\ \int_{\Omega_e} \bar{W}_5 \left\{ -A_{12}^* N_{xx}^a - A_{22}^* N_{yy}^a + \left[\frac{\partial v_0^a}{\partial y} + \frac{1}{2} \left(\frac{\partial w_0^a}{\partial y} \right)^2 \right] \right\} dx dy &= 0 , \\ \int_{\Omega_e} \bar{W}_6 \left[-A_{66}^* N_{xy}^a + \left(\frac{\partial u_0^a}{\partial y} + \frac{\partial v_0^a}{\partial x} + \frac{1}{2} \frac{\partial w_0^a}{\partial x} \frac{\partial w_0^a}{\partial y} + \frac{1}{2} \frac{\partial w_0^a}{\partial x} \frac{\partial w_0^a}{\partial y} \right) \right] dx dy &= 0 , \\ \int_{\Omega_e} \bar{W}_7 \left(-V_x^a + \frac{\partial M_{xx}^a}{\partial x} + \frac{\partial M_{xy}^a}{\partial y} + N_{xx}^a \frac{\partial w_0^a}{\partial x} + N_{xy}^a \frac{\partial w_0^a}{\partial y} \right) dx dy &= 0 , \\ \int_{\Omega_e} \bar{W}_8 \left(-V_y^a + \frac{\partial M_{xy}^a}{\partial x} + \frac{\partial M_{yy}^a}{\partial y} + N_{xy}^a \frac{\partial w_0^a}{\partial x} + N_{yy}^a \frac{\partial w_0^a}{\partial y} \right) dx dy &= 0 , \end{aligned}$$

$$\begin{aligned}
& \int_{\Omega_e} \left(-D_{11}^* \bar{W}_9 M_{xx}^a - D_{12}^* \bar{W}_9 M_{yy}^a + \frac{\partial \bar{W}_9}{\partial x} \frac{\partial w_0^a}{\partial x} \right) dx dy - \oint_{\Gamma_e} \bar{W}_9 \left(n_x \frac{\partial w_0}{\partial x} \right) ds = 0 , \\
& \int_{\Omega_e} \left(-D_{12}^* \bar{W}_{10} M_{xx}^a - D_{22}^* \bar{W}_{10} M_{yy}^a + \frac{\partial \bar{W}_{10}}{\partial y} \frac{\partial w_0^a}{\partial y} \right) dx dy - \oint_{\Gamma_e} \bar{W}_{10} \left(n_y \frac{\partial w_0}{\partial y} \right) ds = 0 , \\
& \int_{\Omega_e} \left(-D_{66}^* \bar{W}_{11} M_{xy}^a + \frac{\partial \bar{W}_{11}}{\partial x} \frac{\partial w_0^a}{\partial y} + \frac{\partial \bar{W}_{11}}{\partial y} \frac{\partial w_0^a}{\partial x} \right) dx dy \\
& - \oint_{\Gamma_e} \bar{W}_{11} \left(n_x \frac{\partial w_0}{\partial y} + n_y \frac{\partial w_0}{\partial x} \right) ds = 0 . \tag{3.1}
\end{aligned}$$

where, Γ_e is the boundary of the element region Ω_e and variables with superscripted letter 'a' denote the approximated variables. The n_i denotes the unit normal vector of the i-direction, where $i = x, y$.

3.1.2 Finite Element Equations of Model I

With the weighted residual statements given in the (3.1), we can develop the finite element the Model I of the plate bending by approximating variables with known interpolation functions and unknown nodal values. But the choice of the known interpolation functions is not arbitrary. By the same reason that we discussed while developing the EBT models in the chapter II, the Lagrange type of the interpolation functions should be used for the approximations of the all variables of the Model I, because no derivative of the variable is involved as nodal unknown. To develop the finite element model based on the displacement model[1], one should approximate the vertical displacement w_0 with the conforming [1, 4] or the nonconforming[1, 4] type of the Hermite interpolation functions, because displacement based model includes the derivatives of the w_0 as nodal values[1]. But for the current Model I, only C^0 continuity of the variables is required. Thus, it allows use of linear interpolation functions as the minimum.

$$\begin{aligned}
u_0 \cong u_0^a &= \sum_{j=1}^m \psi_j^{u_0}(x, y) \mathbb{U}_j, & \bar{W}_1 &= \psi_i^{u_0}(x, y), \\
v_0 \cong v_0^a &= \sum_{j=1}^m \psi_j^{v_0}(x, y) \mathbb{V}_j, & \bar{W}_2 &= \psi_i^{v_0}(x, y), \\
w_0 \cong w_0^a &= \sum_{j=1}^n \psi_j^{w_0}(x, y) \mathbb{W}_j, & \bar{W}_3 &= \psi_i^{w_0}(x, y), \\
N_{xx} \cong N_{xx}^a &= \sum_{j=1}^p \psi_j^{N_{xx}}(x, y) \mathbb{N}_j^1, & \bar{W}_4 &= \psi_i^{N_{xx}}(x, y), \\
N_{yy} \cong N_{yy}^a &= \sum_{j=1}^p \psi_j^{N_{yy}}(x, y) \mathbb{N}_j^2, & \bar{W}_5 &= \psi_i^{N_{yy}}(x, y), \\
N_{xy} \cong N_{xy}^a &= \sum_{j=1}^p \psi_j^{N_{xy}}(x, y) \mathbb{N}_j^3, & \bar{W}_6 &= \psi_i^{N_{xy}}(x, y), \\
V_x \cong V_x^a &= \sum_{j=1}^q \psi_j^{V_x}(x, y) \mathbb{V}_j^1, & \bar{W}_7 &= \psi_i^{V_x}(x, y), \\
V_y \cong V_y^a &= \sum_{j=1}^q \psi_j^{V_y}(x, y) \mathbb{V}_j^2, & \bar{W}_8 &= \psi_i^{V_y}(x, y), \\
M_{xx} \cong M_{xx}^a &= \sum_{j=1}^r \psi_j^{M_{xx}}(x, y) \mathbb{M}_j^1, & \bar{W}_9 &= \psi_i^{M_{xx}}(x, y), \\
M_{yy} \cong M_{yy}^a &= \sum_{j=1}^r \psi_j^{M_{yy}}(x, y) \mathbb{M}_j^2, & \bar{W}_{10} &= \psi_i^{M_{yy}}(x, y), \\
M_{xy} \cong M_{xy}^a &= \sum_{j=1}^r \psi_j^{M_{xy}}(x, y) \mathbb{M}_j^3, & \bar{W}_{11} &= \psi_i^{M_{xy}}(x, y). \tag{3.2}
\end{aligned}$$

The primary variables and the secondary variable of the Model I can be specified as follow:

<The primary variable>

$$u_0$$

$$v_0$$

$$w_0$$

$$M_{xx}$$

$$M_{yy}$$

$$M_{xy}$$

<The secondary variable>

$$n_x N_{xx} + n_y N_{xy}$$

$$n_x N_{xy} + n_y N_{yy}$$

$$n_x V_x + n_y V_y$$

$$n_x \frac{\partial w_0}{\partial x}$$

$$n_y \frac{\partial w_0}{\partial y}$$

$$n_x \frac{\partial w_0}{\partial y} + n_y \frac{\partial w_0}{\partial x}$$

By substituting the equation (3.2) into the (3.1) the finite element Model I of the plate bending can be obtained as follow:

$$\begin{aligned}
& \int_{\Omega_e} \left[\sum_{j=1}^p \left(\frac{\partial \psi_i^{u_0}}{\partial x} \psi_j^{N_{xx}} \right) \mathbb{N}_j^1 + \sum_{j=1}^p \left(\frac{\partial \psi_i^{u_0}}{\partial y} \psi_j^{N_{xy}} \right) \mathbb{N}_j^3 \right] dx dy - \oint_{\Gamma_e} \psi_i^{u_0} \{n_x N_{xx} + n_y N_{xy}\} ds = 0 , \\
& \int_{\Omega_e} \left[\sum_{j=1}^p \left(\frac{\partial \psi_i^{v_0}}{\partial x} \psi_j^{N_{xy}} \right) \mathbb{N}_j^3 + \sum_{j=1}^p \left(\frac{\partial \psi_i^{v_0}}{\partial y} \psi_j^{N_{yy}} \right) \mathbb{N}_j^2 \right] dx dy - \oint_{\Gamma_e} \psi_i^{v_0} \{n_x N_{xy} + n_y N_{yy}\} ds = 0 , \\
& \int_{\Omega_e} \left[\sum_{j=1}^q \left(\frac{\partial \psi_i^{w_0}}{\partial x} \psi_j^{V_x} \right) \mathbb{V}_j^1 + \sum_{j=1}^q \left(\frac{\partial \psi_i^{w_0}}{\partial y} \psi_j^{V_y} \right) \mathbb{V}_j^2 - \psi_i^{w_0} q(x) \right] dx dy \\
& \quad - \oint_{\Gamma_e} \psi_i^{w_0} \{n_x V_x + n_y V_y\} ds = 0 , \\
& \int_{\Omega_e} \left\{ -A_{11}^* \sum_{j=1}^p \left(\psi_i^{N_{xx}} \psi_j^{N_{xx}} \right) \mathbb{N}_j^1 - A_{12}^* \sum_{j=1}^p \left(\psi_i^{N_{xx}} \psi_j^{N_{yy}} \right) \mathbb{N}_j^2 \right. \\
& \quad \left. + \left[\sum_{j=1}^m \left(\psi_i^{N_{xx}} \frac{\partial \psi_j^{u_0}}{\partial x} \right) \mathbb{W}_j + \frac{1}{2} \frac{\partial \mathbf{w}_0^a}{\partial \mathbf{x}} \sum_{j=1}^n \left(\psi_i^{N_{xx}} \frac{\partial \psi_j^{w_0}}{\partial x} \right) \mathbb{W}_j \right] \right\} dx dy = 0 , \\
& \int_{\Omega_e} \left\{ -A_{12}^* \sum_{j=1}^p \left(\psi_i^{N_{yy}} \psi_j^{N_{xx}} \right) \mathbb{N}_j^1 - A_{22}^* \sum_{j=1}^p \left(\psi_i^{N_{yy}} \psi_j^{N_{yy}} \right) \mathbb{N}_j^2 \right. \\
& \quad \left. + \left[\sum_{j=1}^m \left(\psi_i^{N_{yy}} \frac{\partial \psi_j^{v_0}}{\partial y} \right) \mathbb{V}_j + \frac{1}{2} \frac{\partial \mathbf{w}_0^a}{\partial \mathbf{y}} \sum_{j=1}^n \left(\psi_i^{N_{yy}} \frac{\partial \psi_j^{w_0}}{\partial y} \right) \mathbb{W}_j \right] \right\} dx dy = 0 , \\
& \int_{\Omega_e} \left[-A_{66} \sum_{j=1}^p \left(\psi_i^{N_{xy}} \psi_j^{N_{xy}} \right) \mathbb{N}_j^3 \right. \\
& \quad \left. + \left(\sum_{j=1}^m \left(\psi_i^{N_{xy}} \frac{\partial \psi_j^{u_0}}{\partial y} \right) \mathbb{W}_j + \sum_{j=1}^m \left(\psi_i^{N_{xy}} \frac{\partial \psi_j^{v_0}}{\partial x} \right) \mathbb{V}_j + \frac{1}{2} \frac{\partial \mathbf{w}_0^a}{\partial \mathbf{x}} \sum_{j=1}^n \left(\psi_i^{N_{xy}} \frac{\partial \psi_j^{w_0}}{\partial y} \right) \mathbb{W}_j \right. \right. \\
& \quad \left. \left. + \frac{1}{2} \frac{\partial \mathbf{w}_0^a}{\partial \mathbf{y}} \sum_{j=1}^n \left(\psi_i^{N_{xy}} \frac{\partial \psi_j^{w_0}}{\partial x} \right) \mathbb{W}_j \right) \right] dx dy = 0 , \\
& \int_{\Omega_e} \left[-\sum_{j=1}^q \left(\psi_i^{V_x} \psi_j^{V_x} \right) \mathbb{V}_j^1 + \sum_{j=1}^r \left(\psi_i^{V_x} \frac{\partial \psi_j^{M_{xx}}}{\partial x} \right) \mathbb{M}_j^1 + \sum_{j=1}^r \left(\psi_i^{V_x} \frac{\partial \psi_j^{M_{xy}}}{\partial y} \right) \mathbb{M}_j^3 \right. \\
& \quad \left. + \frac{\partial \mathbf{w}_0^a}{\partial \mathbf{x}} \sum_{j=1}^p \left(\psi_i^{V_x} \psi_j^{N_{xx}} \right) \mathbb{N}_j^1 + \frac{\partial \mathbf{w}_0^a}{\partial \mathbf{y}} \sum_{j=1}^p \left(\psi_i^{V_x} \psi_j^{N_{xy}} \right) \mathbb{N}_j^3 \right] dx dy = 0 , \\
& \int_{\Omega_e} \left[-\sum_{j=1}^q \left(\psi_i^{V_y} \psi_j^{V_y} \right) \mathbb{V}_j^2 + \sum_{j=1}^r \left(\psi_i^{V_y} \frac{\partial \psi_j^{M_{xy}}}{\partial x} \right) \mathbb{M}_j^3 + \sum_{j=1}^r \left(\psi_i^{V_y} \frac{\partial \psi_j^{M_{yy}}}{\partial y} \right) \mathbb{M}_j^2 \right. \\
& \quad \left. + \frac{\partial \mathbf{w}_0^a}{\partial \mathbf{x}} \sum_{j=1}^p \left(\psi_i^{V_y} \psi_j^{N_{xy}} \right) \mathbb{N}_j^3 + \frac{\partial \mathbf{w}_0^a}{\partial \mathbf{y}} \sum_{j=1}^p \left(\psi_i^{V_y} \psi_j^{N_{yy}} \right) \mathbb{N}_j^2 \right] dx dy = 0 ,
\end{aligned}$$

$$\begin{aligned}
& \int_{\Omega_e} \left[-D_{11}^* \sum_{j=1}^r (\psi_i^{M_{xx}} \psi_j^{M_{xx}}) \mathbb{M}_j^1 - D_{12}^* \sum_{j=1}^r (\psi_i^{M_{xx}} \psi_j^{M_{yy}}) \mathbb{M}_j^2 \right. \\
& \quad \left. + \sum_{j=1}^n \left(\frac{\partial \psi_i^{M_{xx}}}{\partial x} \frac{\partial \psi_j^{w_0}}{\partial x} \right) \mathbb{W}_j \right] dx dy - \oint_{\Gamma_e} \psi_i^{M_{xx}} \left(n_x \frac{\partial w_0}{\partial x} \right) ds = 0 , \\
& \int_{\Omega_e} \left[-D_{12}^* \sum_{j=1}^r (\psi_i^{M_{yy}} \psi_j^{M_{xx}}) \mathbb{M}_j^1 - D_{22}^* \sum_{j=1}^r (\psi_i^{M_{yy}} \psi_j^{M_{yy}}) \mathbb{M}_j^2 \right. \\
& \quad \left. + \sum_{j=1}^n \left(\frac{\partial \psi_i^{M_{yy}}}{\partial y} \frac{\partial \psi_j^{w_0}}{\partial y} \right) \mathbb{W}_j \right] dx dy - \oint_{\Gamma_e} \psi_i^{M_{yy}} \left(n_y \frac{\partial w_0}{\partial y} \right) ds = 0 , \\
& \int_{\Omega_e} \left[-D_{66}^* \sum_{j=1}^r (\psi_i^{M_{xy}} \psi_j^{M_{xy}}) \mathbb{M}_j^3 + \sum_{j=1}^n \left(\frac{\partial \psi_i^{M_{xy}}}{\partial x} \frac{\partial \psi_j^{w_0}}{\partial y} \right) \mathbb{W}_j \right. \\
& \quad \left. + \sum_{j=1}^n \left(\frac{\partial \psi_i^{M_{xy}}}{\partial y} \frac{\partial \psi_j^{w_0}}{\partial x} \right) \mathbb{W}_j \right] dx dy - \oint_{\Gamma_e} \psi_i^{M_{xy}} \left(n_x \frac{\partial w_0}{\partial y} + n_y \frac{\partial w_0}{\partial x} \right) ds = 0 . \tag{3.3}
\end{aligned}$$

Above equations given in the (3.3) can be rewritten in the algebraic matrix equation in the following form,

$$\begin{aligned}
& [K^e(\{U^e\})]\{U^e\} = \{F^e\} \\
& = \begin{bmatrix} [K^{(1)(1)}] & \dots & [K^{(1)(6)}] & \dots & [K^{(1)(11)}] \\ \vdots & \ddots & \vdots & \ddots & \vdots \\ [K^{(6)(1)}] & \dots & [K^{(6)(6)}] & \dots & [K^{(6)(11)}] \\ \vdots & \ddots & \vdots & \ddots & \vdots \\ [K^{(11)(1)}] & \dots & [K^{(11)(6)}] & \dots & [K^{(11)(11)}] \end{bmatrix} \begin{Bmatrix} \{\mathbb{U}_j\} \\ \vdots \\ \{\mathbb{N}_j^3\} \\ \vdots \\ \{\mathbb{M}_j^3\} \end{Bmatrix} = \begin{Bmatrix} \{F^{(1)}\} \\ \vdots \\ \{F^{(6)}\} \\ \vdots \\ \{F^{(11)}\} \end{Bmatrix} . \tag{3.4}
\end{aligned}$$

where,

$$\begin{aligned}
[K^{14}] &= \int_{\Omega_e} \left\{ \frac{\partial \psi_i^{u_0}}{\partial x} \psi_j^{N_{xx}} \right\} dx dy , & [K^{16}] &= \int_{\Omega_e} \left\{ \frac{\partial \psi_i^{u_0}}{\partial y} \psi_j^{N_{xy}} \right\} dx dy , \\
[K^{25}] &= \int_{\Omega_e} \left\{ \frac{\partial \psi_i^{v_0}}{\partial y} \psi_j^{N_{yy}} \right\} dx dy , & [K^{26}] &= \int_{\Omega_e} \left\{ \frac{\partial \psi_i^{v_0}}{\partial x} \psi_j^{N_{xy}} \right\} dx dy , \\
[K^{37}] &= \int_{\Omega_e} \left\{ \frac{\partial \psi_i^{w_0}}{\partial x} \psi_j^{V_x} \right\} dx dy , & [K^{38}] &= \int_{\Omega_e} \left\{ \frac{\partial \psi_i^{w_0}}{\partial y} \psi_j^{V_y} \right\} dx dy ,
\end{aligned}$$

$$\begin{aligned}
[K^{41}] &= \int_{\Omega_e} \left\{ \psi_i^{N_{xx}} \frac{\partial \psi_j^{u_0}}{\partial x} \right\} dx dy , & [K^{43}] &= \int_{\Omega_e} \left\{ \frac{1}{2} \left(\frac{\partial \mathbf{w}_0^a}{\partial \mathbf{x}} \right) \psi_i^{N_{xx}} \frac{\partial \psi_j^{w_0}}{\partial x} \right\} dx dy \\
[K^{44}] &= \int_{\Omega_e} \left\{ -A_{11}^* \psi_i^{N_{xx}} \psi_j^{N_{xx}} \right\} dx dy , & [K^{45}] &= \int_{\Omega_e} \left\{ -A_{12}^* \psi_i^{N_{xx}} \psi_j^{N_{yy}} \right\} dx dy , \\
[K^{52}] &= \int_{\Omega_e} \left\{ \psi_i^{N_{yy}} \frac{\partial \psi_j^{v_0}}{\partial y} \right\} dx dy , & [K^{53}] &= \int_{\Omega_e} \left\{ \frac{1}{2} \left(\frac{\partial \mathbf{w}_0^a}{\partial \mathbf{y}} \right) \psi_i^{N_{yy}} \frac{\partial \psi_j^{w_0}}{\partial y} \right\} dx dy , \\
[K^{54}] &= \int_{\Omega_e} \left\{ -A_{12}^* \psi_i^{N_{yy}} \psi_j^{N_{xx}} \right\} dx dy , & [K^{55}] &= \int_{\Omega_e} \left\{ -A_{22}^* \psi_i^{N_{yy}} \psi_j^{N_{yy}} \right\} dx dy , \\
[K^{61}] &= \int_{\Omega_e} \left\{ \psi_i^{N_{xy}} \frac{\partial \psi_j^{u_0}}{\partial y} \right\} dx dy , & [K^{62}] &= \int_{\Omega_e} \left\{ \psi_i^{N_{xy}} \frac{\partial \psi_j^{v_0}}{\partial x} \right\} dx dy , \\
[K^{66}] &= \int_{\Omega_e} \left\{ -A_{66}^* \psi_i^{N_{xy}} \psi_j^{N_{xy}} \right\} dx dy , \\
[K^{63}] &= \int_{\Omega_e} \left\{ \frac{1}{2} \left[\left(\frac{\partial \mathbf{w}_0^a}{\partial \mathbf{x}} \right) \psi_i^{N_{xy}} \frac{\partial \psi_j^w}{\partial y} + \left(\frac{\partial \mathbf{w}_0^a}{\partial \mathbf{y}} \right) \psi_i^{N_{xy}} \frac{\partial \psi_j^w}{\partial x} \right] \right\} dx dy , \\
[K^{74}] &= \int_{\Omega_e} \left\{ \left(\frac{\partial \mathbf{w}_0^a}{\partial \mathbf{x}} \right) \psi_i^{V_x} \psi_j^{N_{xx}} \right\} dx dy , & [K^{76}] &= \int_{\Omega_e} \left\{ \left(\frac{\partial \mathbf{w}_0^a}{\partial \mathbf{y}} \right) \psi_i^{V_x} \psi_j^{N_{xy}} \right\} dx dy , \\
[K^{77}] &= \int_{\Omega_e} \left\{ -\psi_i^{V_x} \psi_j^{V_x} \right\} dx dy , & [K^{79}] &= \int_{\Omega_e} \left\{ \psi_i^{V_x} \frac{\partial \psi_j^{M_{xx}}}{\partial x} \right\} dx dy , \\
[K^{7(11)}] &= \int_{\Omega_e} \left\{ \psi_i^{V_x} \frac{\partial \psi_j^{M_{xy}}}{\partial y} \right\} dx dy , \\
[K^{85}] &= \int_{\Omega_e} \left\{ \left(\frac{\partial \mathbf{w}_0^a}{\partial \mathbf{y}} \right) \psi_i^{V_y} \psi_j^{N_{yy}} \right\} dx dy , & [K^{86}] &= \int_{\Omega_e} \left\{ \left(\frac{\partial \mathbf{w}_0^a}{\partial \mathbf{x}} \right) \psi_i^{V_y} \psi_j^{N_{xy}} \right\} dx dy , \\
[K^{88}] &= \int_{\Omega_e} \left\{ -\psi_i^{V_y} \psi_j^{V_y} \right\} dx dy , & [K^{8(10)}] &= \int_{\Omega_e} \left\{ \psi_i^{V_y} \frac{\partial \psi_j^{M_{yy}}}{\partial y} \right\} dx dy , \\
[K^{8(11)}] &= \int_{\Omega_e} \left\{ \psi_i^{V_y} \frac{\partial \psi_j^{M_{xy}}}{\partial x} \right\} dx dy , \\
[K^{93}] &= \int_{\Omega_e} \left\{ \frac{\partial \psi_i^{M_{xx}}}{\partial x} \frac{\partial \psi_j^{w_0}}{\partial x} \right\} dx dy , & [K^{99}] &= \int_{\Omega_e} \left\{ -D_{11}^* \psi_i^{M_{xx}} \psi_j^{M_{xx}} \right\} dx dy , \\
[K^{9(10)}] &= \int_{\Omega_e} \left\{ -D_{12}^* \psi_i^{M_{xx}} \psi_j^{M_{yy}} \right\} dx dy \\
[K^{(10)3}] &= \int_{\Omega_e} \left\{ \frac{\partial \psi_i^{M_{xx}}}{\partial y} \frac{\partial \psi_j^{w_0}}{\partial y} \right\} dx dy , & [K^{(10)9}] &= \int_{\Omega_e} \left\{ -D_{12}^* \psi_i^{M_{yy}} \psi_j^{M_{xx}} \right\} dx dy ,
\end{aligned}$$

$$\begin{aligned}
[K^{(10)(10)}] &= \int_{\Omega_e} \left\{ -D_{22}^* \psi_i^{M_{yy}} \psi_j^{M_{yy}} \right\} dx dy , \\
[K^{(11)3}] &= \int_{\Omega_e} \left\{ \frac{\partial \psi_i^{M_{xy}}}{\partial x} \frac{\partial \psi_j^{w_0}}{\partial y} + \frac{\partial \psi_i^{M_{xy}}}{\partial y} \frac{\partial \psi_j^{w_0}}{\partial x} \right\} dx dy , \\
[K^{(11)(11)}] &= \int_{\Omega_e} \left\{ -D_{66}^* \psi_i^{M_{xy}} \psi_j^{M_{xy}} \right\} dx dy . \\
\{F^1\} &= \oint_{\Gamma_e} \psi_i^u \{n_x N_{xx} + n_y N_{xy}\} ds , & \{F^2\} &= \oint_{\Gamma_e} \psi_i^v \{n_x N_{xy} + n_y N_{yy}\} ds , \\
\{F^3\} &= \int_{\Omega_e} \{ \psi_i^w q(x) \} dx dy + \oint_{\Gamma_e} \psi_i^w Q_n ds & \{F^9\} &= \oint_{\Gamma_e} \psi_i^{M_{xx}} \left(\frac{\partial w_0}{\partial x} n_x \right) ds , \\
\{F^{(10)}\} &= \oint_{\Gamma_e} \psi_i^{M_{yy}} \left(\frac{\partial w_0}{\partial y} n_y \right) ds , \\
\{F^{(11)}\} &= \oint_{\Gamma_e} \left\{ \psi_i^{M_{xy}} \left(\frac{\partial w_0}{\partial y} n_x + \frac{\partial w_0}{\partial x} n_y \right) \right\} ds .
\end{aligned} \tag{3.5}$$

The rest of sub coefficient matrices and force vectors which are not specified in the (3. 5) are zero.

3.2 Model II of Plate Bending

The shear resultant V_x and V_y can be eliminated by substituting the forth and the fifth equilibrium equations into the third equilibrium equation of the CPT. By doing this the symmetry of the linear portion of the coefficient matrix can be achieved and the symmetry of the tangent matrix[1], which will be discussed in the chapter IV, can be also archived.

3.2.1 Weighted Residual Statements of Model II

With the equations of the Model II of the plate bending, the following weighted residual statements can be obtained.

$$\begin{aligned}
& \int_{\Omega_e} \left(\frac{\partial \bar{W}_1}{\partial x} N_{xx}^a + \frac{\partial \bar{W}_1}{\partial y} N_{xy}^a \right) dx dy - \oint_{\Gamma_e} \bar{W}_1 \{n_x N_{xx} + n_y N_{xy}\} ds = 0 , \\
& \int_{\Omega_e} \left(\frac{\partial \bar{W}_2}{\partial x} N_{xy}^a + \frac{\partial \bar{W}_2}{\partial y} N_{yy}^a \right) dx dy - \oint_{\Gamma_e} \bar{W}_2 \{n_x N_{xy} + n_y N_{yy}\} ds = 0 , \\
& \int_{\Omega_e} \left\{ \frac{\partial \bar{W}_3}{\partial x} \left(\frac{\partial M_{xx}^a}{\partial x} + \frac{\partial M_{xy}^a}{\partial y} + N_{xx}^a \frac{\partial w_0^a}{\partial x} + N_{xy}^a \frac{\partial w_0^a}{\partial y} \right) \right. \\
& \quad \left. + \frac{\partial \bar{W}_3}{\partial y} \left(\frac{\partial M_{xy}^a}{\partial x} + \frac{\partial M_{yy}^a}{\partial y} + N_{xy}^a \frac{\partial w_0^a}{\partial x} + N_{yy}^a \frac{\partial w_0^a}{\partial y} \right) - \bar{W}_3 q(x) \right\} dx dy \\
& \quad - \oint_{\Gamma_e} \bar{W}_3 \{n_x V_x + n_y V_y\} ds = 0 , \\
& \int_{\Omega_e} \bar{W}_4 \left\{ -A_{11}^* N_{xx}^a - A_{12}^* N_{yy}^a + \left[\frac{\partial u_0^a}{\partial x} + \frac{1}{2} \left(\frac{\partial w_0^a}{\partial x} \right)^2 \right] \right\} dx dy = 0 , \\
& \int_{\Omega_e} \bar{W}_5 \left\{ -A_{12}^* N_{xx}^a - A_{22}^* N_{yy}^a + \left[\frac{\partial v_0^a}{\partial y} + \frac{1}{2} \left(\frac{\partial w_0^a}{\partial y} \right)^2 \right] \right\} dx dy = 0 , \\
& \int_{\Omega_e} \bar{W}_6 \left[-A_{66}^* N_{xy}^a + \left(\frac{\partial u_0^a}{\partial y} + \frac{\partial v_0^a}{\partial x} + \frac{1}{2} \frac{\partial w_0^a}{\partial x} \frac{\partial w_0^a}{\partial y} + \frac{1}{2} \frac{\partial w_0^a}{\partial x} \frac{\partial w_0^a}{\partial y} \right) \right] dx dy = 0 , \\
& \int_{\Omega_e} \left(-D_{11}^* \bar{W}_7 M_{xx}^a - D_{12}^* \bar{W}_7 M_{yy}^a + \frac{\partial \bar{W}_7}{\partial x} \frac{\partial w_0^a}{\partial x} \right) dx dy - \oint_{\Gamma_e} \bar{W}_7 \left(n_x \frac{\partial w_0}{\partial x} \right) ds = 0 , \\
& \int_{\Omega_e} \left(-D_{12}^* \bar{W}_8 M_{xx}^a - D_{22}^* \bar{W}_8 M_{yy}^a + \frac{\partial \bar{W}_8}{\partial y} \frac{\partial w_0^a}{\partial y} \right) dx dy - \oint_{\Gamma_e} \bar{W}_8 \left(n_y \frac{\partial w_0}{\partial y} \right) ds = 0 , \\
& \int_{\Omega_e} \left(-D_{66}^* \bar{W}_9 M_{xy}^a + \frac{\partial \bar{W}_9}{\partial x} \frac{\partial w_0^a}{\partial y} + \frac{\partial \bar{W}_9}{\partial y} \frac{\partial w_0^a}{\partial x} \right) dx dy - \oint_{\Gamma_e} \bar{W}_9 \left(n_x \frac{\partial w_0}{\partial y} + n_y \frac{\partial w_0}{\partial x} \right) ds = 0 , \quad (3.6)
\end{aligned}$$

3.2.2 Finite Element Equations of Model II

All variables can be approximated with the Lagrange type interpolation functions for the same reason which was discussed with the Model I.

$$\begin{aligned}
u_0 &\cong u_0^a = \sum_{j=1}^m \psi_j^{u_0}(x, y) \mathbb{w}_j , & \bar{W}_1 &= \psi_i^{u_0}(x, y) , \\
v_0 &\cong v_0^a = \sum_{j=1}^m \psi_j^{v_0}(x, y) \mathbb{v}_j , & \bar{W}_2 &= \psi_i^{v_0}(x, y) , \\
w_0 &\cong w_0^a = \sum_{j=1}^n \psi_j^{w_0}(x, y) \mathbb{w}_j , & \bar{W}_3 &= \psi_i^{w_0}(x, y) , \\
N_{xx} &\cong N_{xx}^a = \sum_{j=1}^p \psi_j^{N_{xx}}(x, y) \mathbb{N}_j^1 , & \bar{W}_4 &= \psi_i^{N_{xx}}(x, y) , \\
N_{yy} &\cong N_{yy}^a = \sum_{j=1}^p \psi_j^{N_{yy}}(x, y) \mathbb{N}_j^2 , & \bar{W}_5 &= \psi_i^{N_{yy}}(x, y) , \\
N_{xy} &\cong N_{xy}^a = \sum_{j=1}^p \psi_j^{N_{xy}}(x, y) \mathbb{N}_j^3 , & \bar{W}_6 &= \psi_i^{N_{xy}}(x, y) , \\
M_{xx} &\cong M_{xx}^a = \sum_{j=1}^r \psi_j^{M_{xx}}(x, y) \mathbb{M}_j^1 , & \bar{W}_7 &= \psi_i^{M_{xx}}(x, y) , \\
M_{yy} &\cong M_{yy}^a = \sum_{j=1}^r \psi_j^{M_{yy}}(x, y) \mathbb{M}_j^2 , & \bar{W}_8 &= \psi_i^{M_{yy}}(x, y) , \\
M_{xy} &\cong M_{xy}^a = \sum_{j=1}^r \psi_j^{M_{xy}}(x, y) \mathbb{M}_j^3 , & \bar{W}_9 &= \psi_i^{M_{xy}}(x, y) .
\end{aligned} \tag{3.7}$$

By substituting the (3.7) into the (3.6), the finite element model of the Model II can be obtained as follow:

$$\begin{aligned}
&\int_{\Omega_e} \left[\sum_{j=1}^p \left(\frac{\partial \psi_i^{u_0}}{\partial x} \psi_j^{N_{xx}} \right) \mathbb{N}_j^1 + \sum_{j=1}^p \left(\frac{\partial \psi_i^{u_0}}{\partial y} \psi_j^{N_{xy}} \right) \mathbb{N}_j^3 \right] dx dy - \oint_{\Gamma_e} \psi_i^{u_0} \{n_x N_{xx} + n_y N_{xy}\} ds = 0 , \\
&\int_{\Omega_e} \left[\sum_{j=1}^p \left(\frac{\partial \psi_i^{v_0}}{\partial x} \psi_j^{N_{xy}} \right) \mathbb{N}_j^3 + \sum_{j=1}^p \left(\frac{\partial \psi_i^{v_0}}{\partial y} \psi_j^{N_{yy}} \right) \mathbb{N}_j^2 \right] dx dy - \oint_{\Gamma_e} \psi_i^{v_0} \{n_x N_{xy} + n_y N_{yy}\} ds = 0 , \\
&\int_{\Omega_e} \left[\sum_{j=1}^r \left(\frac{\partial \psi_i^{w_0}}{\partial x} \frac{\partial \psi_j^{M_{xx}}}{\partial x} \right) \mathbb{M}_j^1 + \sum_{j=1}^r \left(\frac{\partial \psi_i^{w_0}}{\partial x} \frac{\partial \psi_j^{M_{xy}}}{\partial y} \right) \mathbb{M}_j^3 + \frac{\partial \mathbf{w}_0^a}{\partial \mathbf{x}} \sum_{j=1}^p \left(\frac{\partial \psi_i^{w_0}}{\partial x} \psi_j^{N_{xx}} \right) \mathbb{N}_j^1 \right. \\
&\quad + \frac{\partial \mathbf{w}_0^a}{\partial \mathbf{y}} \sum_{j=1}^p \left(\frac{\partial \psi_i^{w_0}}{\partial x} \psi_j^{N_{xy}} \right) \mathbb{N}_j^3 + \sum_{j=1}^r \left(\frac{\partial \psi_i^{w_0}}{\partial y} \frac{\partial \psi_j^{M_{xy}}}{\partial x} \right) \mathbb{M}_j^3 + \sum_{j=1}^r \left(\frac{\partial \psi_i^{w_0}}{\partial y} \frac{\partial \psi_j^{M_{yy}}}{\partial y} \right) \mathbb{M}_j^2 \\
&\quad \left. + \frac{\partial \mathbf{w}_0^a}{\partial \mathbf{x}} \sum_{j=1}^p \left(\frac{\partial \psi_i^{w_0}}{\partial y} \psi_j^{N_{xy}} \right) \mathbb{N}_j^3 + \frac{\partial \mathbf{w}_0^a}{\partial \mathbf{y}} \sum_{j=1}^p \left(\frac{\partial \psi_i^{w_0}}{\partial y} \psi_j^{N_{yy}} \right) \mathbb{N}_j^2 - \psi_i^{w_0} q(x) \right] dx dy \\
&\quad - \oint_{\Gamma_e} \psi_i^{w_0} \{n_x V_x + n_y V_y\} ds = 0 ,
\end{aligned}$$

$$\begin{aligned}
& \int_{\Omega_e} \left\{ -A_{11}^* \sum_{j=1}^p (\psi_i^{N_{xx}} \psi_j^{N_{xx}}) \mathbb{N}_j^1 - A_{12}^* \sum_{j=1}^p (\psi_i^{N_{xx}} \psi_j^{N_{yy}}) \mathbb{N}_j^2 \right. \\
& \quad \left. + \left[\sum_{j=1}^m \left(\psi_i^{N_{xx}} \frac{\partial \psi_j^{u_0}}{\partial x} \right) \mathbb{w}_j + \frac{1}{2} \frac{\partial \mathbf{w}_0^a}{\partial \mathbf{x}} \sum_{j=1}^n \left(\psi_i^{N_{xx}} \frac{\partial \psi_j^{w_0}}{\partial x} \right) \mathbb{w}_j \right] \right\} dx dy = 0 , \\
& \int_{\Omega_e} \left\{ -A_{12}^* \sum_{j=1}^p (\psi_i^{N_{yy}} \psi_j^{N_{xx}}) \mathbb{N}_j^1 - A_{22}^* \sum_{j=1}^p (\psi_i^{N_{yy}} \psi_j^{N_{yy}}) \mathbb{N}_j^2 \right. \\
& \quad \left. + \left[\sum_{j=1}^m \left(\psi_i^{N_{yy}} \frac{\partial \psi_j^{v_0}}{\partial y} \right) \mathbb{v}_j + \frac{1}{2} \frac{\partial \mathbf{w}_0^a}{\partial \mathbf{y}} \sum_{j=1}^n \left(\psi_i^{N_{yy}} \frac{\partial \psi_j^{w_0}}{\partial y} \right) \mathbb{w}_j \right] \right\} dx dy = 0 , \\
& \int_{\Omega_e} \left[-A_{66}^* \sum_{j=1}^p (\psi_i^{N_{xy}} \psi_j^{N_{xy}}) \mathbb{N}_j^3 \right. \\
& \quad \left. + \left(\sum_{j=1}^m \left(\psi_i^{N_{xy}} \frac{\partial \psi_j^{u_0}}{\partial y} \right) \mathbb{w}_j + \sum_{j=1}^m \left(\psi_i^{N_{xy}} \frac{\partial \psi_j^{v_0}}{\partial x} \right) \mathbb{v}_j + \frac{1}{2} \frac{\partial \mathbf{w}_0^a}{\partial \mathbf{x}} \sum_{j=1}^n \left(\psi_i^{N_{xy}} \frac{\partial \psi_j^{w_0}}{\partial y} \right) \mathbb{w}_j \right. \right. \\
& \quad \left. \left. + \frac{1}{2} \frac{\partial \mathbf{w}_0^a}{\partial \mathbf{y}} \sum_{j=1}^n \left(\psi_i^{N_{xy}} \frac{\partial \psi_j^{w_0}}{\partial x} \right) \mathbb{w}_j \right) \right] dx dy = 0 , \\
& \int_{\Omega_e} \left[-D_{11}^* \sum_{j=1}^r (\psi_i^{M_{xx}} \psi_j^{M_{xx}}) \mathbb{M}_j^1 - D_{12}^* \sum_{j=1}^r (\psi_i^{M_{xx}} \psi_j^{M_{yy}}) \mathbb{M}_j^2 \right. \\
& \quad \left. + \sum_{j=1}^n \left(\frac{\partial \psi_i^{M_{xx}}}{\partial x} \frac{\partial \psi_j^{w_0}}{\partial x} \right) \mathbb{w}_j \right] dx dy - \oint_{\Gamma_e} \psi_i^{M_{xx}} \left(n_x \frac{\partial w_0}{\partial x} \right) ds = 0 , \\
& \int_{\Omega_e} \left[-D_{12}^* \sum_{j=1}^r (\psi_i^{M_{yy}} \psi_j^{M_{xx}}) \mathbb{M}_j^1 - D_{22}^* \sum_{j=1}^r (\psi_i^{M_{yy}} \psi_j^{M_{yy}}) \mathbb{M}_j^2 \right. \\
& \quad \left. + \sum_{j=1}^n \left(\frac{\partial \psi_i^{M_{yy}}}{\partial y} \frac{\partial \psi_j^{w_0}}{\partial y} \right) \mathbb{w}_j \right] dx dy - \oint_{\Gamma_e} \psi_i^{M_{yy}} \left(n_y \frac{\partial w_0}{\partial y} \right) ds = 0 , \\
& \int_{\Omega_e} \left[-D_{66}^* \sum_{j=1}^r (\psi_i^{M_{xy}} \psi_j^{M_{xy}}) \mathbb{M}_j^3 + \sum_{j=1}^n \left(\frac{\partial \psi_i^{M_{xy}}}{\partial x} \frac{\partial \psi_j^{w_0}}{\partial y} \right) \mathbb{w}_j \right. \\
& \quad \left. + \sum_{j=1}^n \left(\frac{\partial \psi_i^{M_{xy}}}{\partial y} \frac{\partial \psi_j^{w_0}}{\partial x} \right) \mathbb{w}_j \right] dx dy - \oint_{\Gamma_e} \psi_i^{M_{xy}} \left(n_x \frac{\partial w_0}{\partial y} + n_y \frac{\partial w_0}{\partial x} \right) ds = 0 . \tag{3.8}
\end{aligned}$$

Above equation (3. 8) can be rewritten as the matrix form of the algebraic equation as follow:

$$\begin{aligned}
& [\mathbf{K}^e(\{\mathbf{U}^e\})] \{\mathbf{U}^e\} = \{\mathbf{F}^e\} \\
& = \begin{bmatrix} [\mathbf{K}^{(1)(1)}] & \dots & [\mathbf{K}^{(1)(4)}] & \dots & [\mathbf{K}^{(1)(9)}] \\ \vdots & \ddots & \vdots & \ddots & \vdots \\ [\mathbf{K}^{(4)(1)}] & \dots & [\mathbf{K}^{(4)(4)}] & \dots & [\mathbf{K}^{(6)(9)}] \\ \vdots & \ddots & \vdots & \ddots & \vdots \\ [\mathbf{K}^{(9)(1)}] & \dots & [\mathbf{K}^{(9)(6)}] & \dots & [\mathbf{K}^{(9)(9)}] \end{bmatrix} \begin{Bmatrix} \{\mathbb{w}_j\} \\ \{\mathbb{N}_j^1\} \\ \vdots \\ \{\mathbb{M}_j^3\} \end{Bmatrix} = \begin{Bmatrix} \{\mathbf{F}^{(1)}\} \\ \vdots \\ \{\mathbf{F}^{(4)}\} \\ \vdots \\ \{\mathbf{F}^{(9)}\} \end{Bmatrix} . \tag{3.9}
\end{aligned}$$

where,

$$\begin{aligned}
[K^{14}] &= \int_{\Omega_e} \left\{ \frac{\partial \psi_i^{u_0}}{\partial x} \psi_j^{N_{xx}} \right\} dx dy , & [K^{16}] &= \int_{\Omega_e} \left\{ \frac{\partial \psi_i^{u_0}}{\partial y} \psi_j^{N_{xy}} \right\} dx dy , \\
[K^{25}] &= \int_{\Omega_e} \left\{ \frac{\partial \psi_i^{v_0}}{\partial y} \psi_j^{N_{yy}} \right\} dx dy , & [K^{26}] &= \int_{\Omega_e} \left\{ \frac{\partial \psi_i^{v_0}}{\partial x} \psi_j^{N_{xy}} \right\} dx dy , \\
[K^{37}] &= \int_{\Omega_e} \left\{ \frac{\partial \psi_i^{w_0}}{\partial x} \psi_j^{V_x} \right\} dx dy , & [K^{38}] &= \int_{\Omega_e} \left\{ \frac{\partial \psi_i^{w_0}}{\partial y} \psi_j^{V_y} \right\} dx dy , \\
[K^{41}] &= \int_{\Omega_e} \left\{ \psi_i^{N_{xx}} \frac{\partial \psi_j^{u_0}}{\partial x} \right\} dx dy , & [K^{43}] &= \int_{\Omega_e} \left\{ \frac{1}{2} \left(\frac{\partial \mathbf{w}_0^a}{\partial \mathbf{x}} \right) \psi_i^{N_{xx}} \frac{\partial \psi_j^{w_0}}{\partial x} \right\} dx dy \\
[K^{44}] &= \int_{\Omega_e} \left\{ -A_{11}^* \psi_i^{N_{xx}} \psi_j^{N_{xx}} \right\} dx dy , & [K^{45}] &= \int_{\Omega_e} \left\{ -A_{12}^* \psi_i^{N_{xx}} \psi_j^{N_{yy}} \right\} dx dy , \\
[K^{52}] &= \int_{\Omega_e} \left\{ \psi_i^{N_{yy}} \frac{\partial \psi_j^{v_0}}{\partial y} \right\} dx dy , & [K^{53}] &= \int_{\Omega_e} \left\{ \frac{1}{2} \left(\frac{\partial \mathbf{w}_0^a}{\partial \mathbf{y}} \right) \psi_i^{N_{yy}} \frac{\partial \psi_j^{w_0}}{\partial y} \right\} dx dy , \\
[K^{54}] &= \int_{\Omega_e} \left\{ -A_{12}^* \psi_i^{N_{yy}} \psi_j^{N_{xx}} \right\} dx dy , & [K^{55}] &= \int_{\Omega_e} \left\{ -A_{22}^* \psi_i^{N_{yy}} \psi_j^{N_{yy}} \right\} dx dy , \\
[K^{61}] &= \int_{\Omega_e} \left\{ \psi_i^{N_{xy}} \frac{\partial \psi_j^{u_0}}{\partial y} \right\} dx dy , & [K^{62}] &= \int_{\Omega_e} \left\{ \psi_i^{N_{xy}} \frac{\partial \psi_j^{v_0}}{\partial x} \right\} dx dy , \\
[K^{66}] &= \int_{\Omega_e} \left\{ -A_{66}^* \psi_i^{N_{xy}} \psi_j^{N_{xy}} \right\} dx dy , \\
[K^{63}] &= \int_{\Omega_e} \left\{ \frac{1}{2} \left[\left(\frac{\partial \mathbf{w}_0^a}{\partial \mathbf{x}} \right) \psi_i^{N_{xy}} \frac{\partial \psi_j^w}{\partial y} + \left(\frac{\partial \mathbf{w}_0^a}{\partial \mathbf{y}} \right) \psi_i^{N_{xy}} \frac{\partial \psi_j^w}{\partial x} \right] \right\} dx dy , \\
[K^{74}] &= \int_{\Omega_e} \left\{ \left(\frac{\partial \mathbf{w}_0^a}{\partial \mathbf{x}} \right) \psi_i^{V_x} \psi_j^{N_{xx}} \right\} dx dy , & [K^{76}] &= \int_{\Omega_e} \left\{ \left(\frac{\partial \mathbf{w}_0^a}{\partial \mathbf{y}} \right) \psi_i^{V_x} \psi_j^{N_{xy}} \right\} dx dy , \\
[K^{77}] &= \int_{\Omega_e} \left\{ -\psi_i^{V_x} \psi_j^{V_x} \right\} dx dy , \\
[K^{79}] &= \int_{\Omega_e} \left\{ \psi_i^{V_x} \frac{\partial \psi_j^{M_{xx}}}{\partial x} \right\} dx dy , & [K^{7(11)}] &= \int_{\Omega_e} \left\{ \psi_i^{V_x} \frac{\partial \psi_j^{M_{xy}}}{\partial y} \right\} dx dy , \\
[K^{85}] &= \int_{\Omega_e} \left\{ \left(\frac{\partial \mathbf{w}_0^a}{\partial \mathbf{y}} \right) \psi_i^{V_y} \psi_j^{N_{yy}} \right\} dx dy , & [K^{86}] &= \int_{\Omega_e} \left\{ \left(\frac{\partial \mathbf{w}_0^a}{\partial \mathbf{x}} \right) \psi_i^{V_y} \psi_j^{N_{xy}} \right\} dx dy , \\
[K^{88}] &= \int_{\Omega_e} \left\{ -\psi_i^{V_y} \psi_j^{V_y} \right\} dx dy ,
\end{aligned}$$

$$\begin{aligned}
[K^{8(10)}] &= \int_{\Omega_e} \left\{ \psi_i^{V_y} \frac{\partial \psi_j^{M_{yy}}}{\partial y} \right\} dx dy , & [K^{8(11)}] &= \int_{\Omega_e} \left\{ \psi_i^{V_y} \frac{\partial \psi_j^{M_{xy}}}{\partial x} \right\} dx dy , \\
[K^{93}] &= \int_{\Omega_e} \left\{ \frac{\partial \psi_i^{M_{xx}}}{\partial x} \frac{\partial \psi_j^{w_0}}{\partial x} \right\} dx dy , & [K^{99}] &= \int_{\Omega_e} \left\{ -D_{11}^* \psi_i^{M_{xx}} \psi_j^{M_{xx}} \right\} dx dy , \\
[K^{9(10)}] &= \int_{\Omega_e} \left\{ -D_{12}^* \psi_i^{M_{xx}} \psi_j^{M_{yy}} \right\} dx dy , \\
[K^{(10)3}] &= \int_{\Omega_e} \left\{ \frac{\partial \psi_i^{M_{xx}}}{\partial y} \frac{\partial \psi_j^{w_0}}{\partial y} \right\} dx dy , & [K^{(10)9}] &= \int_{\Omega_e} \left\{ -D_{12}^* \psi_i^{M_{yy}} \psi_j^{M_{xx}} \right\} dx dy , \\
[K^{(10)(10)}] &= \int_{\Omega_e} \left\{ -D_{22}^* \psi_i^{M_{yy}} \psi_j^{M_{yy}} \right\} dx dy , & [K^{(11)(11)}] &= \int_{\Omega_e} \left\{ -D_{66}^* \psi_i^{M_{xy}} \psi_j^{M_{xy}} \right\} dx dy . \\
[K^{(11)3}] &= \int_{\Omega_e} \left\{ \frac{\partial \psi_i^{M_{xy}}}{\partial x} \frac{\partial \psi_j^{w_0}}{\partial y} + \frac{\partial \psi_i^{M_{xy}}}{\partial y} \frac{\partial \psi_j^{w_0}}{\partial x} \right\} dx dy , \\
\{F^1\} &= \oint_{\Gamma_e} \psi_i^u \{n_x N_{xx} + n_y N_{xy}\} ds , & \{F^2\} &= \oint_{\Gamma_e} \psi_i^v \{n_x N_{xy} + n_y N_{yy}\} ds , \\
\{F^3\} &= \int_{\Omega_e} \{ \psi_i^w q(x) \} dx dy + \oint_{\Gamma_e} \psi_i^w Q_n ds , \\
\{F^9\} &= \oint_{\Gamma_e} \psi_i^{M_{xx}} \left(\frac{\partial w_0}{\partial x} n_x \right) ds , & \{F^{(10)}\} &= \oint_{\Gamma_e} \psi_i^{M_{yy}} \left(\frac{\partial w_0}{\partial y} n_y \right) ds , \\
\{F^{(11)}\} &= \oint_{\Gamma_e} \left\{ \psi_i^{M_{xy}} \left(\frac{\partial w_0}{\partial y} n_x + \frac{\partial w_0}{\partial x} n_y \right) \right\} ds . & & (3.10)
\end{aligned}$$

The rest of the sub coefficient matrices and the force vectors which are not specified in the (3.10) are equal to zero.

3.3 Model III of Plate Bending

3.3.1 Weighted Residual Statements of Model III

To develop the Model III of the plate bending, the governing equations of the FSDT are modified. The Model III will include the shear rotations ϕ_x and ϕ_y to account

for the shear deformations. The weighed residual statements of this model can be made as follow:

$$\begin{aligned}
& \int_{\Omega_e} \left(\frac{\partial \bar{W}_1}{\partial x} N_{xx}^a + \frac{\partial \bar{W}_1}{\partial y} N_{xy}^a \right) dx dy - \oint_{\Gamma_e} \bar{W}_1 (n_x N_{xx} + n_y N_{xy}) ds = 0 , \\
& \int_{\Omega_e} \left(\frac{\partial \bar{W}_2}{\partial x} N_{xy}^a + \frac{\partial \bar{W}_2}{\partial y} N_{yy}^a \right) dx dy - \oint_{\Gamma_e} \bar{W}_2 (n_x N_{xy} + n_y N_{yy}) ds = 0 , \\
& \int_{\Omega_e} \left[\frac{\partial \bar{W}_3}{\partial x} Q_x^a + \frac{\partial \bar{W}_3}{\partial y} Q_y^a + \frac{\partial \bar{W}_3}{\partial x} \left(N_{xx}^a \frac{\partial w_0^a}{\partial x} + N_{xy}^a \frac{\partial w_0^a}{\partial y} \right) + \frac{\partial \bar{W}_3}{\partial y} \left(N_{xy}^a \frac{\partial w_0^a}{\partial x} + N_{yy}^a \frac{\partial w_0^a}{\partial y} \right) \right. \\
& \quad \left. - \bar{W}_3 q(x) \right] dx dy = 0 \\
& + \oint_{\Gamma_e} \bar{W}_3 \left[\left(Q_x + N_{xx} \frac{\partial w_0}{\partial x} + N_{xy} \frac{\partial w_0}{\partial y} \right) n_x + \left(Q_y + N_{xy} \frac{\partial w_0}{\partial x} + N_{yy} \frac{\partial w_0}{\partial y} \right) n_y \right] ds = 0 , \\
& \int_{\Omega_e} \left(\frac{\partial \bar{W}_4}{\partial x} M_{xx}^a + \frac{\partial \bar{W}_4}{\partial y} M_{xy}^a + \bar{W}_4 Q_x^a \right) dx dy + \oint_{\Gamma_e} \bar{W}_4 (M_{xx} n_x + M_{xy} n_y) ds = 0 , \\
& \int_{\Omega_e} \left(\frac{\partial \bar{W}_5}{\partial x} M_{xy}^a + \frac{\partial \bar{W}_5}{\partial y} M_{yy}^a + \bar{W}_5 Q_y^a \right) dx dy + \oint_{\Gamma_e} \bar{W}_5 (M_{xy} n_x + M_{yy} n_y) ds = 0 , \\
& \int_{\Omega_e} \bar{W}_6 \left\{ -A_{11}^* N_{xx}^a - A_{12}^* N_{yy}^a + \left[\frac{\partial u_0^a}{\partial x} + \frac{1}{2} \left(\frac{\partial w_0^a}{\partial x} \right)^2 \right] \right\} dx dy = 0 , \\
& \int_{\Omega_e} \bar{W}_7 \left\{ -A_{12}^* N_{xx}^a - A_{22}^* N_{yy}^a + \left[\frac{\partial v_0^a}{\partial y} + \frac{1}{2} \left(\frac{\partial w_0^a}{\partial y} \right)^2 \right] \right\} dx dy = 0 , \\
& \int_{\Omega_e} \bar{W}_8 \left[-A_{66}^* N_{xy}^a + \left(\frac{\partial u_0^a}{\partial y} + \frac{\partial v_0^a}{\partial x} + \frac{1}{2} \frac{\partial w_0^a}{\partial x} \frac{\partial w_0^a}{\partial y} + \frac{1}{2} \frac{\partial w_0^a}{\partial x} \frac{\partial w_0^a}{\partial y} \right) \right] dx dy = 0 , \\
& \int_{\Omega_e} \bar{W}_9 \left(-\frac{Q_x^a}{K_s A_{55}} + \frac{\partial w_0^a}{\partial x} + \phi_x^a \right) dx dy = 0 , \\
& \int_{\Omega_e} \bar{W}_{10} \left(-\frac{Q_y^a}{K_s A_{44}} + \frac{\partial w_0^a}{\partial y} + \phi_y^a \right) dx dy = 0 , \\
& \int_{\Omega_e} \bar{W}_{11} \left(-D_{11}^* M_{xx}^a - D_{12}^* M_{yy}^a + \frac{\partial \phi_x^a}{\partial x} \right) dx dy = 0 , \\
& \int_{\Omega_e} \bar{W}_{12} \left(-D_{12}^* M_{xx}^a - D_{22}^* M_{yy}^a + \frac{\partial \phi_y^a}{\partial y} \right) dx dy = 0 , \\
& \int_{\Omega_e} \bar{W}_{13} \left(-D_{66}^* M_{xy}^a + \frac{\partial \phi_x^a}{\partial y} + \frac{\partial \phi_y^a}{\partial x} \right) dx dy = 0 .
\end{aligned} \tag{3.11}$$

where Ω_e and Γ_e denote the element region and the boundary of the element respectively.

3.3.2 Finite Element Equations of Model III

For the Model III, the Lagrange type of interpolation functions can be used to approximate the variables. The weight functions and the approximations of the variables can be chosen as follow:

$$\begin{aligned}
u_0 &\cong u_0^a = \sum_{j=1}^l \psi_j^{u_0}(x, y) \mathbb{U}_j, & \bar{W}_1 &= \psi_i^{u_0}(x, y), \\
v_0 &\cong v_0^a = \sum_{j=1}^l \psi_j^{v_0}(x, y) \mathbb{V}_j, & \bar{W}_2 &= \psi_i^{v_0}(x, y), \\
w_0 &\cong w_0^a = \sum_{j=1}^m \psi_j^{w_0}(x, y) \mathbb{W}_j, & \bar{W}_3 &= \psi_i^{w_0}(x, y), \\
\phi_x &\cong \phi_x^a = \sum_{j=1}^n \psi_j^{\phi_x}(x, y) \mathbb{P}_j^1, & \bar{W}_4 &= \psi_i^{\phi_x}(x, y), \\
\phi_y &\cong \phi_y^a = \sum_{j=1}^n \psi_j^{\phi_y}(x, y) \mathbb{P}_j^2, & \bar{W}_5 &= \psi_i^{\phi_y}(x, y), \\
N_{xx} &\cong N_{xx}^a = \sum_{j=1}^p \psi_j^{N_{xx}}(x, y) \mathbb{N}_j^1, & \bar{W}_6 &= \psi_i^{N_{xx}}(x, y), \\
N_{yy} &\cong N_{yy}^a = \sum_{j=1}^p \psi_j^{N_{yy}}(x, y) \mathbb{N}_j^2, & \bar{W}_7 &= \psi_i^{N_{yy}}(x, y), \\
N_{xy} &\cong N_{xy}^a = \sum_{j=1}^p \psi_j^{N_{xy}}(x, y) \mathbb{N}_j^3, & \bar{W}_8 &= \psi_i^{N_{xy}}(x, y), \\
Q_x &\cong Q_x^a = \sum_{j=1}^q \psi_j^{Q_x}(x, y) \mathbb{Q}_j^1, & \bar{W}_9 &= \psi_i^{Q_x}(x, y), \\
Q_y &\cong Q_y^a = \sum_{j=1}^q \psi_j^{Q_y}(x, y) \mathbb{Q}_j^2, & \bar{W}_{10} &= \psi_i^{Q_y}(x, y), \\
M_{xx} &\cong M_{xx}^a = \sum_{j=1}^r \psi_j^{M_{xx}}(x, y) \mathbb{M}_j^1, & \bar{W}_{11} &= \psi_i^{M_{xx}}(x, y), \\
M_{yy} &\cong M_{yy}^a = \sum_{j=1}^r \psi_j^{M_{yy}}(x, y) \mathbb{M}_j^2, & \bar{W}_{12} &= \psi_i^{M_{yy}}(x, y), \\
M_{xy} &\cong M_{xy}^a = \sum_{j=1}^r \psi_j^{M_{xy}}(x, y) \mathbb{M}_j^3, & \bar{W}_{13} &= \psi_i^{M_{xy}}(x, y).
\end{aligned} \tag{3.12}$$

The primary variables and the secondary variable of the Model III can be specified as follow :

<The primary variable>	<The secondary variable>
u_0	$n_x N_{xx} + n_y N_{xy}$
v_0	$n_x N_{xy} + n_y N_{yy}$
w_0	$V_x n_x + V_y n_y$
ϕ_x	$M_{xx} n_x + M_{xy} n_y$
ϕ_y	$M_{xy} n_x + M_{yy} n_y$

The finite element equations can be obtained by substituting the approximations and the weight functions of the (3.12) into the (3.11).

$$\begin{aligned}
& \int_{\Omega_e} \left(\sum_{j=1}^p \left(\frac{\partial \psi_i^{u_0}}{\partial x} \psi_j^{N_{xx}} \right) \mathbb{N}_j^1 + \sum_{j=1}^p \left(\frac{\partial \psi_i^{u_0}}{\partial y} \psi_j^{N_{xy}} \right) \mathbb{N}_j^3 \right) dx dy - \oint_{\Gamma_e} \psi_i^{u_0} (n_x N_{xx} + n_y N_{xy}) ds = 0 , \\
& \int_{\Omega_e} \left(\sum_{j=1}^p \left(\frac{\partial \psi_i^{v_0}}{\partial x} \psi_j^{N_{xy}} \right) \mathbb{N}_j^3 + \sum_{j=1}^p \left(\frac{\partial \psi_i^{v_0}}{\partial y} \psi_j^{N_{yy}} \right) \mathbb{N}_j^2 \right) dx dy - \oint_{\Gamma_e} \psi_i^{v_0} (n_x N_{xy} + n_y N_{yy}) ds = 0 , \\
& \int_{\Omega_e} \left\{ \sum_{j=1}^q \left(\frac{\partial \psi_i^{w_0}}{\partial x} \psi_j^{Q_x} \right) \mathbb{Q}_j^1 + \sum_{j=1}^q \left(\frac{\partial \psi_i^{w_0}}{\partial y} \psi_j^{Q_y} \right) \mathbb{Q}_j^2 \right. \\
& \quad + \left[\frac{\partial \mathbf{w}_0^a}{\partial \mathbf{x}} \sum_{j=1}^p \left(\frac{\partial \psi_i^{w_0}}{\partial x} \psi_j^{N_{xx}} \right) \mathbb{N}_j^1 + \frac{\partial \mathbf{w}_0^a}{\partial \mathbf{y}} \sum_{j=1}^p \left(\frac{\partial \psi_i^{w_0}}{\partial x} \psi_j^{N_{xy}} \right) \mathbb{N}_j^3 \right] \\
& \quad + \left[\frac{\partial \mathbf{w}_0^a}{\partial \mathbf{x}} \sum_{j=1}^p \left(\frac{\partial \psi_i^{w_0}}{\partial y} \psi_j^{N_{xy}} \right) \mathbb{N}_j^3 + \frac{\partial \mathbf{w}_0^a}{\partial \mathbf{y}} \sum_{j=1}^p \left(\frac{\partial \psi_i^{w_0}}{\partial y} \psi_j^{N_{yy}} \right) \mathbb{N}_j^2 \right] - \psi_i^{w_0} q(x) \left. \right\} dx dy \\
& \quad + \oint_{\Gamma_e} \psi_i^{w_0} \left[\left(Q_x + N_{xx} \frac{\partial w_0}{\partial x} + N_{xy} \frac{\partial w_0}{\partial y} \right) n_x + \left(Q_y + N_{xy} \frac{\partial w_0}{\partial x} + N_{yy} \frac{\partial w_0}{\partial y} \right) n_y \right] ds = 0 , \\
& \int_{\Omega_e} \left[\sum_{j=1}^r \left(\frac{\partial \psi_i^{\phi_x}}{\partial x} \psi_j^{M_{xx}} \right) \mathbb{M}_j^1 + \sum_{j=1}^r \left(\frac{\partial \psi_i^{\phi_x}}{\partial y} \psi_j^{M_{xy}} \right) \mathbb{M}_j^3 + \sum_{j=1}^q \left(\psi_i^{\phi_x} \psi_j^{Q_x} \right) \mathbb{Q}_j^1 \right] dx dy \\
& \quad + \oint_{\Gamma_e} \psi_i^{\phi_x} (M_{xx} n_x + M_{xy} n_y) ds = 0 ,
\end{aligned}$$

$$\begin{aligned}
& \int_{\Omega_e} \left[\sum_{j=1}^r \left(\frac{\partial \psi_i^{\phi_y}}{\partial x} \psi_j^{M_{xy}} \right) \mathbb{M}_j^3 + \sum_{j=1}^r \left(\frac{\partial \psi_i^{\phi_y}}{\partial y} \psi_j^{M_{yy}} \right) \mathbb{M}_j^2 + \sum_{j=1}^q \left(\psi_i^{\phi_y} \psi_j^{Q_y} \right) \mathbb{Q}_j^2 \right] dx dy \\
& \quad + \oint_{\Gamma_e} \psi_i^{\phi_y} (M_{xy} n_x + M_{yy} n_y) ds = 0 , \\
& \int_{\Omega_e} \left\{ -A_{11}^* \sum_{j=1}^p \left(\psi_i^{N_{xx}} \psi_j^{N_{xx}} \right) \mathbb{N}_j^1 - A_{12}^* \sum_{j=1}^p \left(\psi_i^{N_{xx}} \psi_j^{N_{yy}} \right) \mathbb{N}_j^2 \right. \\
& \quad \left. + \left[\sum_{j=1}^m \left(\psi_i^{N_{xx}} \frac{\partial \psi_j^{u_0}}{\partial x} \right) \mathbb{W}_j + \frac{1}{2} \frac{\partial \mathbf{w}_0^a}{\partial \mathbf{x}} \sum_{j=1}^n \left(\psi_i^{N_{xx}} \frac{\partial \psi_j^{w_0}}{\partial x} \right) \mathbb{W}_j \right] \right\} dx dy = 0 , \\
& \int_{\Omega_e} \left\{ -A_{12}^* \sum_{j=1}^p \left(\psi_i^{N_{yy}} \psi_j^{N_{xx}} \right) \mathbb{N}_j^1 - A_{22}^* \sum_{j=1}^p \left(\psi_i^{N_{yy}} \psi_j^{N_{yy}} \right) \mathbb{N}_j^2 \right. \\
& \quad \left. + \left[\sum_{j=1}^m \left(\psi_i^{N_{yy}} \frac{\partial \psi_j^{v_0}}{\partial y} \right) \mathbb{V}_j + \frac{1}{2} \frac{\partial \mathbf{w}_0^a}{\partial \mathbf{y}} \sum_{j=1}^n \left(\psi_i^{N_{yy}} \frac{\partial \psi_j^{w_0}}{\partial y} \right) \mathbb{W}_j \right] \right\} dx dy = 0 , \\
& \int_{\Omega_e} \left\{ - \sum_{j=1}^r \left(\psi_i^{N_{xy}} \psi_j^{M_{xy}} \right) \mathbb{M}_j^3 \right. \\
& \quad + A_{66} \left[\sum_{j=1}^l \left(\psi_i^{N_{xy}} \frac{\partial \psi_j^{u_0}}{\partial y} \right) \mathbb{W}_j + \sum_{j=1}^l \left(\psi_i^{N_{xy}} \frac{\partial \psi_j^{v_0}}{\partial x} \right) \mathbb{V}_j + \frac{1}{2} \frac{\partial \mathbf{w}_0^a}{\partial \mathbf{x}} \sum_{j=1}^m \left(\psi_i^{N_{xy}} \frac{\partial \psi_j^{w_0}}{\partial y} \right) \mathbb{W}_j \right. \\
& \quad \left. + \frac{1}{2} \frac{\partial \mathbf{w}_0^a}{\partial \mathbf{x}} \sum_{j=1}^m \left(\psi_i^{N_{xy}} \frac{\partial \psi_j^{w_0}}{\partial y} \right) \mathbb{W}_j \right] \right\} dx dy = 0 , \\
& \int_{\Omega_e} \left[-\frac{1}{K_s A_{55}} \sum_{j=1}^q \left(\psi_i^{Q_x} \psi_j^{Q_x} \right) \mathbb{Q}_j^1 + \sum_{j=1}^m \left(\psi_i^{Q_x} \frac{\partial \psi_j^{w_0}}{\partial x} \right) \mathbb{W}_j + \sum_{j=1}^n \left(\psi_i^{Q_x} \psi_j^{\phi_x} \right) \mathbb{P}_j^1 \right] dx dy = 0 , \\
& \int_{\Omega_e} \left[-\frac{1}{K_s A_{44}} \sum_{j=1}^q \left(\psi_i^{Q_y} \psi_j^{Q_y} \right) \mathbb{Q}_j^2 + \sum_{j=1}^m \left(\psi_i^{Q_y} \frac{\partial \psi_j^{w_0}}{\partial y} \right) \mathbb{W}_j + \sum_{j=1}^n \left(\psi_i^{Q_y} \psi_j^{\phi_y} \right) \mathbb{P}_j^2 \right] dx dy = 0 , \\
& \int_{\Omega_e} \left[-D_{11}^* \sum_{j=1}^r \left(\psi_i^{M_{xx}} \psi_j^{M_{xx}} \right) \mathbb{M}_j^1 - D_{12}^* \sum_{j=1}^r \left(\psi_i^{M_{xx}} \psi_j^{M_{yy}} \right) \mathbb{M}_j^2 + \sum_{j=1}^n \left(\psi_i^{M_{xx}} \frac{\partial \psi_j^{\phi_x}}{\partial x} \right) \mathbb{P}_j^1 \right] dx dy = 0 , \\
& \int_{\Omega_e} \left[-D_{12}^* \sum_{j=1}^r \left(\psi_i^{M_{yy}} \psi_j^{M_{xx}} \right) \mathbb{M}_j^1 - D_{22}^* \sum_{j=1}^r \left(\psi_i^{M_{yy}} \psi_j^{M_{yy}} \right) \mathbb{M}_j^2 + \sum_{j=1}^n \left(\psi_i^{M_{yy}} \frac{\partial \psi_j^{\phi_y}}{\partial y} \right) \mathbb{P}_j^2 \right] dx dy = 0 , \\
& \int_{\Omega_e} \left[-D_{66}^* \sum_{j=1}^r \left(\psi_i^{M_{xy}} \psi_j^{M_{xy}} \right) \mathbb{M}_j^3 + \sum_{j=1}^n \left(\psi_i^{M_{xy}} \frac{\partial \psi_j^{\phi_y}}{\partial y} \right) \mathbb{P}_j^2 + \sum_{j=1}^n \left(\psi_i^{M_{xy}} \frac{\partial \psi_j^{\phi_x}}{\partial x} \right) \mathbb{P}_j^1 \right] dx dy = 0 .
\end{aligned}
\tag{3.13}$$

Above equations of the (3.14) can be rewritten as the algebraic matrix equation in the form of,

$$\begin{aligned}
& [K^e(\{U^e\})]\{U^e\} = \{F^e\} \\
& = \begin{bmatrix} [K^{(1)(1)}] & \dots & [K^{(1)(7)}] & \dots & [K^{(1)(13)}] \\ \vdots & \ddots & \vdots & \ddots & \vdots \\ [K^{(7)(1)}] & \dots & & \dots & [K^{(7)(13)}] \\ \vdots & \ddots & \vdots & \ddots & \vdots \\ [K^{(13)(1)}] & \dots & [K^{(13)(6)}] & \dots & [K^{(13)(13)}] \end{bmatrix} \begin{Bmatrix} \{\mathbb{U}_j\} \\ \vdots \\ \{\mathbb{N}_j^2\} \\ \vdots \\ \{\mathbb{M}_j^3\} \end{Bmatrix} = \begin{Bmatrix} \{\mathbb{F}^{(1)}\} \\ \vdots \\ \{\mathbb{F}^{(7)}\} \\ \vdots \\ \{\mathbb{F}^{(13)}\} \end{Bmatrix} . \tag{3.14}
\end{aligned}$$

The specific sub coefficient matrices can be obtained from the (3.13) as follow:

$$\begin{aligned}
[K^{16}] &= \int_{\Omega_e} \left\{ \frac{\partial \psi_i^{u_0}}{\partial x} \psi_j^{N_{xx}} \right\} dx dy & [K^{18}] &= \int_{\Omega_e} \left\{ \frac{\partial \psi_i^{u_0}}{\partial y} \psi_j^{N_{xy}} \right\} dx dy \\
[K^{27}] &= \int_{\Omega_e} \left\{ \frac{\partial \psi_i^{v_0}}{\partial y} \psi_j^{N_{yy}} \right\} dx dy & [K^{28}] &= \int_{\Omega_e} \left\{ \frac{\partial \psi_i^{v_0}}{\partial x} \psi_j^{N_{xy}} \right\} dx dy \\
[K^{39}] &= \int_{\Omega_e} \left\{ \frac{\partial \psi_i^{w_0}}{\partial x} \psi_j^{Q_x} \right\} dx dy & [K^{3(10)}] &= \int_{\Omega_e} \left\{ \frac{\partial \psi_i^{w_0}}{\partial y} \psi_j^{Q_y} \right\} dx dy \\
[K^{36}] &= \int_{\Omega_e} \left\{ \left(\frac{\partial \mathbf{w}_0^a}{\partial \mathbf{x}} \right) \frac{\partial \psi_i^{w_0}}{\partial x} \psi_j^{N_{xx}} \right\} dx dy & [K^{37}] &= \int_{\Omega_e} \left\{ \left(\frac{\partial \mathbf{w}_0^a}{\partial \mathbf{y}} \right) \frac{\partial \psi_i^{w_0}}{\partial y} \psi_j^{N_{yy}} \right\} dx dy \\
[K^{38}] &= \int_{\Omega_e} \left\{ \left(\frac{\partial \mathbf{w}_0^a}{\partial \mathbf{y}} \right) \frac{\partial \psi_i^{w_0}}{\partial x} \psi_j^{N_{xy}} + \left(\frac{\partial \mathbf{w}_0^a}{\partial \mathbf{x}} \right) \frac{\partial \psi_i^{w_0}}{\partial y} \psi_j^{N_{xy}} \right\} dx dy \\
[K^{4(11)}] &= \int_{\Omega_e} \left\{ \frac{\partial \psi_i^{\phi_x}}{\partial x} \psi_j^{M_{xx}} \right\} dx dy & [K^{4(13)}] &= \int_{\Omega_e} \left\{ \frac{\partial \psi_i^{\phi_x}}{\partial y} \psi_j^{M_{xy}} \right\} dx dy \\
[K^{49}] &= \int_{\Omega_e} \left\{ \psi_i^{\phi_x} \psi_j^{Q_x} \right\} dx dy \\
[K^{5(12)}] &= \int_{\Omega_e} \left\{ \frac{\partial \psi_i^{\phi_y}}{\partial y} \psi_j^{M_{yy}} \right\} dx dy & [K^{5(13)}] &= \int_{\Omega_e} \left\{ \frac{\partial \psi_i^{\phi_y}}{\partial x} \psi_j^{M_{xy}} \right\} dx dy
\end{aligned}$$

$$\begin{aligned}
[K^{5(10)}] &= \int_{\Omega_e} \{\psi_i^{\phi_y} \psi_j^{Q_y}\} dx dy \\
[K^{61}] &= \int_{\Omega_e} \left\{ \psi_i^{N_{xx}} \frac{\partial \psi_j^{u_0}}{\partial x} \right\} dx dy, & [K^{63}] &= \int_{\Omega_e} \left\{ \frac{1}{2} \left(\frac{\partial \mathbf{w}_0^a}{\partial \mathbf{x}} \right) \psi_i^{N_{xx}} \frac{\partial \psi_j^{w_0}}{\partial x} \right\} dx dy \\
[K^{66}] &= \int_{\Omega_e} \{-A_{11}^* \psi_i^{N_{xx}} \psi_j^{N_{xx}}\} dx dy, & [K^{67}] &= \int_{\Omega_e} \{-A_{12}^* \psi_i^{N_{xx}} \psi_j^{N_{yy}}\} dx dy, \\
[K^{72}] &= \int_{\Omega_e} \left\{ \psi_i^{N_{yy}} \frac{\partial \psi_j^{v_0}}{\partial y} \right\} dx dy, & [K^{73}] &= \int_{\Omega_e} \left\{ \frac{1}{2} \left[\left(\frac{\partial \mathbf{w}_0^a}{\partial \mathbf{y}} \right) \psi_i^{N_{yy}} \frac{\partial \psi_j^{w_0}}{\partial y} \right] \right\} dx dy, \\
[K^{76}] &= \int_{\Omega_e} \{-A_{12}^* \psi_i^{N_{yy}} \psi_j^{N_{xx}}\} dx dy, & [K^{77}] &= \int_{\Omega_e} \{-A_{22}^* \psi_i^{N_{yy}} \psi_j^{N_{yy}}\} dx dy, \\
[K^{88}] &= \int_{\Omega_e} \{-A_{66}^* \psi_i^{N_{xy}} \psi_j^{N_{xy}}\} dx dy & [K^{81}] &= \int_{\Omega_e} \left\{ \psi_i^{N_{xy}} \frac{\partial \psi_j^{u_0}}{\partial y} \right\} dx dy \\
[K^{82}] &= \int_{\Omega_e} \left\{ \psi_i^{N_{xy}} \frac{\partial \psi_j^{v_0}}{\partial x} \right\} dx dy \\
[K^{83}] &= \int_{\Omega_e} \left\{ \frac{1}{2} \left[\left(\frac{\partial \mathbf{w}_0^a}{\partial \mathbf{x}} \right) \psi_i^{N_{xy}} \frac{\partial \psi_j^{w_0}}{\partial y} + \left(\frac{\partial \mathbf{w}_0^a}{\partial \mathbf{y}} \right) \psi_i^{N_{xy}} \frac{\partial \psi_j^{w_0}}{\partial x} \right] \right\} dx dy \\
[K^{99}] &= \int_{\Omega_e} \left\{ -\frac{\psi_i^{Q_x} \psi_j^{Q_x}}{(K_s A_{55})} \right\} dx dy & [K^{93}] &= \int_{\Omega_e} \left\{ \psi_i^{Q_x} \frac{\partial \psi_j^{w_0}}{\partial x} \right\} dx dy \\
[K^{94}] &= \int_{\Omega_e} \{\psi_i^{Q_x} \psi_j^{\phi_x}\} dx dy & [K^{(10)5}] &= \int_{\Omega_e} \{\psi_i^{Q_y} \psi_j^{\phi_y}\} dx dy \\
[K^{(10)(10)}] &= \int_{\Omega_e} \left\{ -\frac{\psi_i^{Q_y} \psi_j^{Q_y}}{(K_s A_{44})} \right\} dx dy & [K^{(10)3}] &= \int_{\Omega_e} \left\{ \psi_i^{Q_y} \frac{\partial \psi_j^{w_0}}{\partial y} \right\} dx dy \\
[K^{(11)(11)}] &= \int_{\Omega_e} \{-D_{11}^* \psi_i^{M_{xx}} \psi_j^{M_{xx}}\} dx dy & [K^{(11)(12)}] &= \int_{\Omega_e} \{-D_{12}^* \psi_i^{M_{xx}} \psi_j^{M_{yy}}\} dx dy \\
[K^{(11)4}] &= \int_{\Omega_e} \left\{ \psi_i^{M_{xx}} \frac{\partial \psi_j^{\phi_x}}{\partial x} \right\} dx dy & [K^{(12)5}] &= \int_{\Omega_e} \left\{ \psi_i^{M_{yy}} \frac{\partial \psi_j^{\phi_y}}{\partial y} \right\} dx dy \\
[K^{(12)(11)}] &= \int_{\Omega_e} \{-D_{12}^* \psi_i^{M_{yy}} \psi_j^{M_{xx}}\} dx dy & [K^{(12)(12)}] &= \int_{\Omega_e} \{-D_{22}^* \psi_i^{M_{yy}} \psi_j^{M_{yy}}\} dx dy \\
[K^{(13)4}] &= \int_{\Omega_e} \left\{ \psi_i^{M_{xy}} \frac{\partial \psi_j^{\phi_x}}{\partial y} \right\} dx dy & [K^{(13)5}] &= \int_{\Omega_e} \left\{ \psi_i^{M_{xy}} \frac{\partial \psi_j^{\phi_y}}{\partial x} \right\} dx dy \\
[K^{(13)(13)}] &= \int_{\Omega_e} \{-D_{66}^* \psi_i^{M_{xy}} \psi_j^{M_{xy}}\} dx dy
\end{aligned}$$

$$\begin{aligned}
\{F^1\} &= \oint_{\Gamma_e} \psi_i^u \{n_x N_{xx} + n_y N_{xy}\} ds , & \{F^2\} &= \oint_{\Gamma_e} \psi_i^{v_0} \{n_x N_{xy} + n_y N_{yy}\} ds , \\
\{F^3\} &= \int_{\Omega_e} \{\psi_i^{w_0} q(x)\} dx dy + \oint_{\Gamma_e} \psi_i^{w_0} [(V_x) n_x + (V_y) n_y] ds , \\
\{F^4\} &= \oint_{\Gamma_e} \psi_i^{\phi_x} \{M_{xx} n_x + M_{xy} n_y\} ds , & \{F^5\} &= \oint_{\Gamma_e} \psi_i^{\phi_y} \{M_{xy} n_x + M_{yy} n_y\} ds , \tag{3.15}
\end{aligned}$$

The rest of sub coefficient matrices and force vectors which are not specified in the (3.15) are equal to zero.

3.4 Model IV of Plate Bending

The membrane resultants (i.e. N_{xx} , N_{xy} and N_{yy}) can be eliminated by substituting the resultant equations of the membrane resultants into the equilibrium equations. By eliminating the in plane force resultants (N_{xx} , N_{xy} and N_{yy}), the size of the coefficient can be reduced while the effect of it will be discussed in the numerical analysis parts of the plate bending.

3.4.1 Weighted Residual Statements of Model IV

The weighted residual statements of the Model IV of the plate bending are given as follow:

$$\begin{aligned}
\int_{\Omega_e} \left\{ \frac{\partial \bar{W}_1}{\partial x} \left[A_{11} \left(\frac{\partial u_0^a}{\partial x} + \frac{1}{2} \left(\frac{\partial w_0^a}{\partial x} \right)^2 \right) + A_{12} \left(\frac{\partial v_0^a}{\partial y} + \frac{1}{2} \left(\frac{\partial w_0^a}{\partial y} \right)^2 \right) \right] \right. \\
\left. + \frac{\partial \bar{W}_1}{\partial y} \left[A_{66} \left(\frac{\partial u_0^a}{\partial y} + \frac{\partial v_0^a}{\partial x} + \frac{\partial w_0^a}{\partial x} \frac{\partial w_0^a}{\partial y} \right) \right] \right\} dx dy - \oint_{\Gamma_e} \bar{W}_1 (n_x N_{xx} + n_y N_{xy}) ds = 0 ,
\end{aligned}$$

$$\int_{\Omega_e} \left\{ \frac{\partial \bar{W}_2}{\partial y} \left[A_{12} \left(\frac{\partial u_0^a}{\partial x} + \frac{1}{2} \left(\frac{\partial w_0^a}{\partial x} \right)^2 \right) + A_{22} \left(\frac{\partial v_0^a}{\partial y} + \frac{1}{2} \left(\frac{\partial w_0^a}{\partial y} \right)^2 \right) \right] \right. \\ \left. + \frac{\partial \bar{W}_2}{\partial x} \left[A_{66} \left(\frac{\partial u_0^a}{\partial y} + \frac{\partial v_0^a}{\partial x} + \frac{\partial w_0^a}{\partial x} \frac{\partial w_0^a}{\partial y} \right) \right] \right\} dx dy - \oint_{\Gamma_e} \bar{W}_2 (n_x N_{xy} + n_y N_{yy}) ds = 0 ,$$

$$\int_{\Omega_e} \left[\frac{\partial \bar{W}_3}{\partial x} Q_x^a + \frac{\partial \bar{W}_3}{\partial y} Q_y^a + \frac{\partial \bar{W}_3}{\partial x} \frac{\partial w_0^a}{\partial x} \left[A_{11} \left(\frac{\partial u_0^a}{\partial x} + \frac{1}{2} \left(\frac{\partial w_0^a}{\partial x} \right)^2 \right) + A_{12} \left(\frac{\partial v_0^a}{\partial y} + \frac{1}{2} \left(\frac{\partial w_0^a}{\partial y} \right)^2 \right) \right] \right. \\ \left. + \frac{\partial \bar{W}_3}{\partial x} \frac{\partial w_0^a}{\partial y} \left[A_{66} \left(\frac{\partial u_0^a}{\partial y} + \frac{\partial v_0^a}{\partial x} + \frac{\partial w_0^a}{\partial x} \frac{\partial w_0^a}{\partial y} \right) \right] \right. \\ \left. + \frac{\partial \bar{W}_3}{\partial y} \frac{\partial w_0^a}{\partial x} \left[A_{66} \left(\frac{\partial u_0^a}{\partial y} + \frac{\partial v_0^a}{\partial x} + \frac{\partial w_0^a}{\partial x} \frac{\partial w_0^a}{\partial y} \right) \right] \right. \\ \left. + \frac{\partial \bar{W}_3}{\partial y} \frac{\partial w_0^a}{\partial y} \left[A_{12} \left(\frac{\partial u_0^a}{\partial x} + \frac{1}{2} \left(\frac{\partial w_0^a}{\partial x} \right)^2 \right) + A_{22} \left(\frac{\partial v_0^a}{\partial y} + \frac{1}{2} \left(\frac{\partial w_0^a}{\partial y} \right)^2 \right) \right] \right. \\ \left. - \bar{W}_3 q(x) \right] dx dy \\ + \oint_{\Gamma_e} \bar{W}_3 \left[\left(Q_x + N_{xx} \frac{\partial w_0}{\partial x} + N_{xy} \frac{\partial w_0}{\partial y} \right) n_x + \left(Q_y + N_{xy} \frac{\partial w_0}{\partial x} + N_{yy} \frac{\partial w_0}{\partial y} \right) n_y \right] ds = 0 ,$$

$$\int_{\Omega_e} \left(\frac{\partial \bar{W}_4}{\partial x} M_{xx}^a + \frac{\partial \bar{W}_4}{\partial y} M_{xy}^a + \bar{W}_4 Q_x^a \right) dx dy + \oint_{\Gamma_e} \bar{W}_4 (M_{xx} n_x + M_{xy} n_y) ds = 0 ,$$

$$\int_{\Omega_e} \left(\frac{\partial \bar{W}_5}{\partial x} M_{xy}^a + \frac{\partial \bar{W}_5}{\partial y} M_{yy}^a + \bar{W}_5 Q_y^a \right) dx dy + \oint_{\Gamma_e} \bar{W}_5 (M_{xy} n_x + M_{yy} n_y) ds = 0 ,$$

$$\int_{\Omega_e} \bar{W}_6 \left(-\frac{Q_x^a}{K_s A_{55}} + \frac{\partial w_0^a}{\partial x} + \phi_x^a \right) dx dy = 0 ,$$

$$\int_{\Omega_e} \bar{W}_7 \left(-\frac{Q_y^a}{K_s A_{44}} + \frac{\partial w_0^a}{\partial y} + \phi_y^a \right) dx dy = 0 ,$$

$$\int_{\Omega_e} \bar{W}_8 \left(-D_{11}^* M_{xx}^a - D_{12}^* M_{yy}^a + \frac{\partial \phi_x^a}{\partial x} \right) dx dy = 0 ,$$

$$\int_{\Omega_e} \bar{W}_9 \left(-D_{12}^* M_{xx}^a - D_{22}^* M_{yy}^a + \frac{\partial \phi_y^a}{\partial y} \right) dx dy = 0 ,$$

$$\int_{\Omega_e} \bar{W}_{10} \left(-D_{66}^* M_{xy}^a + \frac{\partial \phi_x^a}{\partial y} + \frac{\partial \phi_y^a}{\partial x} \right) dx dy = 0 .$$

(3.16)

The primary variables and the secondary variable of the Model IV can be specified as follow:

<The primary variable>	<The secondary variable>
u_0	$n_x N_{xx} + n_y N_{xy}$
v_0	$n_x N_{xy} + n_y N_{yy}$
w_0	$V_x n_x + V_y n_y$
ϕ_x	$M_{xx} n_x + M_{xy} n_y$
ϕ_y	$M_{xy} n_x + M_{yy} n_y$

3.4.2 Finite Element Equations of Model IV

Ten weigh functions and the approximations of ten independent variables can be chosen as the Lagrange type interpolation functions as follow:

$$\begin{aligned}
 u_0 \cong u_0^a &= \sum_{j=1}^l \psi_j^{u_0}(x, y) \mathbb{U}_j, & \bar{W}_1 &= \psi_i^{u_0}(x, y), \\
 v_0 \cong v_0^a &= \sum_{j=1}^l \psi_j^{v_0}(x, y) \mathbb{V}_j, & \bar{W}_2 &= \psi_i^{v_0}(x, y), \\
 w_0 \cong w_0^a &= \sum_{j=1}^m \psi_j^{w_0}(x, y) \mathbb{W}_j, & \bar{W}_3 &= \psi_i^{w_0}(x, y), \\
 \phi_x \cong \phi_x^a &= \sum_{j=1}^n \psi_j^{\phi_x}(x, y) \mathbb{P}_j^1, & \bar{W}_4 &= \psi_i^{\phi_x}(x, y), \\
 \phi_y \cong \phi_y^a &= \sum_{j=1}^n \psi_j^{\phi_y}(x, y) \mathbb{P}_j^2, & \bar{W}_5 &= \psi_i^{\phi_y}(x, y), \\
 Q_x \cong Q_x^a &= \sum_{j=1}^q \psi_j^{Q_x}(x, y) \mathbb{Q}_j^1, & \bar{W}_6 &= \psi_i^{Q_x}(x, y),
 \end{aligned}$$

$$\begin{aligned}
Q_y &\cong Q_y^a = \sum_{j=1}^q \psi_j^{Q_y}(x, y) \mathbb{Q}_j^2, & \bar{W}_7 &= \psi_i^{Q_y}(x, y), \\
M_{xx} &\cong M_{xx}^a = \sum_{j=1}^r \psi_j^{M_{xx}}(x, y) \mathbb{M}_j^1, & \bar{W}_8 &= \psi_i^{M_{xx}}(x, y), \\
M_{yy} &\cong M_{yy}^a = \sum_{j=1}^r \psi_j^{M_{yy}}(x, y) \mathbb{M}_j^2, & \bar{W}_9 &= \psi_i^{M_{yy}}(x, y), \\
M_{xy} &\cong M_{xy}^a = \sum_{j=1}^r \psi_j^{M_{xy}}(x, y) \mathbb{M}_j^3, & \bar{W}_{10} &= \psi_i^{M_{xy}}(x, y).
\end{aligned} \tag{3.17}$$

By substituting the (3.17) into the (3.16), the finite element equations of the Model IV can be obtained as follow:

$$\begin{aligned}
&\int_{\Omega_e} \left\{ \left[A_{11} \left(\sum_{j=1}^l \left(\frac{\partial \psi_i^{u_0}}{\partial x} \frac{\partial \psi_j^{u_0}}{\partial x} \right) \mathbb{w}_j + \frac{1}{2} \frac{\partial w_0^a}{\partial x} \sum_{j=1}^m \left(\frac{\partial \psi_i^{u_0}}{\partial x} \frac{\partial \psi_j^{w_0}}{\partial x} \right) \mathbb{w}_j \right) \right] \right\} dx dy \\
&\quad + \int_{\Omega_e} \left\{ \left[A_{12} \left(\sum_{j=1}^l \left(\frac{\partial \psi_i^{u_0}}{\partial x} \frac{\partial \psi_j^{v_0}}{\partial y} \right) \mathbb{v}_j + \frac{1}{2} \frac{\partial w_0^a}{\partial y} \sum_{j=1}^m \left(\frac{\partial \psi_i^{u_0}}{\partial x} \frac{\partial \psi_j^{w_0}}{\partial y} \right) \mathbb{w}_j \right) \right] \right\} dx dy \\
&\quad + \int_{\Omega_e} \left\{ \left[A_{66} \left(\sum_{j=1}^l \left(\frac{\partial \psi_i^{u_0}}{\partial y} \frac{\partial \psi_j^{u_0}}{\partial y} \right) \mathbb{w}_j + \sum_{j=1}^l \left(\frac{\partial \psi_i^{u_0}}{\partial y} \frac{\partial \psi_j^{v_0}}{\partial x} \right) \mathbb{v}_j + \frac{1}{2} \frac{\partial w_0^a}{\partial y} \sum_{j=1}^m \left(\frac{\partial \psi_i^{u_0}}{\partial y} \frac{\partial \psi_j^{w_0}}{\partial x} \right) \mathbb{w}_j \right. \right. \right. \\
&\quad \left. \left. \left. + \frac{1}{2} \frac{\partial w_0^a}{\partial x} \sum_{j=1}^m \left(\frac{\partial \psi_i^{u_0}}{\partial x} \frac{\partial \psi_j^{w_0}}{\partial y} \right) \mathbb{w}_j \right) \right] \right\} dx dy \\
&\quad - \oint_{\Gamma_e} \bar{W}_1 (n_x N_{xx} + n_y N_{xy}) ds = 0, \\
&\int_{\Omega_e} \left\{ \left[A_{12} \left(\sum_{j=1}^l \left(\frac{\partial \psi_i^{v_0}}{\partial y} \frac{\partial \psi_j^{u_0}}{\partial x} \right) \mathbb{w}_j + \frac{1}{2} \frac{\partial w_0^a}{\partial x} \sum_{j=1}^m \left(\frac{\partial \psi_i^{v_0}}{\partial y} \frac{\partial \psi_j^{w_0}}{\partial x} \right) \mathbb{w}_j \right) \right] \right\} dx dy \\
&\int_{\Omega_e} \left\{ \left[A_{22} \left(\sum_{j=1}^l \left(\frac{\partial \psi_i^{v_0}}{\partial y} \frac{\partial \psi_j^{v_0}}{\partial y} \right) \mathbb{v}_j + \frac{1}{2} \frac{\partial w_0^a}{\partial y} \sum_{j=1}^m \left(\frac{\partial \psi_i^{v_0}}{\partial y} \frac{\partial \psi_j^{w_0}}{\partial y} \right) \mathbb{w}_j \right) \right] \right\} dx dy \\
&\quad + \int_{\Omega_e} \left\{ \left[A_{66} \left(\sum_{j=1}^l \left(\frac{\partial \psi_i^{v_0}}{\partial x} \frac{\partial \psi_j^{u_0}}{\partial y} \right) \mathbb{w}_j + \sum_{j=1}^l \left(\frac{\partial \psi_i^{v_0}}{\partial x} \frac{\partial \psi_j^{v_0}}{\partial x} \right) \mathbb{v}_j + \frac{1}{2} \frac{\partial w_0^a}{\partial y} \sum_{j=1}^m \left(\frac{\partial \psi_i^{v_0}}{\partial x} \frac{\partial \psi_j^{w_0}}{\partial x} \right) \mathbb{w}_j \right. \right. \right. \\
&\quad \left. \left. \left. + \frac{1}{2} \frac{\partial w_0^a}{\partial x} \sum_{j=1}^m \left(\frac{\partial \psi_i^{v_0}}{\partial x} \frac{\partial \psi_j^{w_0}}{\partial y} \right) \mathbb{w}_j \right) \right] \right\} dx dy - \oint_{\Gamma_e} \psi_i^{v_0} (n_x N_{xy} + n_y N_{yy}) ds = 0,
\end{aligned}$$

$$\begin{aligned}
& \int_{\Omega_e} \left\{ \sum_{j=1}^q \left(\frac{\partial \psi_i^{w_0}}{\partial x} \psi_j^{Q_x} \right) \mathbb{Q}_j^1 + \sum_{j=1}^q \left(\frac{\partial \psi_i^{w_0}}{\partial y} \psi_j^{Q_y} \right) \mathbb{Q}_j^2 \right\} dx dy \\
& + \int_{\Omega_e} \left\{ A_{11} \frac{\partial w_0^a}{\partial x} \left[\sum_{j=1}^l \left(\frac{\partial \psi_i^{w_0}}{\partial x} \frac{\partial \psi_j^{u_0}}{\partial x} \right) \mathbb{W}_j + \frac{1}{2} \frac{\partial w_0^a}{\partial x} \sum_{j=1}^m \left(\frac{\partial \psi_i^{w_0}}{\partial x} \frac{\partial \psi_j^{w_0}}{\partial x} \right) \mathbb{W}_j \right] \right\} dx dy \\
& + \int_{\Omega_e} \left\{ A_{12} \frac{\partial w_0^a}{\partial x} \left[\sum_{j=1}^l \left(\frac{\partial \psi_i^{w_0}}{\partial x} \frac{\partial \psi_j^{v_0}}{\partial y} \right) \mathbb{V}_j + \frac{1}{2} \frac{\partial w_0^a}{\partial y} \sum_{j=1}^m \left(\frac{\partial \psi_i^{w_0}}{\partial x} \frac{\partial \psi_j^{w_0}}{\partial y} \right) \mathbb{W}_j \right] \right\} dx dy \\
& + \int_{\Omega_e} \left\{ A_{66} \frac{\partial w_0^a}{\partial y} \left[\sum_{j=1}^l \left(\frac{\partial \psi_i^{w_0}}{\partial x} \frac{\partial \psi_j^{u_0}}{\partial y} \right) \mathbb{W}_j + \sum_{j=1}^l \left(\frac{\partial \psi_i^{w_0}}{\partial x} \frac{\partial \psi_j^{v_0}}{\partial x} \right) \mathbb{V}_j + \frac{1}{2} \frac{\partial w_0^a}{\partial y} \sum_{j=1}^m \left(\frac{\partial \psi_i^{w_0}}{\partial x} \frac{\partial \psi_j^{w_0}}{\partial x} \right) \mathbb{W}_j \right. \right. \\
& \quad \left. \left. + \frac{1}{2} \frac{\partial w_0^a}{\partial x} \sum_{j=1}^m \left(\frac{\partial \psi_i^{w_0}}{\partial x} \frac{\partial \psi_j^{w_0}}{\partial y} \right) \mathbb{W}_j \right] \right\} dx dy \\
& + \int_{\Omega_e} \left\{ A_{66} \frac{\partial w_0^a}{\partial x} \left[\sum_{j=1}^l \left(\frac{\partial \psi_i^{w_0}}{\partial y} \frac{\partial \psi_j^{u_0}}{\partial y} \right) \mathbb{W}_j + \sum_{j=1}^l \left(\frac{\partial \psi_i^{w_0}}{\partial y} \frac{\partial \psi_j^{v_0}}{\partial x} \right) \mathbb{V}_j + \frac{1}{2} \frac{\partial w_0^a}{\partial y} \sum_{j=1}^m \left(\frac{\partial \psi_i^{w_0}}{\partial y} \frac{\partial \psi_j^{w_0}}{\partial x} \right) \mathbb{W}_j \right. \right. \\
& \quad \left. \left. + \frac{1}{2} \frac{\partial w_0^a}{\partial x} \sum_{j=1}^m \left(\frac{\partial \psi_i^{w_0}}{\partial y} \frac{\partial \psi_j^{w_0}}{\partial y} \right) \mathbb{W}_j \right] \right\} dx dy \\
& + \int_{\Omega_e} \left\{ A_{12} \frac{\partial w_0^a}{\partial y} \left[\left(\sum_{j=1}^l \left(\frac{\partial \psi_i^{w_0}}{\partial y} \frac{\partial \psi_j^{u_0}}{\partial x} \right) \mathbb{W}_j + \frac{1}{2} \frac{\partial w_0^a}{\partial x} \sum_{j=1}^m \left(\frac{\partial \psi_i^{w_0}}{\partial y} \frac{\partial \psi_j^{w_0}}{\partial x} \right) \mathbb{W}_j \right) \right] \right\} dx dy \\
& + \int_{\Omega_e} \left\{ A_{22} \frac{\partial w_0^a}{\partial y} \left[\left(\sum_{j=1}^l \left(\frac{\partial \psi_i^{w_0}}{\partial y} \frac{\partial \psi_j^{v_0}}{\partial y} \right) \mathbb{V}_j + \frac{1}{2} \frac{\partial w_0^a}{\partial y} \sum_{j=1}^m \left(\frac{\partial \psi_i^{w_0}}{\partial y} \frac{\partial \psi_j^{w_0}}{\partial y} \right) \mathbb{W}_j \right) \right] \right\} dx dy \\
& - \int_{\Omega_e} \{ \psi_i^{w_0} q(x) \} dx dy + \oint_{\Gamma_e} \bar{W}_3 \left[\left(Q_x + N_{xx} \frac{\partial w_0}{\partial x} + N_{xy} \frac{\partial w_0}{\partial y} \right) n_x + \left(Q_y + N_{xy} \frac{\partial w_0}{\partial x} + N_{yy} \frac{\partial w_0}{\partial y} \right) n_y \right] ds = 0 , \\
& \int_{\Omega_e} \left[\sum_{j=1}^r \left(\frac{\partial \psi_i^{\phi_x}}{\partial x} \psi_j^{M_{xx}} \right) \mathbb{M}_j^1 + \sum_{j=1}^r \left(\frac{\partial \psi_i^{\phi_x}}{\partial y} \psi_j^{M_{xy}} \right) \mathbb{M}_j^3 + \sum_{j=1}^q \left(\psi_i^{\phi_x} \psi_j^{Q_x} \right) \mathbb{Q}_j^1 \right] dx dy \\
& + \oint_{\Gamma_e} \psi_i^{\phi_x} (M_{xx} n_x + M_{xy} n_y) ds = 0 , \\
& \int_{\Omega_e} \left[\sum_{j=1}^r \left(\frac{\partial \psi_i^{\phi_y}}{\partial x} \psi_j^{M_{xy}} \right) \mathbb{M}_j^3 + \sum_{j=1}^r \left(\frac{\partial \psi_i^{\phi_y}}{\partial y} \psi_j^{M_{yy}} \right) \mathbb{M}_j^2 + \sum_{j=1}^q \left(\psi_i^{\phi_y} \psi_j^{Q_y} \right) \mathbb{Q}_j^2 \right] dx dy \\
& + \oint_{\Gamma_e} \psi_i^{\phi_y} (M_{xy} n_x + M_{yy} n_y) ds = 0 , \\
& \int_{\Omega_e} \left[-\frac{1}{K_s A_{55}} \sum_{j=1}^q \left(\psi_i^{Q_x} \psi_j^{Q_x} \right) \mathbb{Q}_j^1 + \sum_{j=1}^m \left(\psi_i^{Q_x} \frac{\partial \psi_j^{w_0}}{\partial x} \right) \mathbb{W}_j + \sum_{j=1}^n \left(\psi_i^{Q_x} \psi_j^{\phi_x} \right) \mathbb{P}_j^1 \right] dx dy = 0 , \\
& \int_{\Omega_e} \left[-\frac{1}{K_s A_{44}} \sum_{j=1}^q \left(\psi_i^{Q_y} \psi_j^{Q_y} \right) \mathbb{Q}_j^2 + \sum_{j=1}^m \left(\psi_i^{Q_y} \frac{\partial \psi_j^{w_0}}{\partial y} \right) \mathbb{W}_j + \sum_{j=1}^n \left(\psi_i^{Q_y} \psi_j^{\phi_y} \right) \mathbb{P}_j^2 \right] dx dy = 0 ,
\end{aligned}$$

$$\begin{aligned}
& \int_{\Omega_e} \left[-D_{11}^* \sum_{j=1}^r (\psi_i^{M_{xx}} \psi_j^{M_{xx}}) \mathbb{M}_j^1 - D_{12}^* \sum_{j=1}^r (\psi_i^{M_{xx}} \psi_j^{M_{yy}}) \mathbb{M}_j^2 + \sum_{j=1}^n \left(\psi_i^{M_{xx}} \frac{\partial \psi_j^{\phi_x}}{\partial x} \right) \mathbb{P}_j^1 \right] dx dy = 0 , \\
& \int_{\Omega_e} \left[-D_{12}^* \sum_{j=1}^r (\psi_i^{M_{yy}} \psi_j^{M_{xx}}) \mathbb{M}_j^1 - D_{22}^* \sum_{j=1}^r (\psi_i^{M_{yy}} \psi_j^{M_{yy}}) \mathbb{M}_j^2 + \sum_{j=1}^n \left(\psi_i^{M_{yy}} \frac{\partial \psi_j^{\phi_y}}{\partial y} \right) \mathbb{P}_j^2 \right] dx dy = 0 , \\
& \int_{\Omega_e} \left[-D_{66}^* \sum_{j=1}^r (\psi_i^{M_{xy}} \psi_j^{M_{xy}}) \mathbb{M}_j^3 + \sum_{j=1}^n \left(\psi_i^{M_{xy}} \frac{\partial \psi_j^{\phi_y}}{\partial y} \right) \mathbb{P}_j^2 + \sum_{j=1}^n \left(\psi_i^{M_{xy}} \frac{\partial \psi_j^{\phi_x}}{\partial x} \right) \mathbb{P}_j^1 \right] dx dy = 0 .
\end{aligned} \tag{3.18}$$

Above equations of the (3.18) can be rewritten in the algebraic matrix equation by the form of,

$$\begin{aligned}
& [\mathbf{K}^e(\{\mathbf{u}^e\})]\{\mathbf{U}^e\} = \{\mathbf{F}^e\} \\
& = \begin{bmatrix} [\mathbf{K}^{(1)(1)}] & \dots & [\mathbf{K}^{(1)(7)}] & \dots & [\mathbf{K}^{(1)(10)}] \\ \vdots & \ddots & \vdots & \ddots & \vdots \\ [\mathbf{K}^{(5)(1)}] & \dots & & \dots & [\mathbf{K}^{(5)(10)}] \\ \vdots & \ddots & \vdots & \ddots & \vdots \\ [\mathbf{K}^{(10)(1)}] & \dots & [\mathbf{K}^{(10)(6)}] & \dots & [\mathbf{K}^{(10)(10)}] \end{bmatrix} \begin{Bmatrix} \{\mathbb{U}_j\} \\ \vdots \\ \{\mathbb{P}_j^2\} \\ \vdots \\ \{\mathbb{M}_j^3\} \end{Bmatrix} = \begin{Bmatrix} \{\mathbf{F}^{(1)}\} \\ \vdots \\ \{\mathbf{F}^{(5)}\} \\ \vdots \\ \{\mathbf{F}^{(10)}\} \end{Bmatrix} .
\end{aligned} \tag{3.19}$$

where,

$$\begin{aligned}
[K^{11}] &= \int_{\Omega_e} \left\{ A_{11} \frac{\partial \psi_i^{u_0}}{\partial x} \frac{\partial \psi_j^{u_0}}{\partial x} + A_{66} \frac{\partial \psi_i^{u_0}}{\partial y} \frac{\partial \psi_j^{u_0}}{\partial y} \right\} dx dy \\
[K^{12}] &= \int_{\Omega_e} \left\{ A_{12} \frac{\partial \psi_i^{u_0}}{\partial x} \frac{\partial \psi_j^{v_0}}{\partial y} + A_{66} \frac{\partial \psi_i^{u_0}}{\partial y} \frac{\partial \psi_j^{v_0}}{\partial x} \right\} dx dy \\
[K^{13}] &= \frac{1}{2} \int_{\Omega_e} \left\{ \frac{\partial \psi_i^{u_0}}{\partial x} \left(A_{11} \frac{\partial \mathbf{w}_0^a}{\partial \mathbf{x}} \frac{\partial \psi_j^{w_0}}{\partial x} + A_{12} \frac{\partial \mathbf{w}_0^a}{\partial \mathbf{y}} \frac{\partial \psi_j^{w_0}}{\partial y} \right) \right. \\
&\quad \left. + A_{66} \frac{\partial \psi_i^{u_0}}{\partial y} \left(\frac{\partial \mathbf{w}_0^a}{\partial \mathbf{x}} \frac{\partial \psi_j^{w_0}}{\partial y} + \frac{\partial \mathbf{w}_0^a}{\partial \mathbf{y}} \frac{\partial \psi_j^{w_0}}{\partial x} \right) \right\} dx dy
\end{aligned}$$

$$[K^{22}] = \int_{\Omega_e} \left\{ A_{22} \frac{\partial \psi_i^{v_0}}{\partial y} \frac{\partial \psi_j^{v_0}}{\partial y} + A_{66} \frac{\partial \psi_i^{v_0}}{\partial x} \frac{\partial \psi_j^{v_0}}{\partial x} \right\} dx dy$$

$$[K^{21}] = \int_{\Omega_e} \left\{ A_{12} \frac{\partial \psi_i^{v_0}}{\partial y} \frac{\partial \psi_j^{u_0}}{\partial x} + A_{66} \frac{\partial \psi_i^{v_0}}{\partial x} \frac{\partial \psi_j^{u_0}}{\partial y} \right\} dx dy$$

$$[K^{23}] = \frac{1}{2} \int_{\Omega_e} \left\{ \frac{\partial \psi_i^{v_0}}{\partial y} \left(A_{22} \frac{\partial \mathbf{w}_0^a}{\partial \mathbf{y}} \frac{\partial \psi_j^{w_0}}{\partial y} + A_{12} \frac{\partial \mathbf{w}_0^a}{\partial \mathbf{x}} \frac{\partial \psi_j^{w_0}}{\partial x} \right) \right. \\ \left. + A_{66} \frac{\partial \psi_i^{v_0}}{\partial x} \left(\frac{\partial \mathbf{w}_0^a}{\partial \mathbf{x}} \frac{\partial \psi_j^{w_0}}{\partial y} + \frac{\partial \mathbf{w}_0^a}{\partial \mathbf{y}} \frac{\partial \psi_j^{w_0}}{\partial x} \right) \right\} dx dy$$

$$[K^{31}] = \int_{\Omega_e} \left\{ \frac{\partial \psi_i^{w_0}}{\partial x} \left(A_{11} \frac{\partial \mathbf{w}_0^a}{\partial \mathbf{x}} \frac{\partial \psi_j^{u_0}}{\partial x} + A_{66} \frac{\partial \mathbf{w}_0^a}{\partial \mathbf{y}} \frac{\partial \psi_j^{u_0}}{\partial y} \right) \right. \\ \left. + \frac{\partial \psi_i^{w_0}}{\partial y} \left(A_{66} \frac{\partial \mathbf{w}_0^a}{\partial \mathbf{x}} \frac{\partial \psi_j^{u_0}}{\partial y} + A_{12} \frac{\partial \mathbf{w}_0^a}{\partial \mathbf{y}} \frac{\partial \psi_j^{u_0}}{\partial x} \right) \right\} dx dy$$

$$[K^{32}] = \int_{\Omega_e} \left\{ \frac{\partial \psi_i^{w_0}}{\partial y} \left(A_{22} \frac{\partial \mathbf{w}_0^a}{\partial \mathbf{y}} \frac{\partial \psi_j^{v_0}}{\partial y} + A_{66} \frac{\partial \mathbf{w}_0^a}{\partial \mathbf{x}} \frac{\partial \psi_j^{v_0}}{\partial x} \right) \right. \\ \left. + \frac{\partial \psi_i^{w_0}}{\partial x} \left(A_{66} \frac{\partial \mathbf{w}_0^a}{\partial \mathbf{y}} \frac{\partial \psi_j^{v_0}}{\partial x} + A_{12} \frac{\partial \mathbf{w}_0^a}{\partial \mathbf{x}} \frac{\partial \psi_j^{v_0}}{\partial y} \right) \right\} dx dy$$

$$[K^{33}] = \frac{1}{2} \int_{\Omega_e} \left\{ \left[A_{11} \left(\frac{\partial \mathbf{w}_0^a}{\partial \mathbf{x}} \right)^2 + A_{66} \left(\frac{\partial \mathbf{w}_0^a}{\partial \mathbf{y}} \right)^2 \right] \frac{\partial \psi_i^{w_0}}{\partial x} \frac{\partial \psi_j^{w_0}}{\partial x} \right. \\ \left. + \left[A_{66} \left(\frac{\partial \mathbf{w}_0^a}{\partial \mathbf{x}} \right)^2 + A_{22} \left(\frac{\partial \mathbf{w}_0^a}{\partial \mathbf{y}} \right)^2 \right] \frac{\partial \psi_i^{w_0}}{\partial y} \frac{\partial \psi_j^{w_0}}{\partial y} \right. \\ \left. + (A_{12} + A_{66}) \frac{\partial \mathbf{w}_0^a}{\partial \mathbf{x}} \frac{\partial \mathbf{w}_0^a}{\partial \mathbf{y}} \left(\frac{\partial \psi_i^{w_0}}{\partial x} \frac{\partial \psi_j^{w_0}}{\partial y} + \frac{\partial \psi_i^{w_0}}{\partial y} \frac{\partial \psi_j^{w_0}}{\partial x} \right) \right\} dx dy$$

$$[K^{36}] = \int_{\Omega_e} \left\{ \frac{\partial \psi_i^{w_0}}{\partial x} \psi_j^{Q_x} \right\} dx dy$$

$$[K^{37}] = \int_{\Omega_e} \left\{ \frac{\partial \psi_i^{w_0}}{\partial y} \psi_j^{Q_y} \right\} dx dy$$

$$[K^{66}] = \int_{\Omega_e} \left\{ -\frac{\psi_i^{Q_x} \psi_j^{Q_x}}{(K_s A_{55})} \right\} dx dy$$

$$[K^{63}] = \int_{\Omega_e} \left\{ \psi_i^{Q_x} \frac{\partial \psi_j^{w_0}}{\partial x} \right\} dx dy$$

$$[K^{64}] = \int_{\Omega_e} \left\{ \psi_i^{Q_x} \psi_j^{\phi_x} \right\} dx dy$$

$$[K^{75}] = \int_{\Omega_e} \left\{ \psi_i^{Q_y} \psi_j^{\phi_y} \right\} dx dy$$

$$[K^{77}] = \int_{\Omega_e} \left\{ -\frac{\psi_i^{Q_y} \psi_j^{Q_y}}{(K_s A_{44})} \right\} dx dy$$

$$[K^{73}] = \int_{\Omega_e} \left\{ \psi_i^{Q_y} \frac{\partial \psi_j^{w_0}}{\partial y} \right\} dx dy$$

$$[K^{88}] = \int_{\Omega_e} \left\{ -D_{11}^* \psi_i^{M_{xx}} \psi_j^{M_{xx}} \right\} dx dy$$

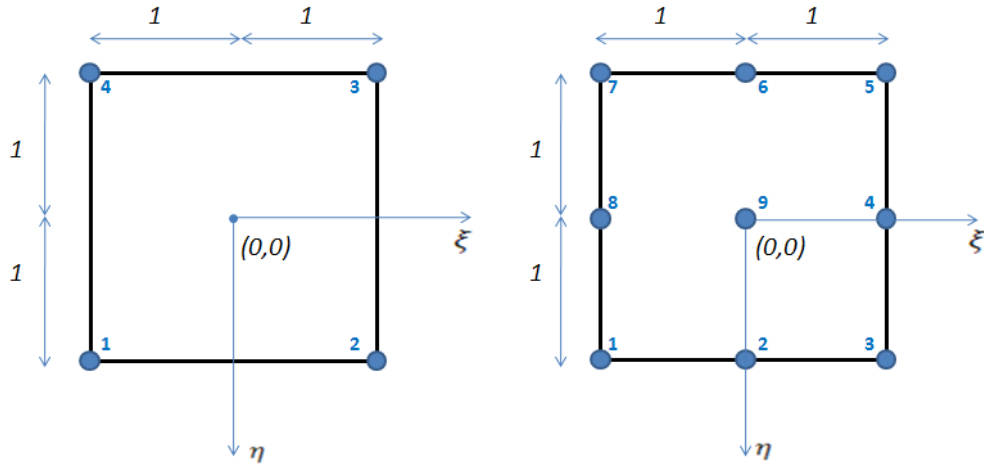
$$[K^{89}] = \int_{\Omega_e} \left\{ -D_{12}^* \psi_i^{M_{xx}} \psi_j^{M_{yy}} \right\} dx dy$$

$$\begin{aligned}
[K^{84}] &= \int_{\Omega_e} \left\{ \psi_i^{M_{xx}} \frac{\partial \psi_j^{\phi_x}}{\partial x} \right\} dx dy & [K^{95}] &= \int_{\Omega_e} \left\{ \psi_i^{M_{yy}} \frac{\partial \psi_j^{\phi_y}}{\partial y} \right\} dx dy \\
[K^{98}] &= \int_{\Omega_e} \left\{ -D_{12}^* \psi_i^{M_{yy}} \psi_j^{M_{xx}} \right\} dx dy & [K^{99}] &= \int_{\Omega_e} \left\{ -D_{22}^* \psi_i^{M_{yy}} \psi_j^{M_{yy}} \right\} dx dy \\
[K^{(10)4}] &= \int_{\Omega_e} \left\{ \psi_i^{M_{xy}} \frac{\partial \psi_j^{\phi_x}}{\partial y} \right\} dx dy & [K^{(10)5}] &= \int_{\Omega_e} \left\{ \psi_i^{M_{xy}} \frac{\partial \psi_j^{\phi_y}}{\partial x} \right\} dx dy \\
[K^{(10)(10)}] &= \int_{\Omega_e} \left\{ -D_{66}^* \psi_i^{M_{xy}} \psi_j^{M_{xy}} \right\} dx dy \\
\{F^1\} &= \oint_{\Gamma_e} \psi_i^u \{n_x N_{xx} + n_y N_{xy}\} ds , & \{F^2\} &= \oint_{\Gamma_e} \psi_i^{v_0} \{n_x N_{xy} + n_y N_{yy}\} ds , \\
\{F^3\} &= \int_{\Omega_e} \{ \psi_i^{w_0} q(x) \} dx dy + \oint_{\Gamma_e} \psi_i^{w_0} [(V_x) n_x + (V_y) n_y] ds , \\
\{F^4\} &= \oint_{\Gamma_e} \psi_i^{\phi_x} \{M_{xx} n_x + M_{xy} n_y\} ds , & \{F^5\} &= \oint_{\Gamma_e} \psi_i^{\phi_y} \{M_{xy} n_x + M_{yy} n_y\} ds , \quad (3.20)
\end{aligned}$$

The rest of the sub coefficient matrices and the force vectors which are not specified above are equal to zero.

3.5 Lagrange Type Plate Finite Elements

For present study, the mixed formula allows a use of the Lagrange type of interpolation functions[4]. The elements that were used for the computer implementation and the numerical analysis are discussed. For the plate problems, 4-node and 9-node Lagrange type of elements were used. The geometry of the elements and the locations of associated interpolations are given in the Fig. 3.1.



(a) 4-node linear element

(b) 9-node quadratic element

Fig. 3.1 Node number and local coordinate of the rectangular elements of the Lagrange family.

And, the associated interpolation functions are as follow:

- 4-node linear element

$$\begin{aligned}
 \psi_1 &= \frac{1}{4}(1 - \xi)(1 - \eta) , \\
 \psi_2 &= \frac{1}{4}(1 + \xi)(1 - \eta) , \\
 \psi_3 &= \frac{1}{4}(1 - \xi)(1 + \eta) , \\
 \psi_4 &= \frac{1}{4}(1 + \xi)(1 + \eta) .
 \end{aligned} \tag{3.21}$$

-9-node quadratic element

$$\begin{aligned}
 \psi_1 &= \frac{1}{4}(\xi^2 - \xi)(\eta^2 - \eta), \quad \psi_2 = \frac{1}{4}(1 - \xi^2)(\eta^2 - \eta), \quad \psi_3 = \frac{1}{4}(\xi^2 + \xi)(\eta^2 - \eta), \\
 \psi_4 &= \frac{1}{2}(\xi^2 + \xi)(1 - \eta^2), \quad \psi_5 = \frac{1}{4}(\xi^2 + \xi)(\eta^2 + \eta), \quad \psi_6 = \frac{1}{2}(1 - \xi^2)(\eta^2 + \eta), \\
 \psi_7 &= \frac{1}{4}(\xi^2 - \xi)(\eta^2 + \eta), \quad \psi_8 = \frac{1}{2}(\xi^2 - \xi)(1 - \eta^2), \quad \psi_9 = (1 - \xi^2)(1 - \eta^2).
 \end{aligned} \tag{3.22}$$

CHAPTER IV

NONLINEAR EQUATION SOLVING PROCEDURES

We obtained matrix form of nonlinear finite element model equations in the previous chapters II and III. In this chapter the non-linear equation solving procedures of equation (2.4), (2.10), (2.18), (2.22), (3.4), (3.9), (3.14) and (3.19) were discussed. These equation solving procedures of the nonlinear mixed finite element models can be generally applied for the developed nonlinear finite element models. The Picard Iteration method[1, 21] and the Newton-Raphson method[1, 22, 23] were used for the present numerical analysis. The solutions obtained from the two different methods can be compared to insure the obtained solutions are well converged one, because the converging characteristic may vary from one method to the other, but the obtained solutions should essentially be the same.

4.1 Direct Iterative Method

The direct method is one of the simplest methods available, because this method only requires update of the coefficient matrix with obtained solutions from the previous iteration at each iteration step. After updating the coefficient matrix the equation solving procedure, which is related to the obtaining of new iterative solutions is just the same as solving linear algebraic equations. The flow chart[1] of the direct iteration method is given in the Fig. 4.1. (for details see Reddy[1]).

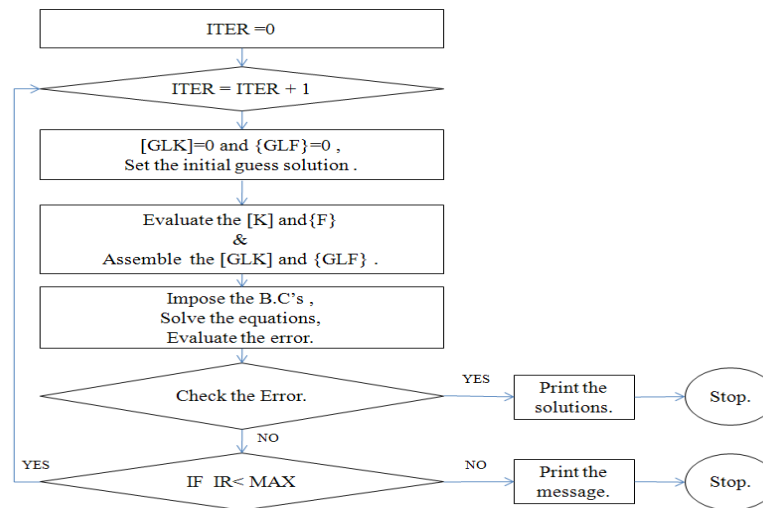


Fig. 4.1 A flow chart[1] of the direct iteration method.

4.1.1 Algorithm of Direct Iterative Method

The element wise matrix form of non-linear finite element equations that we obtained in chapters II and III, i.e., (2.4), (2.10), (2.18), (2.22), (3.4), (3.9), (3.14) and (3.19) can be assembled as global equations [1] which can be written as

$$[K(\{U\})]\{U\} = \{F\} \quad (4.1)$$

where, the $\{U\}$ denotes the global unknowns of the assembled equations.

Because the coefficient matrix $[K]$ is the function of the unknown $\{U\}$, we need to evaluate the $[K]$ by using initial guess solutions or the previous iterative solutions[1]. To imply this concept, the equation (4.1) can be rewritten as,

$$[K(\{U\}^{(r-1)})]\{U\}^{(r)} = \{F\} ,$$

or

$$[K(\{U\}^{(r)})]\{U\}^{(r+1)} = \{F\} , \quad (4.2)$$

where, $\{U\}^r$ is the solution obtained from the r^{th} iteration, $K(\{U\}^{(r-1)})$ is the updated coefficient matrix using the previous solutions $\{U\}^{(r-1)}$ and $\{F\}$ is the force vector.

Now, with the equation (4.2), the simple algorithm can be used to solve the nonlinear finite element equations with the direct method, which can be stated as,

$$\{U\}^r = [K(\{U\}^{(r-1)})]^{-1}\{F\} . \quad (4.3)$$

Above procedure should be repeated until the solutions of r^{th} iteration and the $(r-1)^{\text{th}}$ iteration satisfy the following criterion [1]:

$$\sqrt{\frac{\sum_{l=1}^N (U_l^{(r)} - U_l^{(r-1)})^2}{\sum_{l=1}^N (U_l^{(r)})^2}} < \epsilon , \quad (4.4)$$

where, ϵ is the tolerance[1].

In this study, values of tolerance[1], $\epsilon = 0.01 \sim 0.001$ were chosen for the most of the problems. In many cases, with small values of tolerance (say, $\epsilon = 1.0 \times 10^{-10}$), the iterative solutions may not satisfy the criterion regardless of the iteration numbers.

4.2 Newton-Raphson Iterative Method

Usually the Newton-Raphson iterative method[1, 22] shows faster convergence, compared with the direct method[1, 21]. Also in many cases, the tangent matrix can be symmetry even though the coefficient matrix is not. And with the Newton method, only the tangent matrix is inverted to get the incremental solutions, thus only the symmetry solver can be used, still the calculations of the tangent matrix and implement of the equation solving procedure are substantial. The flow chart[1] of the Newton iteration method is given in the Fig. 3.2.

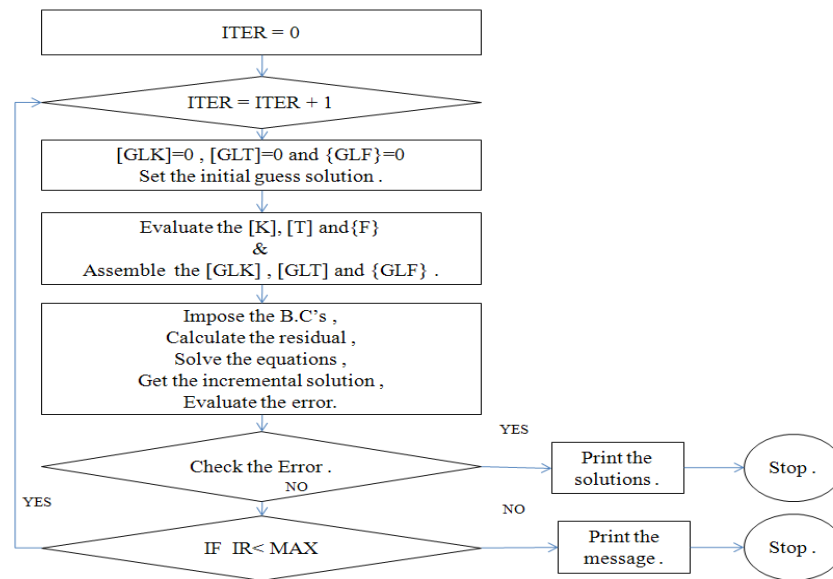


Fig. 4.2 A flow chart[1] of the Newton iteration method.

4.2.1 Algorithm of Newton-Raphson Iterative Method

In the Newton-Raphson iterative method, the residual[1] or the imbalance force vector[1] of the (4.1) can be written as,

$$\{R(\{U\})\} = [K(\{U\})]\{U\} - \{F\} . \quad (4.5)$$

With Taylor's expansion, the residual $\{R\}$ can be expanded to the known solution (i.e. the solution of the previous iteration).

$$\begin{aligned} \{R(\{U\})\} = & \{R(\{U\}^{(r-1)})\} + \left(\frac{\partial \{R(\{U\}^{(r-1)})\}}{\partial \{U\}} \cdot (\{U\} - \{U\}^{(r-1)}) \right) \\ & + \frac{1}{2} \left(\frac{\partial^2 \{R(\{U\}^{(r-1)})\}}{\partial \{U\}^2} \cdot (\{U\} - \{U\}^{(r-1)})^2 \right) + \dots . \end{aligned} \quad (4.6)$$

By omitting all the terms after the third term of the right hand side of the (4.6), and by taking the residual to be zero, i.e. $\{R(\{u\})\} = 0$, we can obtain the following relation.

$$\{R(\{U\}^{(r-1)})\} + \frac{\partial \{R(\{U\}^{(r-1)})\}}{\partial \{U\}} \cdot \{\Delta U\} = 0 , \quad (4.7)$$

where,

$$\{\Delta U\} = \{U\} - \{U\}^{(r-1)} .$$

Here we define the tangent stiffness matrix[1] as follow:

$$[T(\{U\}^{(r-1)})] = \frac{\partial \{R(\{U\}^{(r-1)})\}}{\partial \{U\}}, \quad (4.8)$$

By the substitution of (4.8) into the (4.7), and the inversion of the tangent stiffness matrix, we can obtain the increment of the solution ($\{\Delta U\}$), which can be written as,

$$\{\Delta U\} = -[T(\{U\}^{(r-1)})]^{-1}(\{R(\{U\}^{(r-1)})\}), \quad (4.9)$$

where the residual can be computed from the previous iterative solution as follow:

$$\{R(\{U\}^{(r-1)})\} = \{[K(\{U\}^{(r-1)})]\{U^{(r-1)}\} - \{F\}\}. \quad (4.10)$$

If we can calculate the tangent matrix from the equation (4.8), the solutions can be updated as,

$$\{U\}^{(r)} = \{U\}^{(r-1)} + \{\Delta U\} . \quad (4.11)$$

For the check of the convergence criterion, it can be computed by using the increment of the solutions vector, i.e., $\{\Delta U\}$, as follow:

$$\sqrt{\frac{\sum_{l=1}^N (\Delta U_l)^2}{\sum_{l=1}^N (U_l^{(r)})^2}} < \epsilon . \quad (4.12)$$

4.2.2 Calculation of Tangent Stiffness Matrices

In the Newton-Raphson iterative method, it is required to compute tangent coefficient matrices to get the incremental solution described in the (4.9). The original form of the equation (4.9) can be rewritten as the matrix form of the equation as follow:

$$\begin{aligned} [T(\{U^{(r-1)}\})]\{\Delta U\} &= \{R(\{U\}^{(r-1)})\} \\ &= \begin{bmatrix} [T^{11}(\{U^{(r-1)}\})] & \dots & [T^{1\beta}(\{U^{(r-1)}\})] \\ \vdots & \ddots & \vdots \\ [T^{\alpha 1}(\{U^{(r-1)}\})] & \dots & [T^{\alpha\beta}(\{U^{(r-1)}\})] \end{bmatrix} \begin{Bmatrix} \{\Delta U^{(1)}\} \\ \vdots \\ \{\Delta U^{(\beta)}\} \end{Bmatrix} = \begin{Bmatrix} \{R^1(\{U^{(r-1)}\})\} \\ \vdots \\ \{R^\alpha(\{U^{(r-1)}\})\} \end{Bmatrix}. \end{aligned} \quad (4.13)$$

The component form of this tangent coefficient stiffness matrix and the residual vector can be given as (see Reddy [1]),

$$T_{ij}^{\alpha\beta} = \frac{\partial R_i^\alpha}{\partial U_j^\beta}, \quad (4.14)$$

and

$$R_i^\alpha = \sum_{\gamma=1}^M \sum_{k=1}^N K_{ik}^{\alpha\gamma} U_k^\gamma - F_i^\alpha. \quad (4.15)$$

By substituting the equation (4.15) into the equation (4.14), the following equation can be obtained (see Reddy[1]).

$$T_{ij}^{\alpha\beta} = \frac{\partial}{\partial U_j^\beta} \left(\sum_{\gamma=1}^3 \sum_{k=1}^N K_{ik}^{\alpha\gamma} U_k^\gamma - F_i^\alpha \right)$$

$$= \left(\sum_{\gamma=1}^3 \sum_{k=1}^N \frac{\partial K_{ik}^{\alpha\gamma}}{\partial U_j^\beta} U_k^\gamma + K_{ij}^{\alpha\beta} \right). \quad (4.16)$$

Note that the α denotes the equation number which can be matched to the sub matrix of the α^{th} row in the (4.13), the β denotes β^{th} column in the (4.13), M denotes the total numbers of unknown variables and N is the number of degree of freedom related to the variable. Repeated indices mean summation.

4.2.3 Tangent Stiffness Matrices

The symmetry of the tangent stiffness matrix in Newton iterative method is very important because most of the computational efforts to find the converged solution after obtaining the linear solution (i.e. solutions obtained with zero initial guess solution[1]) are related with the inversion of tangent matrix. By the equation (4.9) and (4.10), the increment of solution can be obtained by inverting the tangent matrix. The inverse of the coefficient matrix is only needed to get the linear solution. Thus the invert of the coefficient matrix does not required after very first step of the iteration. It can be shown that the first linear solution also can be obtained by using the symmetry solver with the choice of a zero initial guess solution. To discuss the symmetry of the tangent matrix, the tangent matrices of the newly developed models were calculated by using the equation given in (4.16). For example the $[T^{32}]$ of the EBT Model I can be calculated with the coefficient matrices $K_{ij}^{3\gamma}$ ($\gamma = 1, 2, \dots, 5$) which can be given by

$$\begin{aligned} K_{ij}^{31} &= \int_{x_a}^{x_b} \left(\psi_i^{N_{xx}} \frac{d\psi_j^{u_0}}{dx} \right) dx, \\ K_{ij}^{32} &= \int_{x_a}^{x_b} \left(\frac{1}{2} \frac{d\mathbf{w}_a}{d\mathbf{x}} \psi_i^{N_{xx}} \frac{d\psi_j^{w_0}}{dx} \right) dx, \\ K_{ij}^{33} &= \int_{x_a}^{x_b} \left(-\frac{\psi_i^{N_{xx}} \psi_j^{N_{xx}}}{EA} \right) dx, \end{aligned}$$

$$K_{ij}^{34} = K_{ij}^{35} = 0.$$

If the degree of the freedom for each variable is N , we can calculate the T_{ij}^{32} by using the equation (4.16) as

$$\begin{aligned}
T_{ij}^{32} &= \left(\sum_{\gamma=1}^5 \sum_{k=1}^N \frac{\partial K_{ik}^{3\gamma}}{\partial \mathbb{w}_j} U_k^\gamma + K_{ij}^{32} \right) \\
&= K_{ij}^{32} + \sum_{k=1}^N \frac{\partial}{\partial \mathbb{w}_j} \left[\int_{x_a}^{x_b} \left(\psi_i^{N_{xx}} \frac{d\psi_k^{u_0}}{dx} \right) dx \right] \mathbb{w}_k \\
&\quad + \sum_{k=1}^N \frac{\partial}{\partial \mathbb{w}_j} \left[\int_{x_a}^{x_b} \left(\frac{1}{2} \frac{d\mathbf{w}_a}{dx} \psi_i^{N_{xx}} \frac{d\psi_k^{w_0}}{dx} \right) dx \right] \mathbb{w}_k \\
&\quad + \sum_{k=1}^N \frac{\partial}{\partial \mathbb{w}_j} \left[\int_{x_a}^{x_b} \left(-\frac{\psi_i^{N_{xx}} \psi_k^{N_{xx}}}{EA} \right) dx \right] \mathbb{N}_k + 0 + 0 \\
&= \int_{x_a}^{x_b} \frac{1}{2} \left[\frac{\partial}{\partial \mathbb{w}_j} \left(\sum_{k=1}^N \frac{d\psi_p^{w_0}}{dx} \mathbb{w}_p \right) \psi_i^{N_{xx}} \left(\sum_{k=1}^N \frac{d\psi_k^{w_0}}{dx} \mathbb{w}_k \right) dx \right] + K_{ij}^{32} \\
&= \frac{1}{2} \int_{x_a}^{x_b} \left[\frac{d\psi_j^{w_0}}{dx} \psi_i^{N_{xx}} \frac{d\mathbf{w}_a}{dx} \right] + K_{ij}^{32} \\
&= K_{ij}^{32} + \int_{x_a}^{x_b} \left(\frac{1}{2} \frac{d\mathbf{w}_a}{dx} \psi_i^{N_{xx}} \frac{d\psi_j^{w_0}}{dx} \right) dx. \tag{4.17}
\end{aligned}$$

where the variables are given by

$$U_k^\gamma = \mathbb{w}_k, \mathbb{w}_k, \mathbb{N}_k, \mathbb{V}_k \text{ and } \mathbb{M}_j \text{ for } \gamma = 1, 2, \dots, M(=5), \text{ respectively.}$$

Likewise, every specific term of the tangent stiffness matrices of newly developed nonlinear beam and plate bending models can be calculated. From the equation (4.15), we can notice that each of the tangent coefficient matrices is consist of the sum of coefficient matrix $K_{ij}^{\alpha\beta}$ and the additional terms. So we can express every tangent matrix as the form of, $T_{ij}^{\alpha\beta} = K_{ij}^{\alpha\beta} + \text{additional terms}$. The results of the calculations of the tangent matrix of the each model can be given as follow:

- Model I of the beam bending

$$\begin{aligned} [T^{32}] &= [K^{32}] + \int_{x_a}^{x_b} \left(\frac{1}{2} \frac{d\mathbf{w}_a}{dx} \psi_i^{N_{xx}} \frac{d\psi_j^{w_0}}{dx} \right) dx, \\ [T^{42}] &= [K^{42}] + \int_{x_a}^{x_b} \left[(N_{xx}^a) \psi_i^V \frac{d\psi_j^w}{dx} \right] dx. \end{aligned} \quad (4.18)$$

- Model II of the beam bending

$$\begin{aligned} [T^{32}] &= [K^{32}] + \int_{x_a}^{x_b} \left(\frac{1}{2} \frac{d\mathbf{w}_a}{dx} \psi_i^{N_{xx}} \frac{d\psi_j^{w_0}}{dx} \right) dx, \\ [T^{22}] &= [K^{22}] + \int_{x_a}^{x_b} \left[(N_{xx}^a) \frac{d\psi_i^w}{dx} \frac{d\psi_j^w}{dx} \right] dx. \end{aligned} \quad (4.19)$$

- Model III of the beam bending

$$\begin{aligned} [T^{43}] &= [K^{43}] + \int_{x_a}^{x_b} \left(\frac{1}{2} \theta_x^a \psi_i^{N_{xx}} \psi_j^{\theta_x} \right) dx, \\ [T^{33}] &= [K^{33}] + \int_{x_a}^{x_b} \left(\theta_x^a \psi_i^{\theta_x} \psi_j^{N_{xx}} \right) dx. \end{aligned} \quad (4.20)$$

- Model IV of the beam bending

$$\begin{aligned} [T^{22}] &= [K^{22}] + \int_{x_a}^{x_b} \left(N_{xx}^a \frac{d\psi_i^{w_0}}{dx} \frac{d\psi_j^{w_0}}{dx} \right) dx, \\ [T^{42}] &= [K^{42}] + \int_{x_a}^{x_b} \left(\frac{1}{2} \frac{d\mathbf{w}_0^a}{dx} \psi_i^{N_{xx}} \frac{d\psi_j^{w_0}}{dx} \right) dx. \end{aligned} \quad (4.21)$$

- Model I of the plate bending

$$[T^{43}] = [K^{43}] + \int_{\Omega_e} \left\{ \frac{1}{2} \left(\frac{\partial \mathbf{w}_0^a}{\partial \mathbf{x}} \right) \psi_i^{N_{xx}} \frac{\partial \psi_j^{w_0}}{\partial \mathbf{x}} \right\} dx dy,$$

$$\begin{aligned}
[T^{53}] &= [K^{53}] + \int_{\Omega_e} \left\{ \frac{1}{2} \left(\frac{\partial \mathbf{w}_0^a}{\partial \mathbf{y}} \right) \psi_i^{N_{yy}} \frac{\partial \psi_j^{w_0}}{\partial y} \right\} dx dy, \\
[T^{63}] &= [K^{63}] + \int_{\Omega_e} \left\{ \frac{1}{2} \left[\left(\frac{\partial \mathbf{w}_0^a}{\partial \mathbf{x}} \right) \psi_i^{N_{xy}} \frac{\partial \psi_j^w}{\partial y} + \left(\frac{\partial \mathbf{w}_0^a}{\partial \mathbf{y}} \right) \psi_i^{N_{xy}} \frac{\partial \psi_j^w}{\partial x} \right] \right\} dx dy, \\
[T^{73}] &= [K^{73}] + \int_{\Omega_e} \left\{ \mathbf{N}_{xx}^a \psi_i^{V_x} \frac{\partial \psi_j^{w_0}}{\partial x} + \mathbf{N}_{xy}^a \psi_i^{V_x} \frac{\partial \psi_j^{w_0}}{\partial y} \right\} dx dy, \\
[T^{83}] &= [K^{83}] + \int_{\Omega_e} \left\{ \mathbf{N}_{xy}^a \psi_i^{V_y} \frac{\partial \psi_j^{w_0}}{\partial x} + \mathbf{N}_{yy}^a \psi_i^{V_y} \frac{\partial \psi_j^{w_0}}{\partial y} \right\} dx dy. \tag{4.22}
\end{aligned}$$

- Model II of the plate bending

$$\begin{aligned}
[T^{33}] &= [K^{33}] \\
&+ \int_{\Omega_e} \left\{ \mathbf{N}_{xx}^a \frac{\partial \psi_i^{w_0}}{\partial x} \frac{\partial \psi_j^{w_0}}{\partial x} + \mathbf{N}_{xy}^a \left(\frac{\partial \psi_i^{w_0}}{\partial x} \frac{\partial \psi_j^{w_0}}{\partial y} + \frac{\partial \psi_i^{w_0}}{\partial y} \frac{\partial \psi_j^{w_0}}{\partial x} \right) \right. \\
&\quad \left. + \mathbf{N}_{yy}^a \frac{\partial \psi_i^{w_0}}{\partial y} \frac{\partial \psi_j^{w_0}}{\partial y} \right\} dx dy, \\
[T^{43}] &= [K^{43}] + \int_{\Omega_e} \left\{ \frac{1}{2} \left(\frac{\partial \mathbf{w}_0^a}{\partial \mathbf{x}} \right) \psi_i^{N_{xx}} \frac{\partial \psi_j^{w_0}}{\partial x} \right\} dx dy, \\
[T^{53}] &= [K^{53}] + \int_{\Omega_e} \left\{ \frac{1}{2} \left(\frac{\partial \mathbf{w}_0^a}{\partial \mathbf{y}} \right) \psi_i^{N_{yy}} \frac{\partial \psi_j^{w_0}}{\partial y} \right\} dx dy, \\
[T^{63}] &= [K^{63}] + \int_{\Omega_e} \left\{ \frac{1}{2} \left[\left(\frac{\partial \mathbf{w}_0^a}{\partial \mathbf{x}} \right) \psi_i^{N_{xy}} \frac{\partial \psi_j^{w_0}}{\partial y} + \left(\frac{\partial \mathbf{w}_0^a}{\partial \mathbf{y}} \right) \psi_i^{N_{xy}} \frac{\partial \psi_j^{w_0}}{\partial x} \right] \right\} dx dy. \tag{4.23}
\end{aligned}$$

- Model III of the plate bending

$$\begin{aligned}
[T^{33}] &= [K^{33}] \\
&+ \int_{\Omega_e} \left\{ \mathbf{N}_{xx}^a \frac{\partial \psi_i^{w_0}}{\partial x} \frac{\partial \psi_j^{w_0}}{\partial x} + \mathbf{N}_{xy}^a \left(\frac{\partial \psi_i^{w_0}}{\partial x} \frac{\partial \psi_j^{w_0}}{\partial y} + \frac{\partial \psi_i^{w_0}}{\partial y} \frac{\partial \psi_j^{w_0}}{\partial x} \right) \right. \\
&\quad \left. + \mathbf{N}_{yy}^a \frac{\partial \psi_i^{w_0}}{\partial y} \frac{\partial \psi_j^{w_0}}{\partial y} \right\} dx dy, \\
[T^{63}] &= [K^{63}] + \int_{\Omega_e} \left\{ \frac{1}{2} \left(\frac{\partial \mathbf{w}_0^a}{\partial \mathbf{x}} \right) \psi_i^{N_{xx}} \frac{\partial \psi_j^{w_0}}{\partial x} \right\} dx dy, \\
[T^{73}] &= [K^{73}] + \int_{\Omega_e} \left\{ \frac{1}{2} \left(\frac{\partial \mathbf{w}_0^a}{\partial \mathbf{y}} \right) \psi_i^{N_{yy}} \frac{\partial \psi_j^{w_0}}{\partial y} \right\} dx dy, \\
[T^{83}] &= [K^{83}] + \int_{\Omega_e} \left\{ \frac{1}{2} \left[\left(\frac{\partial \mathbf{w}_0^a}{\partial \mathbf{x}} \right) \psi_i^{N_{xy}} \frac{\partial \psi_j^{w_0}}{\partial y} + \left(\frac{\partial \mathbf{w}_0^a}{\partial \mathbf{y}} \right) \psi_i^{N_{xy}} \frac{\partial \psi_j^{w_0}}{\partial x} \right] \right\} dx dy. \tag{4.24}
\end{aligned}$$

- Model IV of the plate bending

$$\begin{aligned}
[T^{13}] &= [K^{13}] \\
&+ \frac{1}{2} \int_{\Omega_e} \left\{ \frac{\partial \psi_i^{u_0}}{\partial x} \left(A_{11} \frac{\partial \mathbf{w}_0^a}{\partial x} \frac{\partial \psi_j^{w_0}}{\partial x} + A_{12} \frac{\partial \mathbf{w}_0^a}{\partial y} \frac{\partial \psi_j^{w_0}}{\partial y} \right) \right. \\
&\quad \left. + A_{66} \frac{\partial \psi_i^{u_0}}{\partial y} \left(\frac{\partial \mathbf{w}_0^a}{\partial x} \frac{\partial \psi_j^{w_0}}{\partial y} + \frac{\partial \mathbf{w}_0^a}{\partial y} \frac{\partial \psi_j^{w_0}}{\partial x} \right) \right\} dx dy, \\
[T^{23}] &= [K^{23}] \\
&\frac{1}{2} \int_{\Omega_e} \left\{ \frac{\partial \psi_i^{v_0}}{\partial y} \left(A_{22} \frac{\partial \mathbf{w}_0^a}{\partial y} \frac{\partial \psi_j^{w_0}}{\partial y} + A_{12} \frac{\partial \mathbf{w}_0^a}{\partial x} \frac{\partial \psi_j^{w_0}}{\partial x} \right) \right. \\
&\quad \left. + A_{66} \frac{\partial \psi_i^{v_0}}{\partial x} \left(\frac{\partial \mathbf{w}_0^a}{\partial x} \frac{\partial \psi_j^{w_0}}{\partial y} + \frac{\partial \mathbf{w}_0^a}{\partial y} \frac{\partial \psi_j^{w_0}}{\partial x} \right) \right\} dx dy, \\
[T^{33}] &= [K^{33}] \\
&+ \frac{1}{2} \int_{\Omega_e} \left\{ \left[A_{11} \left(\frac{\partial \mathbf{w}_0^a}{\partial x} \right)^2 + A_{66} \left(\frac{\partial \mathbf{w}_0^a}{\partial y} \right)^2 \right] \frac{\partial \psi_i^{w_0}}{\partial x} \frac{\partial \psi_j^{w_0}}{\partial x} \right. \\
&\quad + \left[A_{66} \left(\frac{\partial \mathbf{w}_0^a}{\partial x} \right)^2 + A_{22} \left(\frac{\partial \mathbf{w}_0^a}{\partial y} \right)^2 \right] \frac{\partial \psi_i^{w_0}}{\partial y} \frac{\partial \psi_j^{w_0}}{\partial y} \\
&\quad \left. + (A_{12} + A_{66}) \frac{\partial \mathbf{w}_0^a}{\partial x} \frac{\partial \mathbf{w}_0^a}{\partial y} \left(\frac{\partial \psi_i^{w_0}}{\partial x} \frac{\partial \psi_j^{w_0}}{\partial y} + \frac{\partial \psi_i^{w_0}}{\partial y} \frac{\partial \psi_j^{w_0}}{\partial x} \right) \right\} dx dy \\
&+ \int_{\Omega_e} \left\{ A_{11} \left[\frac{\partial \mathbf{u}_0^a}{\partial x} + \frac{1}{2} \left(\frac{\partial \mathbf{w}_0^a}{\partial x} \right)^2 \right] + A_{12} \left[\frac{\partial \mathbf{v}_0^a}{\partial y} + \frac{1}{2} \left(\frac{\partial \mathbf{w}_0^a}{\partial y} \right)^2 \right] \right\} \frac{\partial \psi_i^{w_0}}{\partial x} \frac{\partial \psi_j^{w_0}}{\partial x} dx dy \\
&+ \int_{\Omega_e} \left\{ A_{12} \left[\frac{\partial \mathbf{u}_0^a}{\partial x} + \frac{1}{2} \left(\frac{\partial \mathbf{w}_0^a}{\partial x} \right)^2 \right] + A_{22} \left[\frac{\partial \mathbf{v}_0^a}{\partial y} + \frac{1}{2} \left(\frac{\partial \mathbf{w}_0^a}{\partial y} \right)^2 \right] \right\} \frac{\partial \psi_i^{w_0}}{\partial y} \frac{\partial \psi_j^{w_0}}{\partial y} dx dy \\
&+ \int_{\Omega_e} (A_{12} + A_{66}) \frac{\partial \mathbf{w}_0^a}{\partial x} \frac{\partial \mathbf{w}_0^a}{\partial y} \left(\frac{\partial \psi_i^{w_0}}{\partial x} \frac{\partial \psi_j^{w_0}}{\partial y} + \frac{\partial \psi_i^{w_0}}{\partial y} \frac{\partial \psi_j^{w_0}}{\partial x} \right) dx dy.
\end{aligned} \tag{4.25}$$

Rest components of the tangent matrix which are not specified above is the same as the components of the coefficient matrix, which can be written as

$$T_{ij}^{\alpha\beta} = K_{ij}^{\alpha\beta} + [0]. \tag{4.26}$$

As mentioned, the symmetry of the tangent matrix can be obtained in every Model except for the beam Model I and the plate Model I. Because of shear terms (i. e., V_x and

V_y) included we cannot expect the symmetry of the tangent matrix in the beam Model I and the plate Model I. Then these two models should be solved by asymmetry solver[1], which is based on the Gauss Eliminations[24] to invert a matrix. The numerical results will be discussed in the chapter V.

4.3 Load Increment Vector

In the applications of the direct iterative method in nonlinear finite element analysis of the structural problems, the load increment is very critical to get converged nonlinear solution under a large applied distributed load (q_0). Without proper increment load, the solution may not converge with the direct iterative method. But the Newton iterative method can be applied at the more general range of applied distributed load (q_0) without load increment to get the converged solutions, while more iterative time is substantial. The details of the load increment will be discussed in chapter V with the numerical results of the examples.

CHAPTER V

NUMERICAL RESULTS

In this chapter we will discuss the numerical results of the nonlinear finite element models of the beam and plates bending problems. Comparisons of various models are presented with linear analysis and non linear analysis.

5.1. Numerical Analysis of Nonlinear Beam Bending

5.1.1 Description of Problem[1]

A beam made of steel ($E = 30 \times 10^6 \text{ psi}$) whose geometry is given in the Fig. 5.1, was chosen for the study of the 1D nonlinear analysis. Three different boundary conditions, i.e. HH, PP and CC, were considered to see the performance of the beam.

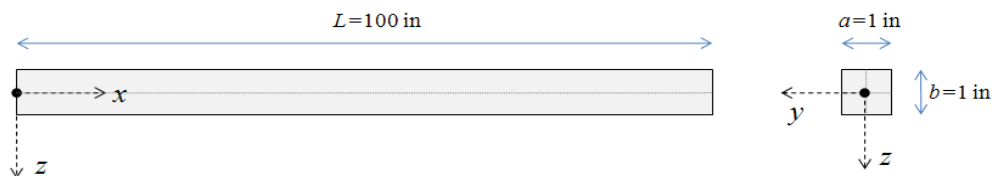


Fig. 5.1 Description of the beam geometry.

Three types of boundary conditions under the distributed load q_0 are considered with 4 nonlinear beam bending models developed in the chapter II. The descriptions of three boundary conditions are given in the Fig. 5.2. Under evenly distributed load q_0 and the given boundary conditions, we can use the symmetry part of the beam as a computational domain of the finite element analysis. To use the symmetry part of the beam as the computational domain, the mathematical boundary conditions at the middle

point (i.e., $x=L/2$) of the beam should be specified. By the geometry of the beam bending under the given boundary conditions and evenly distributed load, the mathematical boundary conditions of the middle point can be specified in addition to the boundary conditions of the one edge of the beam as shown in the Fig. 5.2. It can be seen that the current EBT mixed nonlinear Model I and II do not includes the slope, i.e., $-dw_0/dx$, as a primary variable. It is important to specify either primary or secondary variable as a boundary condition. In the same sense we should specify only the moment, $M_{xx}(0) = 0$, as a primary variable at the edge of the beam because the slope, $-dw_0/dx$, is not known there. Thus it is clear that if any specified boundary condition exists, one should specify either the primary or the secondary variable at the typical nodal point. This can be clarified by using the pairs of the primary and secondary variables that we classified in the chapter III. With the beam Model IV, the shear rotation of the beam cross section ϕ_x was included, so it can be specified as shown in the Fig. 5.2.

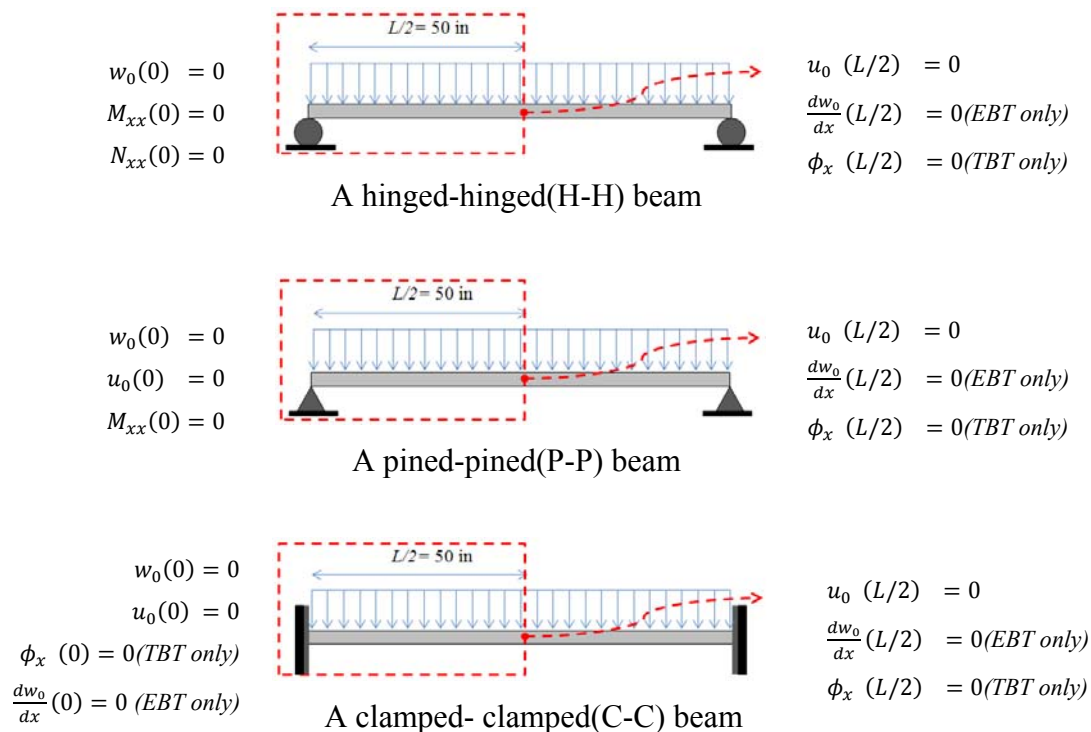


Fig. 5.2. Symmetry boundary conditions of beams.

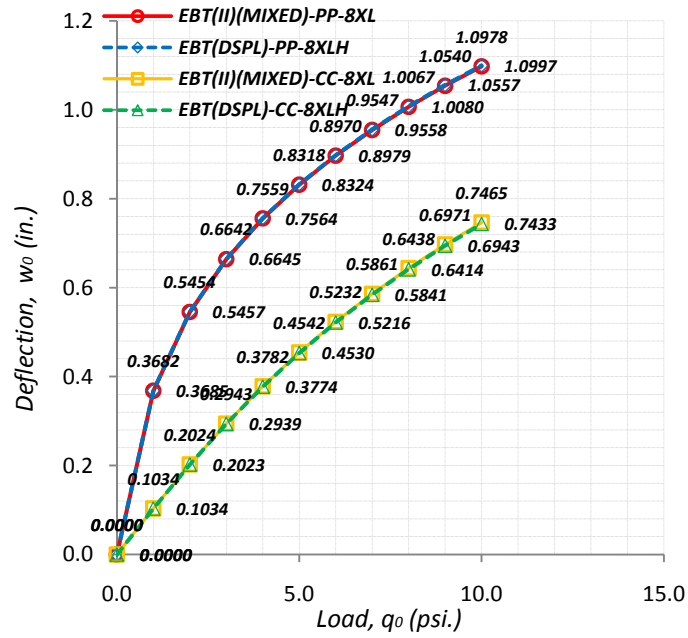
5.1.2 Numerical Results

First, the results of the mixed models and the displacement based models[1] are compared to see the validness of the solutions. The center deflections of the mixed Model I and IV, using eight linear elements ($8 \times L$) mesh are presented in the Table 5.1, along with the results of the displacement based Models of the EBT and the TBT using eight linear-Hermite($8 \times LH$) and eight linear elements($8 \times L$) respectively. Every converged solution was obtained by using the Newton-Raphson iterative method.

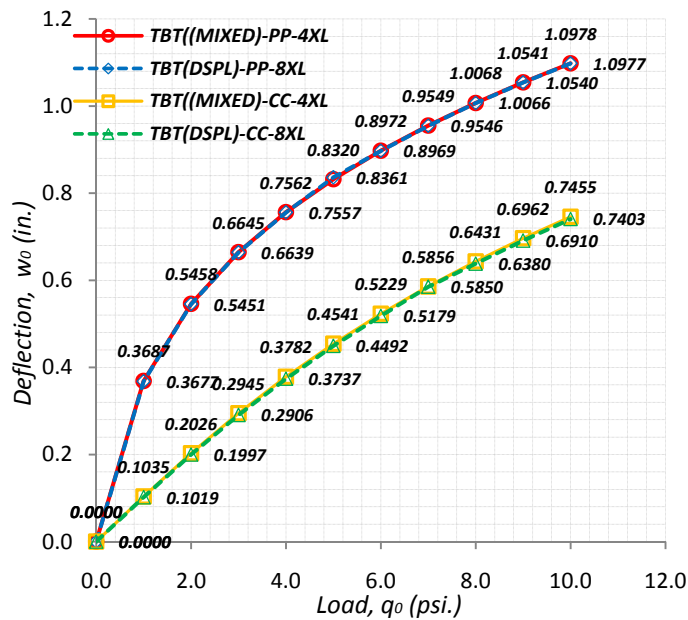
The graph of the mixed models and the displacement based models, which are given in the Fig. 5.3, shows almost the same results for the two different boundary conditions. With the same eight linear elements mesh, the difference of the converged solutions is not considerable. And the difference of the solutions between the TBT and the EBT beams is also negligible.

Table 5.1
Comparison of mixed models and displacement based models.

The load q_0 (psi/in)	The center deflection w_0 (in)							
	Mixed nonlinear Models				Displacement based nonlinear Models[1]			
	The Model (I) - $8 \times L$		The Model (IV) - $8 \times L$		EBT - $8 \times LH$		TBT - $8 \times L$	
	CC	PP	CC	PP	CC	PP	CC	PP
0.0	0.000000	0.000000	0.000000	0.000000	0.0000	0.0000	0.0000	0.0000
1.0	0.103380(3)	0.368892(5)	0.103492(3)	0.368715(5)	0.1034(3)	0.3685(5)	0.1019(3)	0.3677(5)
2.0	0.202427(3)	0.546221(4)	0.202587(3)	0.545838(4)	0.2023(3)	0.5457(4)	0.1997(3)	0.5451(4)
3.0	0.294349(3)	0.665046(4)	0.294469(3)	0.664527(4)	0.2939(3)	0.6645(4)	0.2906(3)	0.6639(4)
4.0	0.378187(3)	0.756797(4)	0.378194(3)	0.756180(4)	0.3774(3)	0.7564(4)	0.3737(3)	0.7557(4)
5.0	0.454206(3)	0.832666(4)	0.454054(3)	0.831972(4)	0.4530(3)	0.8324(4)	0.4492(3)	0.8316(4)
6.0	0.523212(3)	0.897967(4)	0.522877(3)	0.897212(4)	0.5216(3)	0.8979(4)	0.5179(3)	0.8969(4)
7.0	0.586135(3)	0.955668(4)	0.585607(3)	0.954862(4)	0.5841(3)	0.9558(4)	0.5805(3)	0.9546(4)
8.0	0.643848(3)	1.007606(4)	0.643129(3)	1.006757(4)	0.6414(3)	1.0080(4)	0.6380(3)	1.0066(4)
9.0	0.697107(3)	1.055004(4)	0.696202(3)	1.054117(4)	0.6943(3)	1.0557(4)	0.6910(3)	1.0540(4)
10.0	0.746547(3)	1.098719(4)	0.745463(3)	1.097800(4)	0.7433(3)	1.0997(4)	0.7403(3)	1.0977(4)



(a) Comparison of the Model I with EBT displacement based Model.



(b) Comparison of the Model IV with the TBT displacement Model.

Fig. 5.3. A comparison of the non-linear solutions of beams.

But under the hinged-hinged boundary condition, current mixed models showed much better results compared with displacement based models. The displacement Model showed the membrane locking[14]. The membrane locking occurs because of the inconsistent presence the polynomial degree in the approximations. To examine it, we consider a hinged-hinged boundary condition with the Model I, II and IV. For the hinged-hinged boundary condition, total applied load should contribute for the bending of the beam element, because there is no horizontal constrain to cause membrane strain, i.e., ε_{xx} . In the finite element models, the strain ε_{xx} can be expressed as follow: (see Reddy [1])

$$\varepsilon_{xx} = \frac{du_0}{dx} + \left(\frac{dw_0}{dx}\right)^2. \quad (5. 1)$$

To satisfy the physics under the given boundary conditions, strain ε_{xx} should be zero. But because of the use of polynomial approximations, there can be inconsistency[1] of the degree of terms in the strain. Especially, in the displacement based model, u_0 was approximated with linear interpolation function, and w_0 was approximated by using cubic interpolations functions. For this typical pair of approximations, the degree of the each term in the strain ε_{xx} can be given by

$$\varepsilon_{xx} \cong 0 = \frac{du_0}{dx} [= \mathbf{constant}] + \left(\frac{dw_0}{dx}\right)^2 [\mathbf{4th order}]. \quad (5. 2)$$

Thus it is not easy for du_0/dx to make whole strain term to be zero, because it is presented as constant. This phenomenon is very well known drawback of the nonlinear EBT and TBT finite element model.

And for the TBT models, another locking can be observed from the shear strain relations[1] which can be given as,

$$\gamma_{xz} \cong \phi_x + \frac{dw_0}{dx} [= \textit{constant}] . \quad (5. 3)$$

To fix these defect, the reduced integrations[1, 7], use of consistent approximations and use of higher order interpolations can be used. The effects of the locking with full integration in different models are given in the Table 5.2.

Table 5.2
Membrane locking in mixed models and misplacement models.

The load (q_0)	The center deflection (in) -HH			
	TBT(Model IV) 4 x L	TBT(DSPL) 4 x L	EBT(I)(Model I) 4 x L	EBT(DSPL) 4 x LH
0.0	0.0000	0.0000	0.0000	0.0000
1.0	0.5181	0.1223	0.5208	0.5108
2.0	1.0361	0.2446	1.0417	1.0213
3.0	1.5542	0.3669	1.5625	1.4986
4.0	2.0723	0.4892	2.0833	1.9453
5.0	2.5904	0.6115	2.6042	2.3607
6.0	3.1084	0.7338	3.1250	2.7467
7.0	3.6265	0.8561	3.6458	3.1074
8.0	4.1446	0.9784	4.1667	3.4422
9.0	4.6626	1.1007	4.6875	3.7564
10.0	5.1807	1.2230	5.2083	4.0523

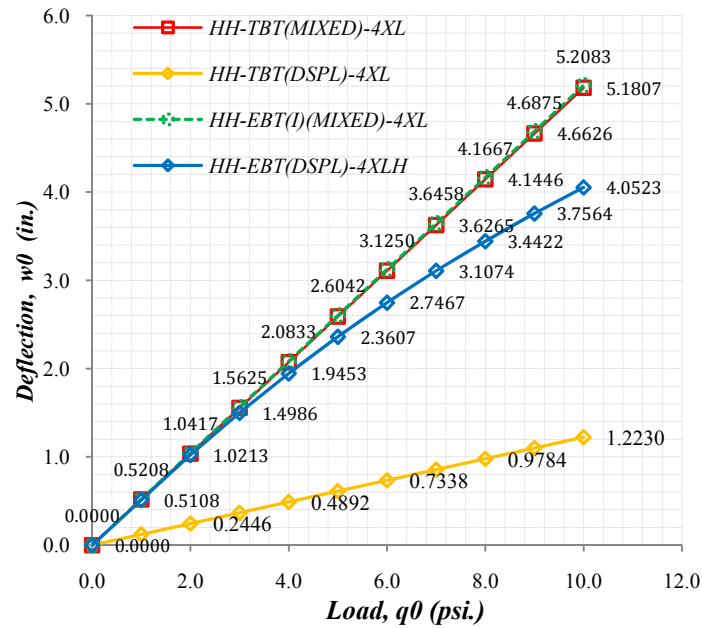
The results presented in the Table 5.2 are showing that the membrane locking can be eliminated by using the mixed nonlinear model in both of the TBT and the EBT beams. Usually the locking can be mitigated by using a more refined mesh, but the mixed Model I and IV didn't showed any locking even with 2 linear elements mesh as shown in the Table 5.2.

But, among current mixed models, the membrane locking appeared in different levels. For example, the comparison of the Model I and the Model II shows that the Model I is showing better performance compared with the Model II. But the Model II is still showing better result compared with the displacement based model. The result of the hinged-hinged(HH) boundary condition of the Model I and II with 2 linear elements mesh is given in the Table 5.3.

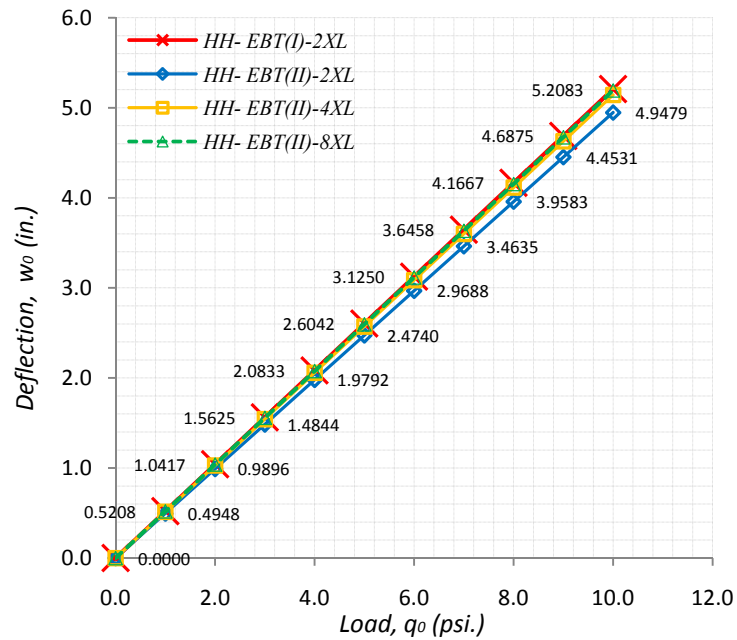
The graph (a) given in the Fig. 5.4, shows that the locking can be eliminated with the mixed Model I and IV. While the graph (b) shows that the Model II still has membrane locking. Even though the Model II has the membrane locking, the effect of it is not significant compared to the displacement based model.

Table 5. 3
Effect of the membrane locking in the mode I and II.

The load (q_0)	The center deflection (in)-HH			
	EBT(I) 2 x L	EBT(II) 2 x L	EBT(II) 4 x L	EBT(II) 8 x L
0.0	0.0000	0.0000	0.0000	0.0000
1.0	0.5208	0.4948	0.5143	0.5192
2.0	1.0417	0.9896	1.0286	1.0384
3.0	1.5625	1.4844	1.5430	1.5576
4.0	2.0833	1.9792	2.0573	2.0768
5.0	2.6042	2.4740	2.5716	2.5960
6.0	3.1250	2.9688	3.0859	3.1152
7.0	3.6458	3.4635	3.6003	3.6344
8.0	4.1667	3.9583	4.1146	4.1536
9.0	4.6875	4.4531	4.6289	4.6729
10.0	5.2083	4.9479	5.1432	5.1921



(a) Comparison of the membrane locking of various Models.



(b) Comparison of the membrane locking in the EBT Model I and Model II

Fig. 5.4 A comparison of the membrane locking in various models.

Next the effect of the length-to-thickness ratio on the deflections is presented in the Tables 5.4 and 5.5. The data in the Table 5.4 is showing that as the beam becomes thicker, it acts almost linearly, while thin beam shows nonlinearity more strongly.

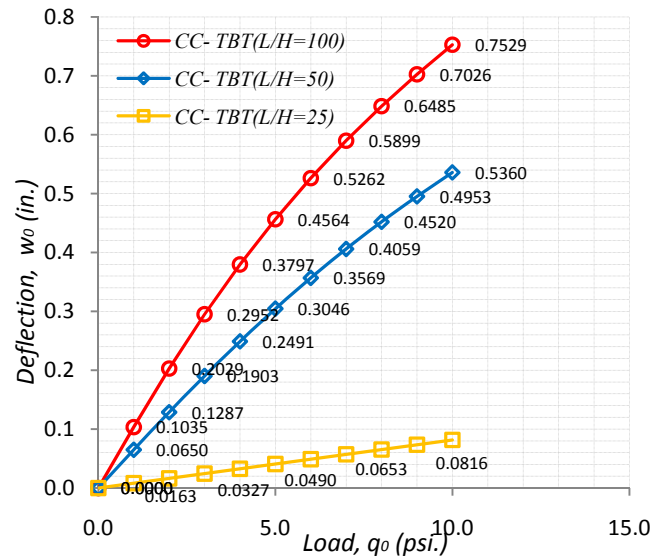
Table 5.4
Effect of the length-to-thickness ratio on the deflections in TBT beam.

The load (q_0)	TBT(L/H=100)	TBT(L/H=50)	TBT(L/H=25)
0.0	0.000000	0.000000	0.000000
1.0	0.103530	0.064961	0.008169
2.0	0.202854	0.128734	0.016338
3.0	0.295229	0.190329	0.024505
4.0	0.379677	0.249076	0.032671
5.0	0.456414	0.304625	0.040834
6.0	0.526203	0.356888	0.048994
7.0	0.589944	0.405950	0.057150
8.0	0.648490	0.451996	0.065302
9.0	0.702587	0.495260	0.073449
10.0	0.752860	0.535983	0.081591

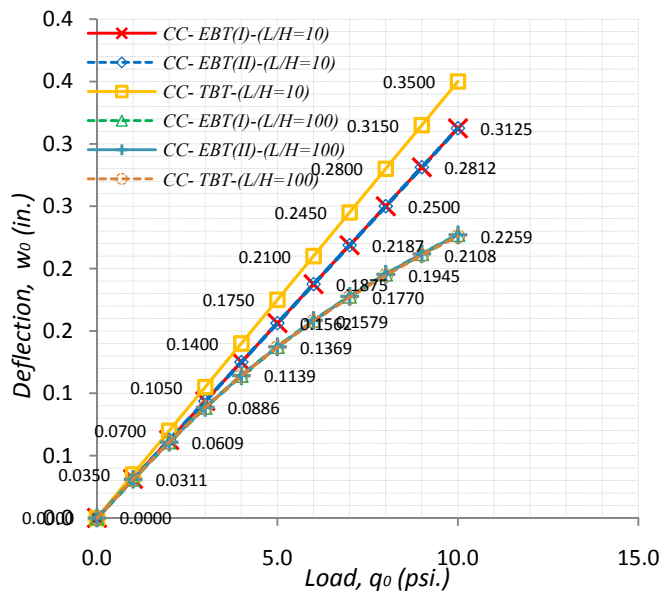
It can be shown that the differences of the solutions between the TBT and the EBT are negligible when the beam is thin, but it is not when the beam is thick.

Table 5.5
Comparison of the effect of the length-to-thickness ratio in the EBT and the TBT beams.

The load (q_0)	L/H=10			L/H=100		
	EBT(I)	EBT(II)	TBT	EBT(I)	EBT(II)	TBT
0.0	0.0000	0.0000	0.0000	0.0000	0.0000	0.0000
1.0	0.0313	0.0313	0.0350	0.0310	0.0310	0.0311
2.0	0.0625	0.0625	0.0700	0.0608	0.0608	0.0609
3.0	0.0937	0.0938	0.1050	0.0886	0.0886	0.0886
4.0	0.1250	0.1250	0.1400	0.1141	0.1141	0.1139
5.0	0.1562	0.1562	0.1750	0.1373	0.1373	0.1369
6.0	0.1875	0.1875	0.2100	0.1584	0.1584	0.1579
7.0	0.2187	0.2187	0.2450	0.1777	0.1777	0.1770
8.0	0.2500	0.2500	0.2800	0.1954	0.1955	0.1945
9.0	0.2812	0.2812	0.3150	0.2118	0.2118	0.2108
10.0	0.3125	0.3125	0.3500	0.2271	0.2271	0.2259



(a) Effect of the length-to-thickness ratio on deflections in the TBT beam



(b) Comparison of the effect of length-to-thickness ratio on deflections in the EBT and the TBT beams.

Fig. 5.5 Comparison of effect of the length-to-thickness ratio on the beam.

The model III showed poor performance compared with other newly developed models, but with cubic element it showed good accuracy and convergence. Some results of the model III presented in the Table 5. 6.

Table 5.6
Comparison of Model III with other mixed models.

The load q_0 (psi/in)	The center deflection w_0 (in)							
	The Model (III) - 2×C		The Model (III) - 4×C		The Model (I) - 2×C		The Model (II) - 2×C	
	CC	PP	CC	PP	CC	PP	CC	PP
0.0	0.0000	0.0000	0.0000	0.0000	0.0000	0.0000	0.0000	0.0000
1.0	0.1034	0.3685	0.1034	0.3685	0.1034	0.3685	0.1034	0.3685
2.0	0.2023	0.5454	0.2023	0.5454	0.2023	0.5454	0.2023	0.5454
3.0	0.2939	0.6639	0.2939	0.6639	0.2939	0.6639	0.2939	0.6639
4.0	0.3774	0.7554	0.3774	0.7555	0.3774	0.7555	0.3774	0.7555
5.0	0.4529	0.8311	0.4530	0.8312	0.4530	0.8312	0.4530	0.8312
6.0	0.5213	0.8963	0.5215	0.8963	0.5215	0.8963	0.5215	0.8963
7.0	0.5836	0.9539	0.5839	0.9539	0.5839	0.9539	0.5839	0.9539
8.0	0.6407	1.0057	0.6411	1.0057	0.6412	1.0057	0.6412	1.0057
9.0	0.6933	1.0530	0.6939	1.0531	0.6939	1.0530	0.6939	1.0530
10.0	0.7421	1.0966	0.7429	1.0967	0.7429	1.0967	0.7429	1.0967

The poor performance of Model III can be explained by the (2.12).

$$\theta_x - \frac{dw_0}{dx} = 0. \quad (5.5)$$

As discussed with the membrane locking and the shear locking, this typical relation created other kind of locking, because of the inconsistent approximation for the θ_x and w_0 . Since we included this relation only in the Model III, only Model III showed new kind of locking. But this locking was not fixed with reduced integration when lower order interpolation functions (i.e., linear and quadratic) are used. Only higher order interpolation function with reduced integration showed good results.

5.2. Numerical analysis of Nonlinear Plate Bending

5.2.1 Description of Problem[1]

Next, we consider a non-linear plate bending problems using the newly developed mixed models in the chapter III. A square plate with the following material properties was considered.

$$\begin{aligned} a = b = 10 \text{ in}, \quad h = 1 \text{ in}, \quad E = 7.8 \times 10^6 \text{ psi}, \\ \nu = 0.3(\text{or } 0.25 \text{ for linear analysis}), \end{aligned} \quad (5.4)$$

The origin of the coordinate was chosen to be located at the center of the plated. The geometry and the coordinate of the plate are described in the Fig. 5.6.

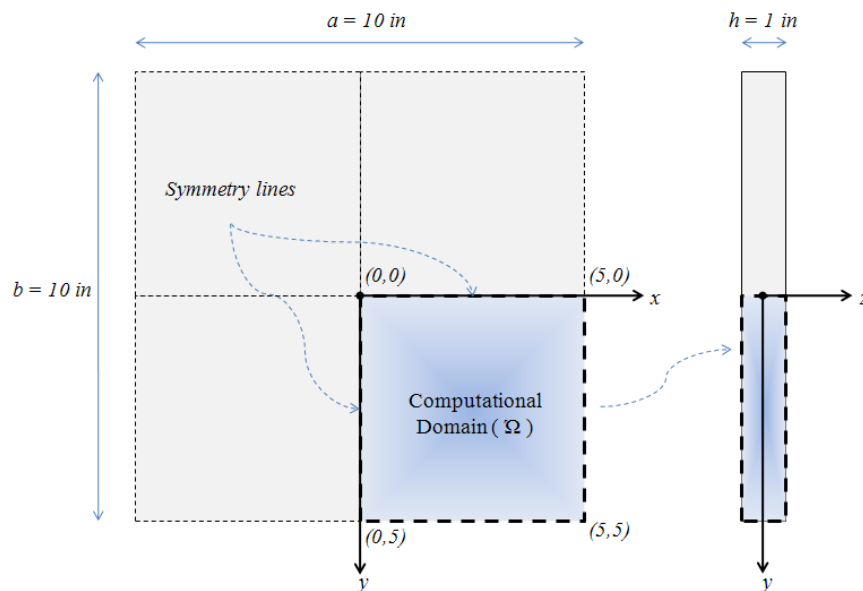


Fig. 5.6. A description of the plate bending problem.

As it was discussed in the beam bending problem, due to the given boundary conditions and the geometry of the plate and the applied load, the boundary conditions of

the rectangular plate with biaxial symmetry were considered. Here three symmetry boundary conditions were considered with common mathematical boundary condition along the symmetry lines of the quadrant of the plate. The specific boundary conditions are given in the Fig. 5.7. Note that for the SS1, at the singular points, i.e. point (5, 5), both boundary conditions of $y = 5$ and $x = 5$, were specified.

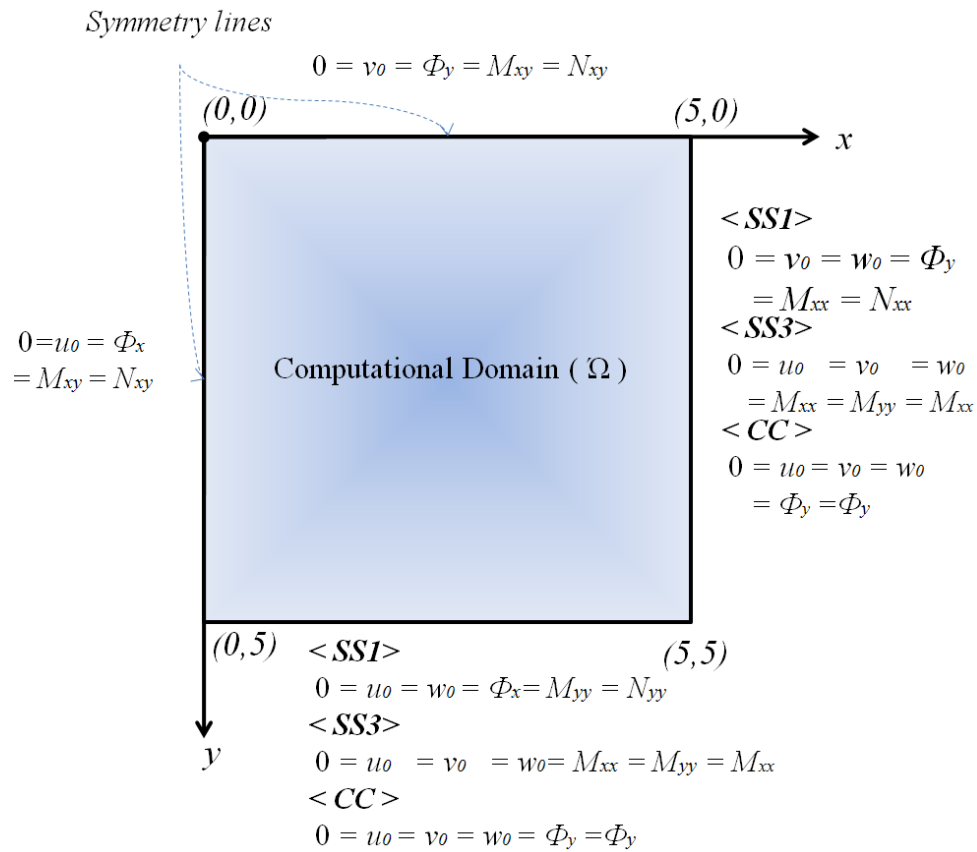


Fig. 5.7. Symmetry boundary conditions[1, 25] of a quadrant of the square plate.

5.2.2 Non-dimensional Analysis of Linear Solutions

To check the accuracy of the newly developed plate bending models, solutions of the new models were compared with those of the existing models [3, 26, 27] and analytic

solutions. First, the linear solutions of the mixed CPT models will be discussed by comparing the data obtained with displacement based model[1, 7].

It can be clearly shown, that the linear solution of the Model II is the same as that of the mixed model developed by Reddy[7], because both models includes the same variables(i.e. vertical displacement, and bending moments) which are related to the bending of the plate, while the Model I includes shear resultants also in addition to those. The comparison of the results of the various models under the simple support I (SS1) and clamped (CC) boundary conditions are given in the Tables 5.7 and 5.8.

For the simple support (SS1) boundary condition, the Model II showed best accuracy for the center vertical deflection, while the Model I provided better accuracy for the center bending moment as shown in the Table 5.7.

Table 5.7
Comparison of the linear solution of various CPT Models, isotropic ($\nu = 0.3$) square plate, simple supported (SS1).

Mesh size	Current Models		Mixed (Reddy [7])	Mixed (Herrmann[26])	Hybrid (Allman[27])	Compatible cubic displacement Model[1]
	MODEL I	Model II				
Liner (4-node)	Center deflection (* equivalent quadratic), $\bar{w} = w \times D_{11} \times 10^2 / (q_0 \times a^4)$ (Exact solution, 0.4062 [7])					
1×1	0.4613 (* -)	0.4613 (-)	0.4613	0.9018	0.347	0.220
2×2	0.4383 (0.4154)	0.4237 (0.4154)	0.4237	0.5127	0.392	0.371
4×4	0.4135 (0.4067)	0.4106 (0.4067)	0.4106	0.4316	0.403	0.392
6×6	0.4094 (0.4063)	0.4082 (0.4063)	0.4082	0.4172	-	-
8×8	0.4079 (0.4063)	0.4073 (0.4063)	-	-	-	-
Liner (4-node)	Center bending moment(equivalent quadratic), $\bar{M} = M \times 10 / (q_0 \times a^2)$ (Exact solution, 0.479 [7])					
1×1	0.7196 (-)	0.7196 (-)	0.7196	0.328	0.604	-
2×2	0.5029 (0.4906)	0.5246 (0.4096)	0.5246	0.446	0.515	-
4×4	0.4850 (0.4797)	0.4892 (0.4796)	0.4892	0.471	0.487	-
6×6	0.4816 (0.4790)	0.4834 (0.4790)	0.4834	0.476	-	-
8×8	0.4804 (0.4788)	0.4814 (0.4789)	-	-	-	-

Table 5.8
Comparison of the linear solution of various CPT Models, isotropic ($\nu = 0.3$)
square plate, clamped (CC).

Mesh size	Current Models		Mixed (Reddy [7])	Mixed (Herrmann[26])	Hybrid (Allman[27])	Compatible cubic displacement Model[1]
	Model I	Model II				
Liner (4-node)	Center deflection(*equivalent quadratic), $\bar{w} = w \times D_{11} \times 10^2 / (q_0 \times a^4)$ (Exact 0.1265 [7])					
1×1	0.1576 (* -)	1.6644 (-)	1.6644	0.7440	0.087	0.026
2×2	0.1502 (0.1512)	0.1528 (0.1512)	0.1528	0.2854	0.132	0.120
4×4	0.1310 (0.1279)	0.1339 (0.1278)	0.1339	0.1696	0.129	0.121
6×6	0.1284 (0.1268)	0.1299 (0.1268)	0.1299	0.1463	-	-
8×8	0.1265 (0.1265)	0.1270 (0.1266)	-	-	-	-
Liner (4-node)	Center bending moment(equivalent quadratic), $\bar{M} = M \times 10 / (q_0 \times a^2)$ (Exact 0.230 [7])					
1×1	0.4918 (-)	0.5193 (-)	0.5193	0.208	0.344	-
2×2	0.2627 (0.2552)	0.3165 (0.2552)	0.3165	0.242	0.314	-
4×4	0.2354 (0.2312)	0.2478 (0.2310)	0.2478	0.235	0.250	-
6×6	0.2318 (0.2295)	0.2374 (0.2295)	0.2374	0.232	-	-
8×8	0.2286 (0.2290)	0.2310 (0.2291)	-	-	-	-

For the clamped (CC) boundary condition, the Model I showed best accuracy both for the center vertical deflection and the center bending moment as shown in the Table 5.8. The difference of the solution between Model I and Model II was caused by the presence or absence of the shear resultant in the finite element models. Thus, by including the shear resultants (i.e., V_x and V_y) as nodal values in the CPT mixed finite element model, more accurate center bending moment and center vertical deflection were obtained.

Next, current CPT mixed models were compared with the displacement based model. For the CPT displacement based model, non-conforming [4] and the conforming[4] elements should be used because of the continuity requirement of the weak formulation[1]. Current mixed models provided better accuracy when the compatible nine-node quadratic element was used. But the four-node liner element also

provided acceptable accuracy compared with the non-conforming displacement based model. And, for the SS1 boundary condition with the Poisson's ratio, $\nu = 0.25$, the Model II also showed better accuracy as it did with $\nu = 0.3$. In both cases, stresses obtained from the current mixed model showed better accuracy, because the stresses can be directly computed by using bending moment or shear resultant obtained at the node, not including any derivative. Stresses in the Table 5.9, were obtained by the following equations. See equation (1.25) of the chapter I for specific terms of the matrix Q (i.e. Q_{ij} , $i, j = 1, 2, 6$), while Q_x is the vertical shear resultant of the FSDT. And D_{ij}^* is the component of the invert of matrix $[D]$ given in the (1.24) and (1.29).

$$\begin{aligned}\sigma_{xx} &= Q_{11}\varepsilon_{xx} + Q_{12}\varepsilon_{yy} = Q_{11}\varepsilon_{xx}^0 + Q_{12}\varepsilon_{yy}^0 + [Q_{11}(z\varepsilon_{xx}^1) + Q_{12}(z\varepsilon_{yy}^1)] \\ &= Q_{11}\varepsilon_{xx}^0 + Q_{12}\varepsilon_{yy}^0 + z \left[Q_{11} \left(-\frac{\partial^2 w_0}{\partial x^2} \right) + Q_{12} \left(-\frac{\partial^2 w_0}{\partial y^2} \right) \right]\end{aligned}\quad (5.6)$$

$$\begin{aligned}\sigma_{xy} &= Q_{66}\gamma_{xy} = Q_{66}\gamma_{xy}^0 + Q_{66}(z\gamma_{xy}^0) \\ &= Q_{66}\gamma_{xy}^0 + z \left[Q_{66} \left(-2\frac{\partial^2 w_0}{\partial x \partial y} \right) \right]\end{aligned}\quad (5.7)$$

$$\begin{aligned}\sigma_{xz} &= Q_{55}\gamma_{xz} = Q_{55}\gamma_{xz}^0 = \frac{Q_x}{(h K_s)} \quad (\text{Only for the FSDT, with } K_s = 5/6.) .\end{aligned}\quad (5.8)$$

Not only vertical deflection but also stresses showed better accuracy under simple supported I (SS1) boundary condition, when they were compared with those of the displacement based model. In most of the cases results obtained with 9-node quadratic element presented better accuracy. Results of isotropic plate, under SS1 boundary condition are given in the Table 5.9.

Table 5.9

Comparison of the CPT linear solution with that of the displacement model, isotropic ($\nu = 0.25$) square plate, simple supported (SS1). $\bar{w} = wE_{22} \times 10^2/(q_0a^4)$, $\bar{\sigma} = \sigma h^2/(q_0a^2)$, $\sigma_{xx}(0, 0, h/2)$, $\sigma_{xy}(a/2, b/2, h/2)$

Mesh type		Linear (4-node)			Quadratic (9-node)			Exact[1]
		2×2	4×4	8×8	1×1	2×2	4×4	
Model I	\bar{w}	4.9407	4.6534	4.5903	4.6753	4.5752	4.5704	4.5701
	$\bar{\sigma}_{xx}$	0.2912	0.2800	0.2772	0.2835	0.2859	0.2762	0.2762
	$\bar{\sigma}_{xy}$	0.2132	0.2114	0.2097	0.2498	0.2288	0.2162	0.2085
Model II	\bar{w}	4.7801	4.6221	4.5831	4.6753	4.5749	4.5704	4.5701
	$\bar{\sigma}_{xx}$	0.3035	0.2823	0.2864	0.2835	0.2767	0.2762	0.2762
	$\bar{\sigma}_{xy}$	0.1987	0.2054	0.2078	0.2498	0.2283	0.2160	0.2085
Mesh type		Linear(4-node) and Non-conforming (12 - node)			Linear (4-node) and Conforming (16 - node)			Exact[1]
		2×2	4×4	8×8	2×2	4×4	8×8	
DSPL. [1]	\bar{w}	4.8571	4.6425	4.5883	4.7619	4.5952	4.5739	4.5701
	$\bar{\sigma}_{xx}$	0.2405	0.2673	0.2740	0.2637	0.2637	0.2731	0.2762
	$\bar{\sigma}_{xy}$	0.1713	0.1964	0.2050	0.1688	0.1935	0.2040	0.2085

Table 5.10

Comparison of the CPT linear solution with that of the displacement Model, isotropic ($\nu = 0.25$) square plate, clamped(CC). $\bar{w} = wE_{22} \times 10^2/(q_0a^4)$, $\bar{\sigma} = \sigma h^2/(q_0a^2)$, $\sigma_{xx}(0, 0, h/2)$, $\sigma_{xy}(a/2, b/2, h/2)$

Mesh type		Linear (4-node)			Quadratic (9-node)			Exact
		2×2	4×4	8×8	1×1	2×2	4×4	
Model I	\bar{w}	1.6933	1.4746	1.4220	1.7043	1.4386	1.4234	1.4231
	$\bar{\sigma}_{xx}$	0.1528	0.1360	0.1318	0.1486	0.1335	0.1321	-
	$\bar{\sigma}_{xy}$	0.0433	0.0144	0.0062	0.0318	0.0067	0.0071	-
Model II	\bar{w}	1.7239	1.5080	1.4278	1.7043	1.4381	1.4248	1.4231
	$\bar{\sigma}_{xx}$	0.1839	0.1431	0.1331	0.1486	0.1333	0.1321	-
	$\bar{\sigma}_{xy}$	0.0378	0.0127	0.0068	0.0318	0.0065	0.0071	-
Mesh type		Linear(4-node) and Non-conforming (12 - node)			Linear (4-node) and Conforming (16 - node)			Exact
		2×2	4×4	8×8	2×2	4×4	8×8	
DSPL. [1]	\bar{w}	1.5731	1.4653	1.4342	1.4778	1.4370	1.4249	1.4231
	$\bar{\sigma}_{xx}$	0.0987	0.1238	0.1301	0.0861	0.1197	0.1288	-
	$\bar{\sigma}_{xy}$	0.0497	0.0222	0.0067	0.0489	0.0224	0.0068	-

Improvement was noticed with clamped boundary condition. The comparison of the results with isotropic plate ($\nu = 0.25$), under CC boundary condition are given in the Table 5.10.

Next, the numerical results of the Model III and IV are compared with the results of the Reddy's mixed model[1]. The mixed model developed by Reddy included bending moments as independent nodal value in the finite element model, while current Model III and IV included vertical shear resultants (i.e., Q_x and Q_y), as independent nodal value. Note that the difference between Model III and VI comes from the presence or absence of membrane forces (i.e., N_{xx} , N_{yy} and N_{xy}) in the finite element models. Thus, the solution of the linear bending of each model is essentially the same as shown in the Table 5.11.

Table 5.11
Comparison of the current mixed FSDT linear solution with that of the other mixed model (Reddy[7]), with isotropic ($\nu = 0.25$, $K_s = 5/6$) square plate, simple supported (SS1).

Mesh size	Current Models		Mixed (Reddy[7])	Current Models		Mixed (Reddy[7])
	Model(III)	Model(IV)		Model(III)	Model(IV)	
Liner (4-node)	Center deflection, $\bar{w} = wD_{11} \times 10^2 / (q_0 a^4)$, (Exact 0.427[8])			Center bending moment $\bar{M} = M \times 10 / (q_0 a^2)$, (Exact 0.479[8])		
1×1	0.4174 (* -)	0.4174 (-)	0.4264	0.6094 (-)	0.6094 (-)	0.6094
2×2	0.4293 (0.4345)	0.4293 (0.4345)	0.4321	0.5060 (0.4779)	0.5060 (0.4779)	0.5070
4×4	0.4280 (0.4277)	0.4280 (0.4277)	0.4285	0.4849 (0.4779)	0.4849 (0.4779)	0.4850
8×8	0.4275 (0.4273)	0.4275 (0.4273)	-	0.4803 (0.4785)	0.4803 (0.4785)	-

Also the comparison of the center deflection and stresses of current models with those of the displacement based model is presented in the Table 5.12. In most of cases, current models showed better accuracy for both of the center vertical displacement and stresses.

Table 5.12

Comparison of the linear solution of the FSDT with isotropic ($\nu = 0.25, K_s = 5/6$) square plate, simple supported (SS1). $\bar{w} = wE_{22} \times 10^2 / (q_0 a^4)$, $\bar{\sigma} = \sigma h^2 / (q_0 a^2)$, $\sigma_{xx}(0, 0, h/2)$, $\sigma_{xy}(a/2, b/2, h/2)$, $\sigma_{xz}(a/2, 0, h/2)$

Model type	Mesh type	Linear (4-node)			Quadratic (9-node)			Exact[1]
		2×2	4×4	8×8	1×1	2×2	4×4	
Model (III)	\bar{w}	4.8139	4.7987	4.7931	4.8727	4.7950	4.7913	4.7914
	$\bar{\sigma}_{xx}$	0.2920	0.2797	0.2771	0.2756	0.2755	0.2762	0.2762
	$\bar{\sigma}_{xy}$	0.2093	0.2098	0.2097	0.2399	0.2216	0.2135	0.2085
	$\bar{\sigma}_{xz}$	0.3962	0.4025	0.4047	0.3576	0.3907	0.4002	0.3927
Model (IV)	\bar{w}	4.8139	4.7987	4.7931	4.8727	4.7950	4.7913	4.7914
	$\bar{\sigma}_{xx}$	0.2920	0.2797	0.2771	0.2756	0.2755	0.2762	0.2762
	$\bar{\sigma}_{xy}$	0.2093	0.2098	0.2097	0.2399	0.2216	0.2135	0.2085
	$\bar{\sigma}_{xz}$	0.3962	0.4025	0.4047	0.3576	0.3907	0.4002	0.3927
DSPL.[1]	\bar{w}	4.8887	4.8137	4.7866	4.9711	4.8005	4.7917	4.7914
	$\bar{\sigma}_{xx}$	0.2441	0.2684	0.2737	0.2645	0.2716	0.2750	0.2762
	$\bar{\sigma}_{xy}$	0.1504	0.1869	0.2737	0.1652	0.1943	0.2044	0.2085
	$\bar{\sigma}_{xz}$	0.2750	0.3356	0.2008	0.2886	0.3425	0.3735	0.3927

5.2.3 Non-linear Analysis

Total 12 load step was used to see the significance of the non-linearity with the following incremental load parameter vector [1], $P = q_0 a^4 / (E_{22} h^4)$.

$$P = \{ 6.25, 12.5, 25.0, 25.0, 25.0, 25.0, 25.0, 25.0, 25.0, 25.0, 25.0, 25.0 \} \quad (5.9)$$

A tolerance $\epsilon = 0.01$ was used for convergence in the Newton – Raphson iteration scheme. Model I and II was compared with the CPT displacement base model to see its non-linear behavior. In non-linear analysis of the CPT, center deflection, normal stress and membrane stress were compared with the results of the non-conforming and conforming displacement based models.

First, the center deflection, w_0 , of the newly developed models are presented in the Table 5.13. In every load step, converged solution was obtained within 4 iterations. To investigate the effect of reduced integration, results of full integration and the reduced integration were presented in the Table 5.13. In both of the model, the locking was not severe and the effect of reduced integration was not significant.

Table 5.13
Effect of reduced integration in Model I and II.

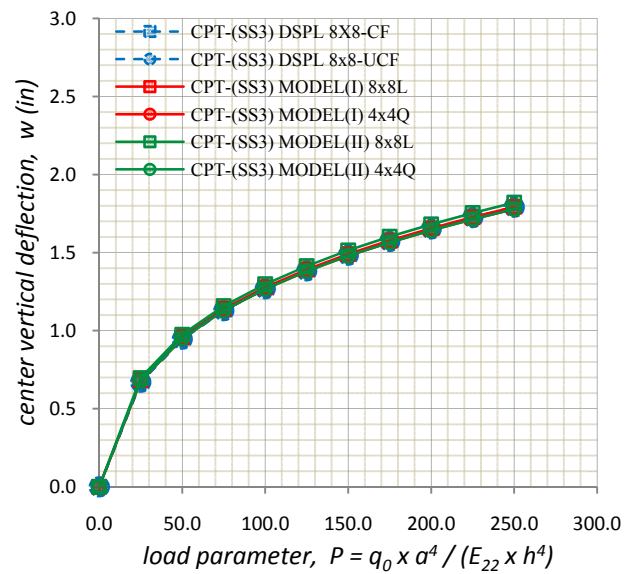
$P = \frac{q_0 a^4}{(E_{22} h^4)}$	Center deflection, w, CPT-(SS1)							
	MODEL I				MODEL II			
	4x4-Linear		2x2-Quadratic		4x4-Linear		2x2-Quadratic	
	FI	RI	FI	RI	FI	RI	FI	RI
6.25	0.2736	0.2737	0.2691	0.2691	0.2718	0.2719	0.2691	0.2691
12.50	0.5090	0.5096	0.5005	0.5007	0.5059	0.5064	0.5005	0.5007
25.00	0.8608	0.8629	0.8468	0.8475	0.8565	0.8579	0.8470	0.8476
50.00	1.3119	1.3163	1.2923	1.2943	1.3061	1.3093	1.2932	1.2947
75.00	1.6185	1.6244	1.5960	1.5997	1.6114	1.6157	1.5977	1.6004
100.00	1.8572	1.8641	1.8328	1.8383	1.8488	1.8539	1.8357	1.8394
125.00	2.0559	2.0637	2.0302	2.0377	2.0462	2.0521	2.0339	2.0391
150.00	2.2280	2.2365	2.2011	2.2107	2.2171	2.2235	2.2059	2.2125
175.00	2.3811	2.3900	2.3529	2.3649	2.3689	2.3757	2.3588	2.3669
200.00	2.5196	2.5289	2.4901	2.5045	2.5062	2.5133	2.4971	2.5068
225.00	2.6465	2.6562	2.6158	2.6327	2.6320	2.6394	2.6240	2.6352
250.00	2.7641	2.7741	2.7321	2.7515	2.7484	2.7561	2.7414	2.7541

Then, using 8×8 linear and 4×4 quadratic elements, non-linear normal stresses and center deflection of the Model I were compared with those of the non-conforming and the conforming displacement based models. The results of vertical deflection and the normal stress is presented in the Table 5.14

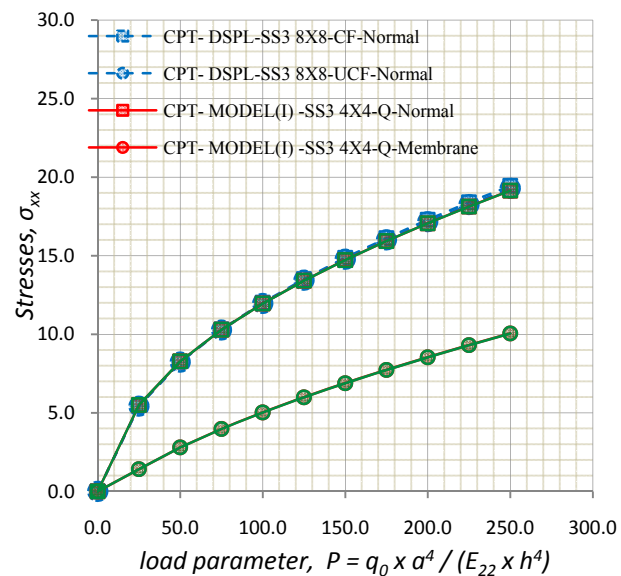
Table 5.14
Comparison of the center deflection and normal stress of Model I and II with the CPT displacement model.

$P = \frac{q_0 a^4}{(E_{22} h^4)}$	Center deflection, w, CPT-(SS3)					
	MODEL I		MODEL II		DSPL	DSPL
	8x8-L	4x4-Q	8x8-L	4x4-Q	8X8-CF	8x8-UCF
0.00	0.0000	0.0000	0.0000	0.0000	0.0000	0.0000
25.00	0.6836	0.6774	0.6966	0.6771	0.6690	0.6700
50.00	0.9581	0.9501	0.9743	0.9497	0.9450	0.9460
75.00	1.1388	1.1296	1.1572	1.1293	1.1270	1.1280
100.00	1.2775	1.2675	1.2977	1.2672	1.2670	1.2680
125.00	1.3919	1.3813	1.4137	1.3809	1.3830	1.3830
150.00	1.4902	1.4791	1.5134	1.4787	1.4830	1.4830
175.00	1.5770	1.5654	1.6015	1.5650	1.5710	1.5710
200.00	1.6552	1.6432	1.6809	1.6428	1.6510	1.6510
225.00	1.7265	1.7142	1.7533	1.7138	1.7240	1.7240
250.00	1.7923	1.7796	1.8201	1.7793	1.7910	1.7910
$P = \frac{q_0 a^4}{(E_{22} h^4)}$	Normal stresses, $\sigma_{xx}^{normal}(0,0,0.5h) \times a^2/E_{11}$, CPT-(SS3)					
	MODEL I		MODEL II		DSPL	DSPL
	8x8-L	4x4-Q	8x8-L	4x4-Q	8X8-CF	8x8-UCF
0.00	0.0000	0.0000	0.0000	0.0000	0.0000	0.0000
25.00	5.5195	5.5008	5.3402	5.4980	5.4260	5.4230
50.00	8.2751	8.2782	8.0297	8.2741	8.2470	8.2270
75.00	10.2633	10.2937	9.9885	10.2901	10.3090	10.2710
100.00	11.8988	11.9589	11.6072	11.9541	12.0170	11.9610
125.00	13.2682	13.4106	13.0238	13.4098	13.5130	13.4400
150.00	14.6077	14.7273	14.3036	14.7196	14.8670	14.7770
175.00	15.8033	15.9322	15.4838	15.9311	16.1170	16.0090
200.00	16.8734	17.0628	16.5872	17.0613	17.2870	17.1620
225.00	17.8924	18.1308	17.6290	18.1271	18.3930	18.2510
250.00	18.9188	19.1385	18.6199	19.1411	19.4460	19.2870

The non linear load versus deflection and load versus stress graphs are given in the Fig.5.8. Under the SS3 boundary condition, both of the vertical deflection and stresses of the Model I and II showed very close value when they are compared with the displacement based model. The normal stresses and the membrane stresses were computed at the (0,0,0.5h) and (0,0,0) respectively. 9-nodel quadratic element showed closer solutions to that of the displacement based FSDT model.



(a) Load verses center deflection



(b) Load verses center normal stress

Fig. 5.8. Plots of the membrane and normal stress of Model I, II and CPT displacement model under SS3 boundary condition.

To see the convergence of the various models, center deflections of previously developed models with 2×2 quadratic and 4×4 linear meshes under SS1 and SS3

boundary conditions were compared. Every model showed good convergence with a tolerance, $\epsilon = 0.01$, except for the Model IV. The Model IV showed acceptable convergence with SS3 boundary condition, but with SS1 it took more iteration times to converge than other models. The iterative times taken to get converged solutions of the various models are presented in the table 5.15.

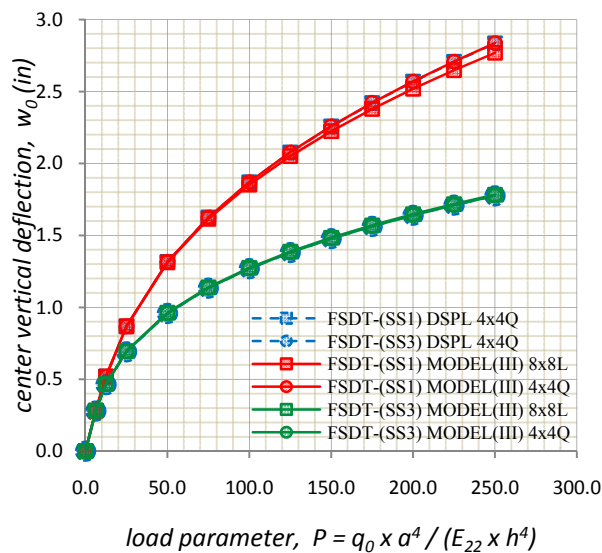
Table 5.15
Comparison of the convergence of Model I, II, III and IV under the SS1 and SS3 boundary conditions.

$P = \frac{q_0 a^4}{(E_{22} h^4)}$	Center deflection, w (*iteration times to converge), SS1 various models					
	Model (III)		Model (IV)		Model (I)	Model (II)
	4x4-L	2x2-Q	4x4-L	2x2-Q	2x2-Q	2x2-Q
0.00	0.0000(3)	0.0000(3)	0.0000(3)	0.0000(3)	0.0000(3)	0.0000(3)
6.25	0.2821(3)	0.2816(3)	0.2877(3)	0.2847(3)	0.2691(3)	0.2691(3)
12.50	0.5213(3)	0.5195(3)	0.5281(5)	0.5233(5)	0.5007(3)	0.5007(4)
25.00	0.8730(3)	0.8695(3)	0.8801(6)	0.8736(6)	0.8475(3)	0.8476(4)
50.00	1.3195(3)	1.3187(3)	1.3237(7)	1.3169(7)	1.2943(3)	1.2947(3)
75.00	1.6228(3)	1.6282(3)	1.6302(7)	1.6256(7)	1.5997(3)	1.6004(3)
100.00	1.8589(3)	1.8720(3)	1.8684(7)	1.8663(7)	1.8383(3)	1.8394(3)
125.00	2.0553(3)	2.0769(2)	2.0682(7)	2.0688(7)	2.0377(3)	2.0391(3)
150.00	2.2251(3)	2.2552(2)	2.2420(6)	2.2456(6)	2.2107(3)	2.2125(3)
175.00	2.3757(3)	2.4141(2)	2.3914(6)	2.3973(6)	2.3649(3)	2.3669(2)
200.00	2.5116(3)	2.5580(2)	2.5308(6)	2.5392(6)	2.5045(2)	2.5068(2)
225.00	2.6376(2)	2.6898(2)	2.6592(6)	2.6704(6)	2.6327(2)	2.6352(2)
250.00	2.7521(2)	2.8117(2)	2.7717(5)	2.7850(5)	2.7515(2)	2.7541(2)
$P = \frac{q_0 a^4}{(E_{22} h^4)}$	Center deflection, w (*iteration times to converge), SS3 various models					
	Model (III)		Model (IV)		Model (I)	Model (II)
	4x4-L	2x2-Q	4x4-L	2x2-Q	2x2-Q	2x2-Q
0.00	0.0000	0.0000	0.0000	0.0000	0.000	0.000
6.25	0.2911(4)	0.2865(4)	0.2912(4)	0.2866(4)	0.2718(4)	0.2713(4)
12.50	0.4779(3)	0.4709(3)	0.4784(3)	0.4716(3)	0.4561(3)	0.4552(3)
25.00	0.7076(3)	0.6978(3)	0.7080(3)	0.6982(3)	0.6872(3)	0.6860(3)
50.00	0.9763(3)	0.9626(3)	0.9760(4)	0.9622(4)	0.9578(3)	0.9563(4)
75.00	1.1542(3)	1.1375(3)	1.1535(4)	1.1367(4)	1.1360(3)	1.1345(4)
100.00	1.2914(3)	1.2724(3)	1.2908(4)	1.2715(4)	1.2730(3)	1.2714(4)
125.00	1.4050(2)	1.3841(2)	1.4046(4)	1.3832(4)	1.3861(3)	1.3845(4)
150.00	1.5030(2)	1.4803(2)	1.5015(3)	1.4783(3)	1.4834(2)	1.4818(3)
175.00	1.5897(2)	1.5655(2)	1.5885(3)	1.5636(3)	1.5693(2)	1.5678(3)
200.00	1.6679(2)	1.6422(2)	1.6669(3)	1.6405(3)	1.6467(2)	1.6452(3)
225.00	1.7393(2)	1.7124(2)	1.7385(3)	1.7107(3)	1.7173(2)	1.7159(3)
250.00	1.8054(2)	1.7773(2)	1.8047(3)	1.7757(3)	1.7825(2)	1.7811(3)

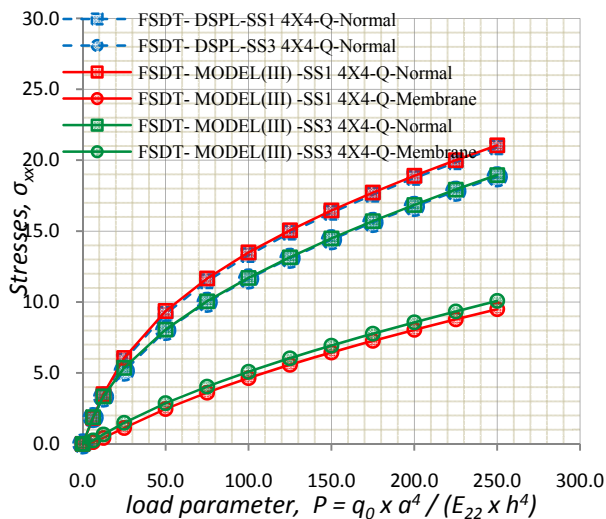
In the nonlinear analysis of the FSDT, the non-linear center deflection, normal stress and membrane stress of the Model III were compared with the results of displacement based models. The results are presented in the Table 5.16. A 4x4 quadratic mesh showed the closest result to the displacement FSDT model's result as shown in the Fig. 5.9.

Table 5.16
Comparison of the center deflection and normal stress of Model III with the FSDT displacement model under SS1 and SS3 boundary conditions.

$P = \frac{q_0 a^4}{(E_{22} h^4)}$	Center deflection, w, FSDT-Model (III)					
	SS1		SS3		DSPL(SS1)	DSPL(SS3)
	8x8-L	4x4-Q	8x8-L	4x4-Q	4x4-Q	4x4-Q
0.00	0.0000	0.0000	0.0000	0.0000	0.0000	0.0000
6.25	0.2815	0.2813	0.2823	0.2804	0.2813	0.2790
12.50	0.5192	0.5187	0.4671	0.4645	0.5186	0.4630
25.00	0.8678	0.8677	0.6956	0.6922	0.8673	0.6911
50.00	1.3117	1.3159	0.9626	0.9582	1.3149	0.9575
75.00	1.6148	1.6254	1.1389	1.1339	1.6241	1.1333
100.00	1.8522	1.8702	1.2748	1.2693	1.8687	1.2688
125.00	2.0509	2.0769	1.3872	1.3812	2.0758	1.3809
150.00	2.2241	2.2583	1.4840	1.4777	2.2567	1.4774
175.00	2.3786	2.4213	1.5697	1.5631	2.4194	1.5628
200.00	2.5191	2.5702	1.6470	1.6401	2.5681	1.6398
225.00	2.6480	2.7080	1.7176	1.7104	2.7056	1.7102
250.00	2.7684	2.8366	1.7828	1.7754	2.8338	1.7752
$P = \frac{q_0 a^4}{(E_{22} h^4)}$	Normal stresses, $\sigma_{xx}(0,0,0.5h) \times a^2/E_{11}$, FSDT-Model(III), 4x4Q					
	SS1		SS3		DSPL(SS1)	DSPL(SS3)
	$\sigma_{xx}^{Membrane}$	σ_{xx}^{Normal}	$\sigma_{xx}^{Membrane}$	σ_{xx}^{Normal}	σ_{xx}^{Normal}	σ_{xx}^{Normal}
0.00	0.0000	0.0000	0.0000	0.0000	0.000	0.000
6.25	0.1228	1.8382	0.2415	1.8836	1.780	1.856
12.50	0.4124	3.5098	0.6646	3.3424	3.398	3.300
25.00	1.1211	6.0584	1.4838	5.3620	5.885	5.137
50.00	2.4550	9.3685	2.8656	8.0544	9.165	8.001
75.00	3.6076	11.6627	4.0327	10.0497	11.465	9.983
100.00	4.6341	13.4941	5.0765	11.7036	13.308	11.634
125.00	5.5698	15.0596	6.0326	13.1587	14.889	13.085
150.00	6.4411	16.4546	6.9241	14.4891	16.290	14.398
175.00	7.2587	17.7226	7.7666	15.7033	17.567	15.610
200.00	8.0353	18.8989	8.5692	16.8457	18.748	16.743
225.00	8.7770	20.0025	9.3372	17.9294	19.854	17.812
250.00	9.4916	21.0468	10.0764	18.9536	20.898	18.829



(a) Load verses center deflection



(b) Load verses center normal and membrane stress

Fig. 5.9 Plots of the center deflection, normal and membrane stress of Model III with that of the FSDT displacement model under SS1 and SS3 boundary conditions.

To see distributions of the variables other than displacements, images of the distribution of each variable are presented in the Fig. 5.10 and 5.11. The data was post processed inside of each element using 10 gauss points ranging from -0.975 to 0.975, in both newly developed models (i.e., Model I and III) and FSDT displacement based

model. Converged solutions of SS3 at the load parameter, $P = 250.0$, were used for the post processing

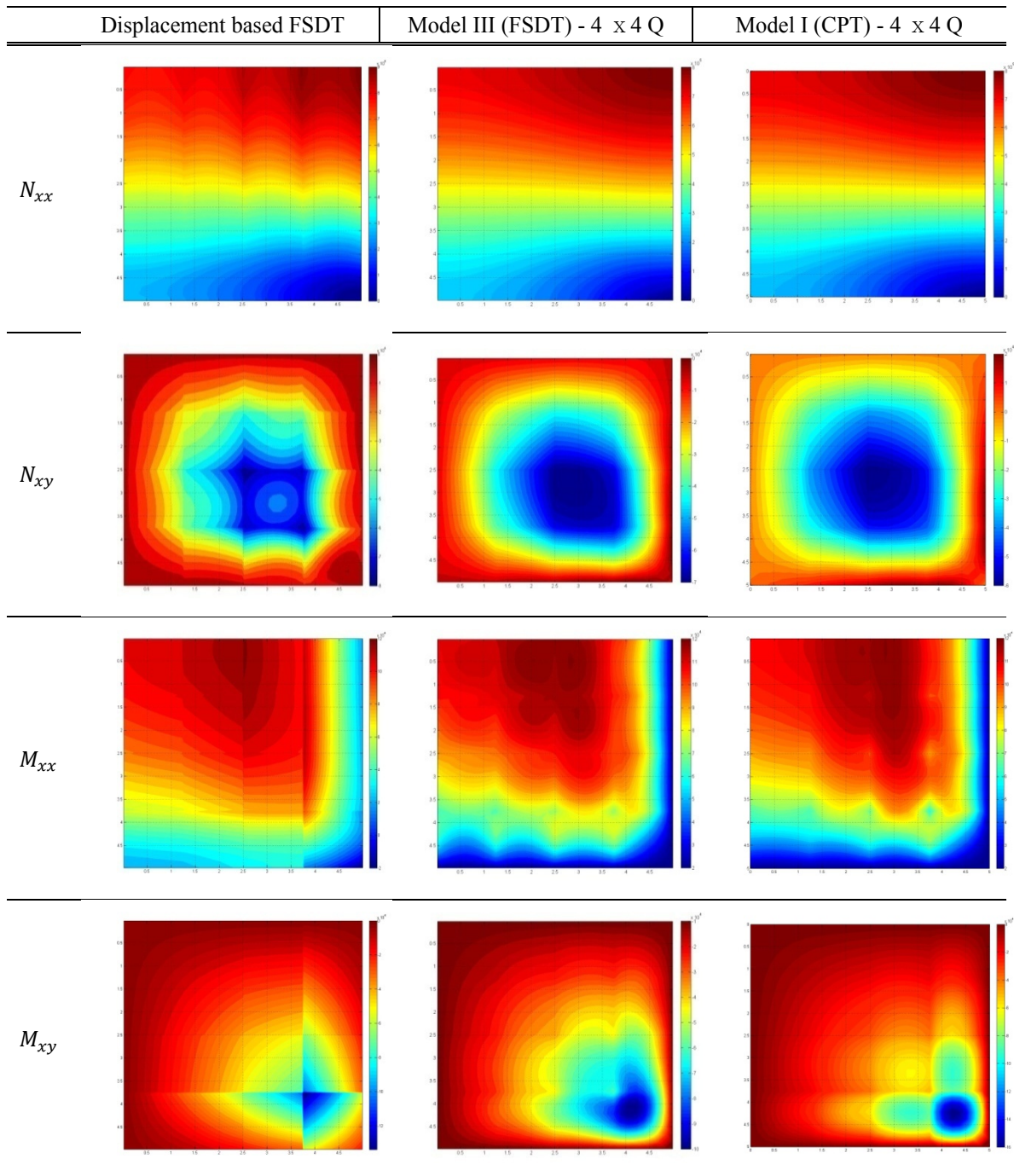
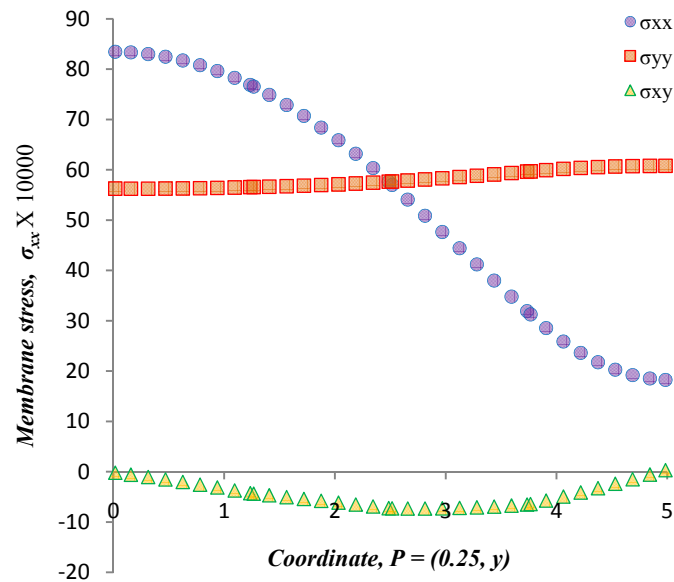
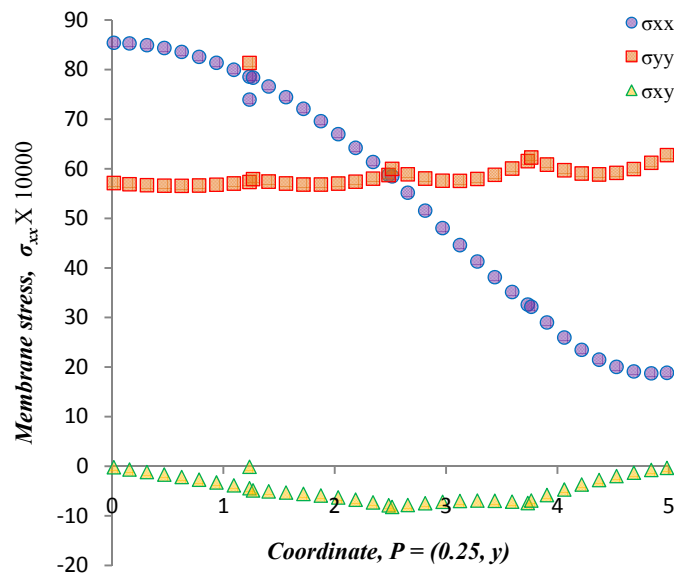


Fig. 5.10 Post processed quadrant images of the variables in various models, SS3, with converged solution at load parameter $\bar{P} = 250$.

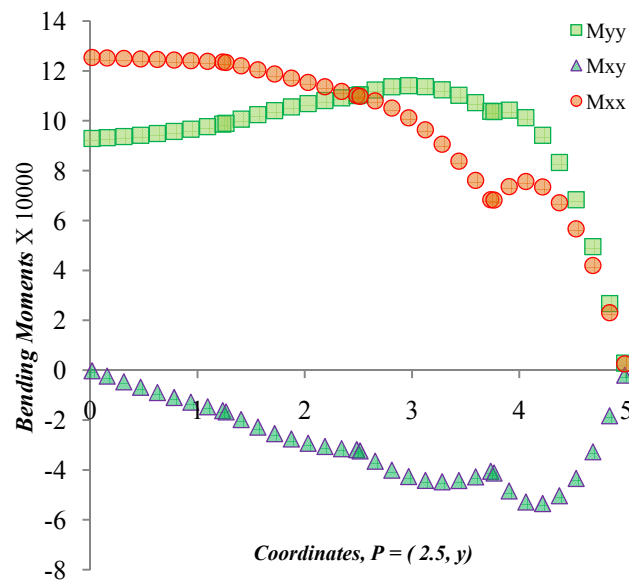


(a) Model III

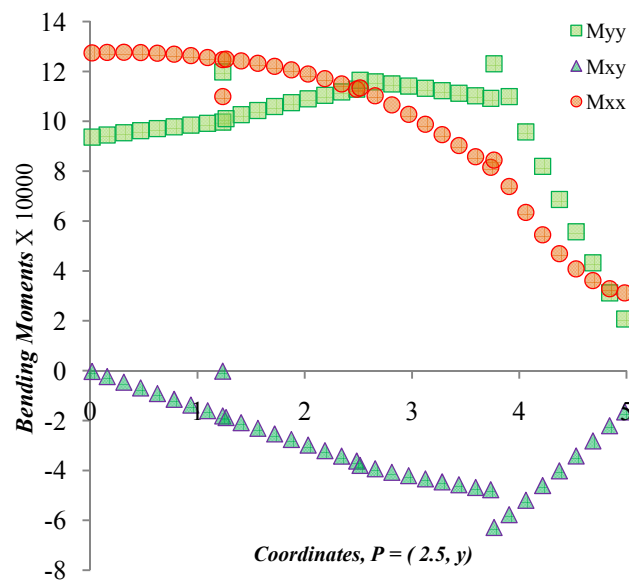


(b) FSDT displacement model

Fig. 5.11. Plots of the non-linear membrane stresses of Model III and FSDT displacement model along the $x = 2.5$.



(a) Model III



(a) FSDT displacement model

Fig. 5.12. Plots of the non-linear bending moments of Model III and FSDT displacement model along the $x = 2.5$.

Even though all of them are showing similar patterns for each variable as shown in the Fig. 5.10, one can easily notice that the images obtained from the current mixed models offer better picture at the boundaries of the elements, while the images obtained from the displacement based model shows discontinuous states. And more obviously, the graphs of the Fig. 5.11 and 5.12 are showing that the distribution of stresses and bending moments of Model III is better than the displacement FSDT, even though bending moments of Model III have some oscillations at the element boundary. This is the merit of the current mixed models which cannot be achieved without including force like variables as independent nodal value.

CHAPTER VI

CONCLUSION

In this study, advantages and disadvantages of newly developed nonlinear finite element models of beams and plates bending were discussed with numerical simulations under various boundary conditions.

As an advantage, the locking of the beam element was eliminated or attenuated with newly developed beam models, depending on the inclusion of variables and also choice of the interpolation functions. Especially with the model III, the effect of including some variable was shown, and to fix new locking, use of high order interpolation function (i.e., cubic interpolation function) was adopted.

For almost every case, newly developed plate bending models provided better accuracy for linear solutions of the vertical deflection and force like variables. When it was compared with the analytic solutions, both new models and traditional models showed good accuracy for the displacement (i.e., vertical deflection w_0), but new mixed models presented much better accuracy for the stress fields. The 9-node quadratic element performed better than 4-node linear element in most of cases, while linear element still provided acceptable accuracy compared with existing traditional models.

In non linear analysis, most of the newly developed mixed models showed good convergence of non-linear solutions, when it was compared with the displacement based non-linear models. But inclusion of the some variable affected convergence of non-linear solution in the FSDT models. The Model IV showed poor convergence compared with other models, because of the absence of typical variable in the mixed formula.

The post processed data of newly developed plate bending models presented better continuity at the element boundary, while displacement based FSDT model showed noticeable discontinuity at the element boundary. Even if these defects of displacement based model can be overcome by more refined mesh or other post processing techniques,

the essentially the level of accuracy for force like variables cannot be the same as that of current mixed models.

We can conclude that two main advantages of the mixed model are the reduction of the continuity requirements for the vertical displacement, and the increase of the accuracy for the resultants included in the finite element models. The disadvantages of current models are the sacrificed computational cost caused by the increased numbers of degrees of freedoms included in the finite element models.

REFERENCES

- [1] J. N. Reddy, *An Introduction to Nonlinear Finite Element Analysis*, Oxford University Press, Oxford, 2004.
- [2] J. N. Reddy, *An Introduction to Continuum Mechanics : With Applications*, Cambridge University Press, New York, 2008.
- [3] J. N. Reddy, *Theory and Analysis of Elastic Plates and Shells*, 2nd ed., CRC, Boca Raton, FL, 2007.
- [4] J. N. Reddy, *An Introduction to the Finite Element Method*, 3rd ed., McGraw-Hill, New York, 2006.
- [5] J. N. Reddy, *Mechanics of Laminated Composite Plates and Shells : Theory and Analysis*, 2nd ed., CRC Press, Boca Raton, FL, 2004.
- [6] N. S. Putcha, A Refined Mixed Shear Flexible Finite Element for the Nonlinear Analysis of Laminated Plates, *Comput. Struct.* 22(1986), 529 – 538.
- [7] J. N. Reddy, Mixed Finite Element Models for Laminated Composite Plate, *J. Engrg. Indus.* 109(1987), 39 – 45.
- [8] J. N. Reddy, *Energy Principles and Variational Methods in Applied Mechanics*, J. Wiley, New York, 2002.
- [9] C. M. Wang, J. N. Reddy, and K. H. Lee, *Shear deformable beams and plates : relationships with classical solutions*, Elsevier, New York, 2000.
- [10] H. V. Smith, *Numerical Methods of Integration*, Studentlitteratur, Chartwell-Bratt, England, 1993.
- [11] J. H. Davis, *Differential Equations with Maple : An Interactive Approach*, Birkhäuser, Boston , 2001.
- [12] L. R. Nyhoff, and S. Leestma, *Introduction to Fortran 90 for Engineers and Scientists*, Prentice Hall, Upper Saddle River, NJ, 1997.
- [13] W. J. Palm, *MATLAB for Engineering Applications*, WCB/McGraw-Hill, Boston , 1998.

- [14] J. N. Reddy, On Locking-free Shear Deformable Beam Finite Elements, *Comput. Methods Appl. Mech. Engrg.* 149(1997) 113-132.
- [15] S. J. Colley, *Vector Calculus*, Prentice Hall, Upper Saddle River, NJ, 1997.
- [16] W. M. Lai, D. Rubin, and E. Krempl, *Introduction to Continuum Mechanics*, Oxford ; Pergamon Press, New York, 1993.
- [17] R. L. Panton, *Incompressible Flow*, J. Wiley, Hoboken, NJ, 2005.
- [18] S. Timoshenko, and J. N. Goodier, *Theory of Elasticity*, McGraw-Hill, New York , 1970.
- [19] W. D. Callister, *Materials Science and Engineering : An Introduction*, John Wiley & Sons, New York, 2007.
- [20] S. J. Lee, and J. N. Reddy, Nonlinear Finite Element Analysis of Laminated Composite Shell with Actuating Layers, *Finite Elements in Analysis and Design* 43(2006) 1-21.
- [21] J. L. Batoz, G. Dhatt, Incremental Displacement Algorithms for Non-linear Problems, *Int. J. Numer. Methods Engrg.* 14(1979) 1262-1267.
- [22] E. Riks, The Application of Newton's Method to Problem of Elastic Stability, *J. Appl. Mech.* 39(1972) 1060-1066.
- [23] F. Cajori, Historical Note on the Newton-Raphson Method of Approximations, *American Mathematical Monthly* 18(1911) 29-32.
- [24] S. J. Leon, *Linear Algebra with Applications*, Prentice Hall, Upper Saddle River, NJ, 2002.
- [25] F. Moleiro, C. M. Mota Soares, C. A. Mota Soares, Mixed Least-squares Finite Element Model for the Static Analysis of Laminated Composite Plates, *Comput. Struct* 86 (2008) 826-838.
- [26] L. R. Herrmann, Mixed Finite Element Method for Bending of Plates, *Int. J. Numerical Method*, 9 (1975) 3-5.
- [27] D. J. Allman, Triangular Finite Element for Plate Bending with Constant and Linearly Varying Bending Moments, *High Speed Computing of Elastic Struct.* 1 (1971) 106-136.

VITA

Wooram Kim was born in Uijeongbu, Republic of Korea. He received his B.S. in weapons engineering from the Korea Military Academy in 2004, and he was commissioned as an Armor officer in the same year. He served in the ROK Army from 2004 to 2005 as a tank platoon leader of the 59th tank battalion. He entered the Mechanical Engineering Department at Texas A&M University in 2006 as a graduate student and received his M.S. in August 2008.

Permanent Address: Department of Mechanical Engineering, 3123, TAMU,
College Station, Texas, 77843-3123, USA.

Chair of Committee: Dr. J.N. Reddy

E-mail Address: c14445@kma.ac.kr